



Norwegian University of
Science and Technology

Analysis of low Frequency content from the Circulatory System

Kristian L Stenerud

Master of Science in Electronics

Submission date: June 2016

Supervisor: Ilangko Balasingham, IET

Norwegian University of Science and Technology
Department of Electronics and Telecommunications

Preface

This thesis has been done as partial fulfilment of the requirements for the degree of Master of Science(M.Sc) at the Norwegian University of Science and Technology (NTNU). The work presented has been done during the spring semester 2016.

The thesis has been part of a project led by Nils Kristian Skjærvold, studying the cardiovascular system and the underlying regulation. The findings in this thesis has been used by other parts of the project. The medical students Bjørn Gardsjord Lio and Fredrik Axelsson collected the data, they used the the frequency analysis done in this thesis in their "Hovedoppgave". Their medical analysis of the results are seen in their thesis [1].

Trondheim, June 2016

Kristian Stenerud

Acknowledgment

I would like to thank my supervisor Ilangko Balasingham and his phd. students for great help, with insightful discussions and leading me in the right directions.

I would also like to specially thank Nils Kristian Skjærvold and the entire project team for allowing me to contribute to their project and getting an insight into such an interesting field of research. Special thanks to Bjørn Lio, Fredrik Axelsson and Kathrine Knai for collecting the data and our interdisciplinary exchange of knowledge.

K.S.

Problem Description

Hemodynamic and physiological parameters such as blood pressure, electrocardiogram (ECG), blood flow, muscle sympathetic nerve activity, etc. can provide information about the health status of a patient. If the patient is given intervention in terms of physical and orthostatic challenges or pharmacological manipulations, then the hemodynamic and physiological parameters can change. The changes can provide important clinical information regarding the individual patient's underlying physiologic regulation, about pathophysiological state of diseases and their progress. As for now, there are no existing mathematical tools available in order to access and understand this circulatory dynamics as a function of health condition, age and gender or predict the outcome in a robust manner.

This thesis aims to study the low frequency oscillations in circulatory variables from pre- and post cardiac surgery patients to see how these evolve as a function of time. The understanding of biological signals behavior and therefor the behavior of the cardiovascular system helps to characterize patients state and might represent a step toward a better care.

Abstract

This thesis has investigated the low frequency content from the cardiovascular system. Three different signals; heart rate variability(HRV), blood pressure(BP) and a flow signal of the blood(Laser doppler flow, LDF) all being global variables of the cardiovascular system collected independently of each other has been used. The low frequency content from these three different signals has been compared for patients doing cardiac surgery. Four time segments of one hour each has been collected, one before the surgery and three after surgery. The frequency analysis has been done using a continuous wavelet transform. This produces three frequency spectrum's for each time segment, corresponding to a signal. A Poincare analysis for the HRV signal has been done to verify some of the results. The study of the evolution of the frequency spectrum's over the time segments then shows two main findings.

First finding is a similar trend in the sub-bands *HR*, *resp* and partly the *myo* sub-band. Where the peak frequency for all shows a similar evolution over the time segments. Also for the power variable there is a similar trend over the time segments.

Second finding is the similar trend in the lower sub-bands *neuro*, *eMeta* and *VLF*. For the mentioned sub-bands the peak value variable has all the same evolution over the time segments. These variables also shows a statistical significant change from before the surgery to the last and most stable segment after the surgery. The trend from the peak value also recur in the variables from the Poincare analysis. The values from the Poincare analysis show significant decrease from before to after surgery.

The results are produced from a limited amount of data. In order to increase the statistical strength of the results a larger data set should be evaluated.

Sammendrag

Denne oppgaven er et studie av det lavfrekvente innholdet fra det kardiovaskulære systemet. Analysen har tatt utgangspunkt i tre forskjellige signaler, hjertefrekvens variasjon (HRV), blodtrykk (BP) og et strømningsignal av blodet (Laser doppler flow, LDF). Dette gir tre globale variabler i det kardiovaskulære systemet, målt på uavhengige måter. Det lavfrekvente innholdet i disse signalene er sammenlignet for pasienter som er inne til hjerteroperasjon. Det er valgt ut 4 tidssegmenter for sammenligningen, et før operasjon og tre etter. Frekvensanalysen av signalene er utført med kontinuerlig wavelet transformasjon. En Poincare analyse for HRV signalet er gjort for å verifisere noen av resultatene. Evolusjonen av de korresponderende frekvensspektrene over de gitte tidssegment gir to hovedfunn.

Første funn er en sammenheng i utviklingen for del-båndene *HR*, *resp* og delvis *myo*, den viser lignende utvikling for den sterkeste frekvensen i del-båndene (*peak_frequency*). *Power* variabelen viser også en lignende utvikling for disse del-båndene.

Andre funn er en lignende utvikling i de lavere del-båndene, *neuro*, *eMeta* og *VLF*. Verdien på den sterkeste frekvens (*peak_value*) i disse båndene viser samme utvikling over de fire tidssegmentene. Denne variabelen viser også en statistisk signifikant endring fra før operasjon til siste segment etter operasjon for alle signalene og de nevnte del-båndene. Utviklingen i *peak_value* variabelen viser seg også i variablene fra Poincare analysen. Fra Poincare analysen viser SD1 og SD2 en signifikant nedgang fra før til etter operasjonen.

Resultatene i denne analysen er fra en begrenset mengde data. For å bedre det statistiske grunnlaget bør et større datasett vurderes.

Table of Contents

Preface	i
Acknowledgment	ii
Problem Description	iii
Abstract	iv
Sammendrag	v
Table of Contents	vii
List of Tables	viii
List of Figures	xi
Acronyms	xii
1 Introduction	1
1.1 Motivation/Background	1
1.2 Approach	2
1.3 Previous work/Litterateur survey	2
1.4 Structure of thesis	2
2 Background	5
2.1 Circulatory system	5
2.1.1 Heart and Blood vessels	5
2.1.2 Cardiac cycle	7
2.1.3 The heart's electrical conduction system	8
2.2 ECG signal	10
2.2.1 Noise sources in ECG	13
2.3 Blood Pressure	14
2.4 Laser Doppler flowmetry	15
2.5 Heart rate and HRV	15
2.6 Analysis methods	17
2.6.1 Frequency analysis	17
2.6.2 Poincarè analysis	19
3 Methods and Implementation	21
3.1 Signal acquisition	21
3.1.1 ECG recordings	22
3.1.2 Blood pressure recordings	22
3.1.3 Laser Doppler Flow	22
3.2 Noise analysis	22

3.2.1	ECG	22
3.2.2	Laser Doppler Flow	25
3.2.3	Blood Pressure	28
3.3	The application	32
3.3.1	Pre program	32
3.3.2	Analysis program	35
3.4	Analysis set up	40
3.4.1	Poincarè analysis	44
4	Results	45
4.1	Frequency analysis application	45
4.2	Patient analysis	45
4.2.1	Averaged evolution	46
4.2.2	Peak detection	54
4.2.3	Pre vs Post3	54
4.2.4	Poincare analysis	54
5	Discussion	65
5.1	Application and analysis set up	65
5.2	Peak detections	65
5.3	Trend analysis	66
5.3.1	Heart rate	66
5.3.2	Respiratory rate	66
5.3.3	Myogenic activity	66
5.3.4	Neurogenic activity	67
5.3.5	Metabolic activity	67
5.3.6	VLF	67
5.3.7	Similarities	67
5.4	Pre vs Post3	68
5.5	Poincarè analysis	68
6	Summary and Conclusion	69
6.1	Conclusion	69
6.2	Recommendations for Further Work	70
A	Cwt mean plots	71
B	Poincare plots	82
C	Attached files	93
	Bibliography	94

List of Tables

2.1	Electrode names and placement for 12 lead ECG	11
3.1	Standardized way of saving the files from the pre program	34
3.2	Time segments chosen for the post segments	42
3.3	Frequency sub-bands	42
4.1	Number of peaks detected for the HR sub-band	48
4.2	Number of peaks detected for the respiratory sub-band	49
4.3	Number of peaks detected for the myo sub-band	50
4.4	Number of peaks detected for the neuro sub-band	51
4.5	Number of peaks detected for the eMeta sub-band	52
4.6	Number of peaks detected for the VLF sub-band	53
4.7	Number of peaks detected for the sub-bands	61
4.8	T test for variables	62
4.9	Poincare analysis	62
5.1	Number of statistical significatn changed variables from pre to post3	68
A.1	Shows set up for the cwt mean plots	71

List of Figures

2.1	Circulatory system, showing the arterial system in red and the venous system in blue. from [2]	6
2.2	Diagram of the human heart from [2]	7
2.3	Cardiac events from [3]	8
2.4	Electrical conduction in a heart from [4]	9
2.5	Placement for a 12 lead ECG. A 12 lead ECG using only 10 electrodes figures from [5]	10
2.6	Limb leads and augmented limb leads, captured from [5]	12
2.7	Illustration of recorded signal by an electrode, captured from [5]	12
2.8	Typical ECG waveform from a healthy person, captured from [5]	13
2.9	Change in frequency due to a moving source, from [6]	15
2.10	The upper plot shows the ECG signal and how the R-R interval is extracted, the lower plot shows the R-R intervals, from [7]	16
2.11	Continuous wavelet, Morlet	18
2.12	Poincare plot showing the fitted ellipse and the variables SD1 and SD2, figure from [8]	20
3.1	A raw ECG signal where the upper one showing a period without any motion artifact and the two lower plots show the same motion artifact	23
3.2	Showing the frequency spectrum of ECG signal where the upper one showing a period without any motion artifact and the lower plot shows with motion artifact	23
3.3	Showing the time-frequency spectrum of ECG signal	24
3.4	Top plot's shows original signal with motion artifact, lower plots show the original signals filtered.	26
3.5	Top plot's shows original signal with motion artifact, lower plots show the original signal after removing the motion artifact using the polyfit technique.	27
3.6	Upper plot shows a noisy part of a LDF signal the lower plot shows a noise free LDF signal, , both are from the same patient with some overlap at 8-10min.	28
3.7	Frequency analysis of the laser doppler flow signal from FFT and CWT. Top plot's is of the noisy LDF and bottom is of the normal LDF	29
3.8	Using the LDF signal with motion artifact from figure 3.6, the black boxes shows the outliers and the red and orange lines shows the thresholds	30
3.9	Using the LDF signal with motion artifact from figure 3.6, zoomed into a segment, the black boxes shows the outliers and the red and orange lines shows the thresholds	30
3.10	Using the LDF signal with motion artifact from figure 3.6, the black boxes shows the outliers and the red and orange lines shows the thresholds	31

3.11	Using the LDF signal with motion artifact from figure 3.6, zoomed into a segment, the black boxes shows the outliers and the red and orange lines shows the thresholds	31
3.12	FFT of the LDF signal with motion artifact from figure 3.6, on top with the outlier techniques adaptive and hard threshold following	32
3.13	The plot shows a ECG signal with R peaks detected buy the function used in the pre program	33
3.14	Screen shot of the program <i>data_exc_GUI.m</i>	35
3.15	Screen shot of the program <i>master_GUI.m</i> at start up.	36
3.16	Screen shot from <i>master_GUI.m</i> with a FFT analysis	37
3.17	CWT using different mother wavelets	38
3.18	Screen shot from <i>master_GUI.m</i> with a CWT time frequency analysis	39
3.19	Screen shot from <i>master_GUI.m</i> with a CWT frequency analysis	39
3.20	Screen shot from <i>master_GUI.m</i> with a CWT frequency analysis and findPeaks function	41
3.21	Comparing FFT and CWT mean method	43
4.1	CWT mean of 160317 from pre(plot 1:3), post1(plot 4:6), post2(plot 7:9) and post3(plot 10:12)	46
4.2	CWT mean of 160329 from pre(plot 1:3), post1(plot 4:6), post2(plot 7:9) and post3(plot 10:12)	47
4.3	Peak frequency's for the HR sub-band	48
4.4	Peak value's for the HR sub-band	49
4.5	Power for the HR sub-band	50
4.6	Showing frequency content from ECG,BP,LDF and respiratory signal.	51
4.7	Peak frequency's for the resp sub-band	52
4.8	Peak value's for the resp sub-band	53
4.9	Power for the resp sub-band	54
4.10	Peak frequency's for the myo sub-band	55
4.11	Peak value's for the myo sub-band	56
4.12	Power for the myo sub-band	56
4.13	Peak frequency's for the neuro sub-band	57
4.14	Peak value's for the neuro sub-band	57
4.15	Power for the neuro sub-band	58
4.16	Peak frequency's for the eMeta sub-band	58
4.17	Peak value's for the eMeta sub-band	59
4.18	Power for the eMeta sub-band	59
4.19	Peak frequency's for the VLF sub-band	60
4.20	Peak value's for the VLF sub-band	60
4.21	Power for the VLF sub-band	61
4.22	Poincare plots of 160317 from pre(top left), post1(top right), post2(bottom left) and post3(bottom right)	63
4.23	Evolution for SD1 and SD2	63
4.24	Evolution for the ratio $SD1/SD2$	64
A.1	CWT mean of 160317	72

A.2	CWT mean of 160329	73
A.3	CWT mean of 160331	74
A.4	CWT mean of 160406	75
A.5	CWT mean of 160407	76
A.6	CWT mean of 160413	77
A.7	CWT mean of 160421	78
A.8	CWT mean of 160510	79
A.9	CWT mean of 160512	80
A.10	CWT mean of 160524	81
B.1	Poincare plots of 160317	82
B.2	Poincare plots of 160329	83
B.3	Poincare plots of 160331	84
B.4	Poincare plots of 160406	85
B.5	Poincare plots of 160407	86
B.6	Poincare plots of 160413	87
B.7	Poincare plots of 160421	88
B.8	Poincare plots of 160510	89
B.9	Poincare plots of 160512	90
B.10	Poincare plots of 160524	91

Acronyms

HR Heart rate

HRV Heart rate variability

BP Blood pressure

LDF Laser doppler flow

ECG Electrocardiogram

SYS Systolic (often pressure)

DIA Diastolic (often pressure)

CWT Continous wavelet transform

FFT Fast fourier transform

Resp Respiratory

myo Myogenic

neuro Neurogenic

eMeta Metabolic

VLF very low frequency

GUI Graphical user interface

FIR Finite impulse response

Chapter 1

Introduction

1.1 Motivation/Background

The circulatory system is controlled by complex regulation with multiple feed-back and -forward loops over a large temporal and spatial scale. The spatial scale varies from the heart and lungs and out to the smallest capillaries and finally cells which are dependent on the blood delivered by the blood vessels. The temporal scale ranges from autonomic nerve potentials in microseconds to circadian rhythms over several hours[9].

During homeostasis, circulatory system is not stationary but on the contrary a healthy circulatory system exhibits a considerable variation at all times. When assessing global circulatory signals, these exhibit distinct oscillatory patterns. These patterns are consequences of underlying complex regulations. The most prominent oscillations is the oscillations around 1Hz and 0.2-0.3Hz constituted by heart rate and the respiratory system. Less studied and less known are the lower frequency's below the respiratory frequency.

This study is being done in collaboration with a medical team from St.Olavs. The medical team consists of the medical students at St.Olavs hospital Bjørn Gardsjord Lio and Fredrik Axelson as a their working on their "Hovedoppgave", also Kathrine Knai as a medical student on the "Forskerlinjen" is a part of the team all which is supervised by the team founder Nils Kristian Skjærvold, post.doc at Department of circulation and medical imaging and consultant anaesthesiologist at the Department of cardiothoracic anaesthesia and –intensive care medicine. The medical team are the problem owners in this project. Some of the following points are from their project description [9].

The medical team believes the oscillatory patterns in the circulatory system exhibited in individual patients can be used to unmask some of the patients underlying circulatory regulation and thus their stability. A main focus in these studies are to examine changes in frequency pattern over time in different variables and patient groups and further to look for synchronization patterns between these different oscillations.

Cardiac surgery patients are as a consequence of their illness and advanced age circulatory compromised, and an important role for the cardiothoracic anaesthesiologist is to evaluate the patient's stability and reserve. In this study we will look into the circulatory oscillatory pattern of patients pre- and postoperative to gain insight into the nature of these patters and how they change during the course of major surgical and anaesthesiological intervention. This will gain insight into the complex regulation of the circulatory system. Understanding biological signals

behavior helps to characterize patient's state and might represent a step toward a better care.

Aim:

- To study oscillations in circulatory variables from pre- and post cardiac surgery patients to see how these evolve as a function of time and to compare them with variables obtained preoperative in the same patients. [9]

The study is performed in accordance with the Helsinki Declaration under patient's approval after institutional approval from regional authorities (REK, Regional etisk komité).

1.2 Approach

To provide the medical team with frequency analysis of the circulatory system. It was decided to make an application to do frequency analysis which takes an input which is medical data provided by the medical team. This medical data would be global variables from the circulatory system. The application would process the data and give an output, which displays the frequency content of the data and any wanted variables for doing a quantitative analysis. The application will be made in Matlab.

General inspection and understanding of the signal is considered important to know what they measure and how they measure the global variables of the circulatory system. This will give a basic idea of what to expect when doing the frequency analysis. This study will also look into what frequency analysis methods most suitable for this project, with the Fast Fourier Transform is fast and easy while the wavelet transform is better suited for not perfect harmonic signals. The interesting low frequency content of this thesis would be from the heart rate and lower. This corresponds to approximately 2Hz and lower.

1.3 Previous work/Litterateur survey

Some interesting studies has previously be done on the low frequency content from different biological signals. Stefanovska et al. has done some analysis of the low frequency differences between a control group and a group of athletes. Looking at the low frequency differences using laser doppler flow signal. The frequency analysis has been done using wavelet transform, and the comparison has been done using some hypothesised frequency bands and comparing chosen values in these sub-bands. [10].

There has also been done several studies on heart rate variability(HRV). One of the more interesting studies regarding this thesis is from Lakusic et al.[11]. The study looked into the change in HRV after coronary artery bypass surgery. They found a decrease in complexity in HRV after a coronary artery bypass grafting(CABG) surgery. They have then used a mix of time and frequency variables to compare pre and post operative.

1.4 Structure of thesis

The structure of this thesis is as follows:

Chapter 1 provides a introduction to this thesis. In chapter 2 follows a theoretical introduction to the biological signals recorded from the circulatory system and some frequency analysis methods. This chapter will give enough theory to follow the rest of the thesis.

Chapter 3 describes the proses of making the application for frequency analysis and the steps for doing the frequency analysis of the signals from the medical team.

The results from this thesis will be described and discussed in chapter 4 and 5. The conclusion and recommendations for further work follows in chapter 6.

Chapter 2

Background

This chapter will give a background to the subjects covered in this thesis. It will start with general anatomy and a description of the circulatory system and hemodynamics, which is the study of blood flow. It will then move on to an explanation of different signals used in the analysis of the circulatory system.

Section 2.1 will cover what must be known about the circulatory system and hemodynamics to get a basic understanding of how the signals used to monitor the circulatory system is being produced. Section 2.2, 2.3 and 2.4 will describe the ECG, Blood pressure and Laser Doppler Flow signals respectively. These sections will describe the signals themselves, how these signals are obtained and their normal behavior. Section 2.6 will present some analysis methods for biological signals. It will emphasize frequency analysis and different ways to find the frequencies in a signal.

After reading this chapter one should be able to understand the rest of this thesis's technical terms and have a good understanding of the cardiovascular system.

2.1 Circulatory system

The circulatory system is a system of organs that circulates blood and thus transports nutrients around the body[2]. This is vital for nourishing cells, helping cells fighting diseases and maintain human homeostasis. The circulatory system could be separate in two systems, the cardiovascular system and lymphatic system. This thesis will focus about the cardiovascular system.

The cardiovascular system comprises the heart, blood vessels and the blood. 2.1. The cardiovascular system could be divide in two "loops" with the heart in the center, the *pulmonary* circulation which takes deoxygenated blood from the heart to the lungs and returns oxygenated blood back to the heart. The other "loop" is the *systemic* circulation which supplies the body with oxygen-rich blood [2].

2.1.1 Heart and Blood vessels

The heart works as a pulsating pump that supply all the parts of the body with oxygenated blood and collects the deoxygnated it then pumps the blood to lungs be oxygenated. These two functions are earlier called systemic circulation, supplying oxygen-rich blood to the body and retrieving it and the pulmonary circulation, that oxygenates the blood in the lungs. For each of

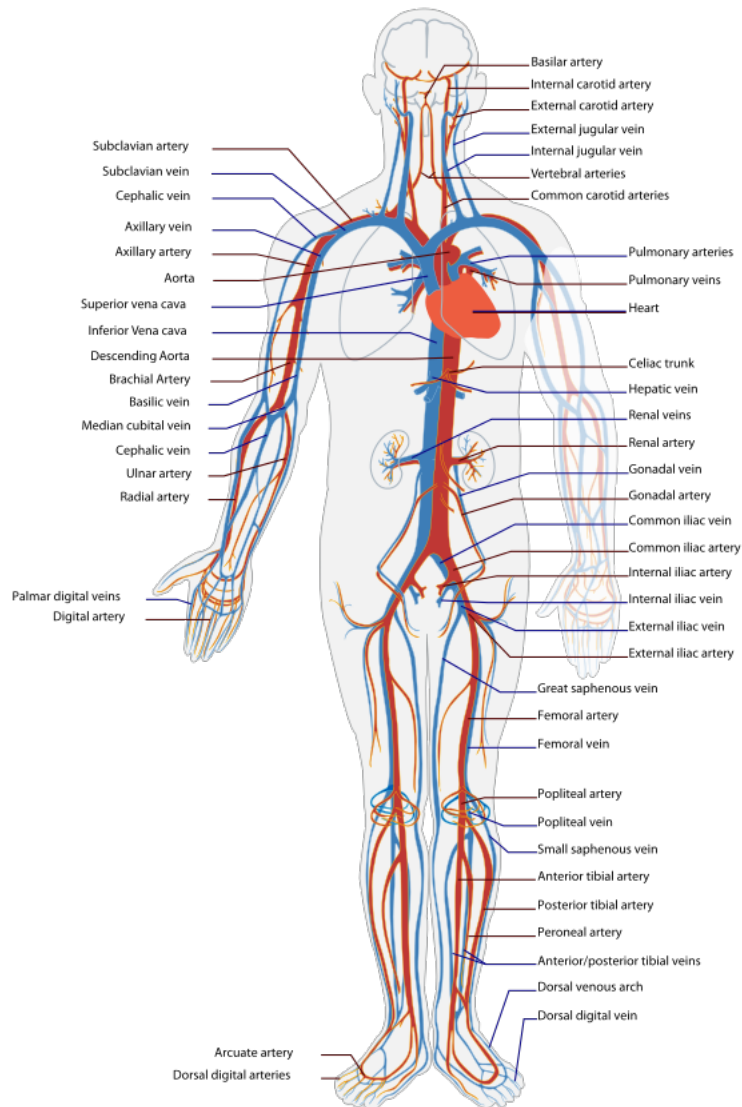


Figure 2.1: Circulatory system, showing the arterial system in red and the venous system in blue. from [2]

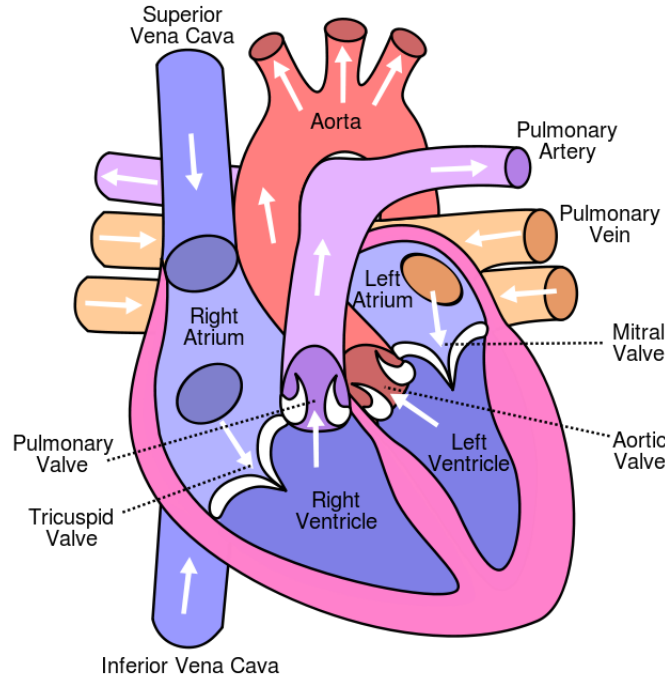


Figure 2.2: Diagram of the human heart from [2]

these "loops" the heart has one atrium and one ventricle, this is chambers separated by valves. This makes it a total of 4 chambers in the heart muscle.

The right atrium receives the oxygen poor blood from the superior and interior *vena cava*, which collects the deoxygenated blood from the whole body. From the right atrium the blood is passing through the *tricuspid valve* to the right ventricle, where it its pumped to the lungs for re-oxygenation. The left atrium receives the newly oxygenated blood from the lungs trough the pulmonary vein passing it through *mitral valve* to the left ventricle. From the left ventricle the oxygen rich blood is pumped out to the organs of the body through the *aorta*. Because of the distance out in extremities of the body is greater than the distance to the lungs, the left side of the heart is stronger than the right, especially than the left ventricle.

The aorta is the start of systemic "loop", distributing the blood to arteries which brings blood to the organs. The arteries then split up into smaller blood vessels called *arterioles* these are again split into even smaller vessels called *capillaries*. The cells are then using the oxygen in there process leaving the blood deoxygenated, the oxygen poor blood is then transported back to the heart through the *veins*, and the systemic "loop" is closed.

Figure 2.1 shows an illustration of the human circulatory system, including the blood vessels and the heart. Figure 2.2 shows an simplified presentation of the anatomy of the heart.

2.1.2 Cardiac cycle

As described earlier is the cardiovascular system driven by the heart muscle as biological pump. To get a brief understanding of the biological signals from the cardiovascular system it is important to know how the heart "pump" works. The cardiac cycle refers to a complete heartbeat from its generation to the beginning of the next one. The frequency of the cardiac cycle or a

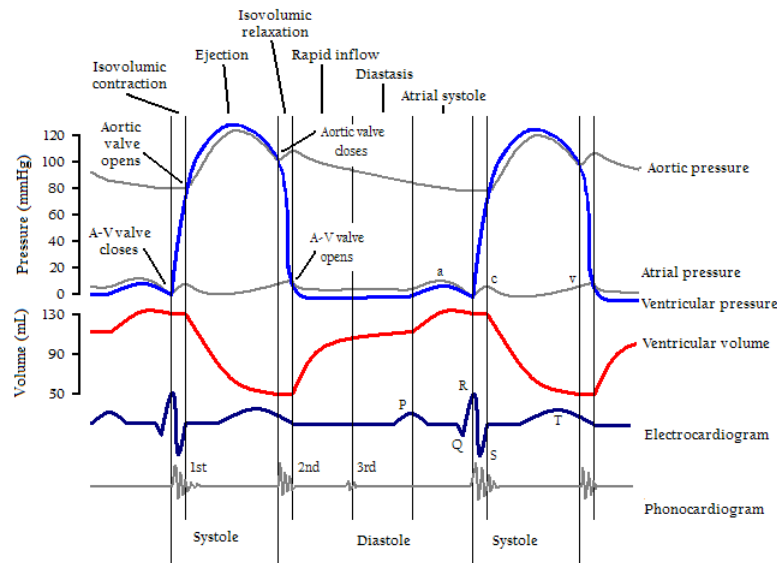


Figure 2.3: Cardiac events from [3]

heartbeat is referred to as the heart rate. The cardiac cycle is divided into two states, *systolic* and *diastolic*, but it could also be divided into five stages describing the cycle including the *systolic* and *diastolic* [3].

The first stage, "ventricular filling" is the start of the diastolic state, this is where the semilunar valves (pulmonary valve and the aortic valve) are closed and the atrioventricular (AV) valves (mitral and tricuspid valves) are open, and the heart is relaxed. The second stage, "atrial systole" is when the atrium contracts and pumps blood into the ventricle. The third stage is called the "isovolumic contraction", is the start of the systolic state. This is where the AV and semilunar valves close and ventricles start to contract. There is no change in volume in the ventricles but the pressure increases. The fourth stage is the "ventricular ejection" the semilunar valves open and ventricles are contracting and pumping the blood out in the pulmonary artery and the aorta. During the last and fifth stage, "isovolumic relaxation time", the ventricle starts relaxing and the semilunar valves close due to the higher pressure in the aorta and pulmonary artery than the ventricles.

To sum up the diastolic and systolic commonly refers to the diastolic and systolic stages of the ventricles. This is systolic when the ventricle is contracting and ejecting blood and diastolic when it is filling up.

Figure 2.3 shows the relation between pressure, volume, electrocardiogram (ECG) and heart sounds (Phonocardiogram, PCG) over two heartbeats also showing the different stages. PCG is sound recordings typically from valves closing. The ECG signal will be described later on.

2.1.3 The heart's electrical conduction system

A muscle contraction is initiated by an electrical impulse, an action potential [12]. As the heart is a muscle this is true for the heart as well, but the heart muscle has other important differences from skeletal and smooth muscles.

The cardiac muscle is different from skeletal muscles in that way that it is not controlled

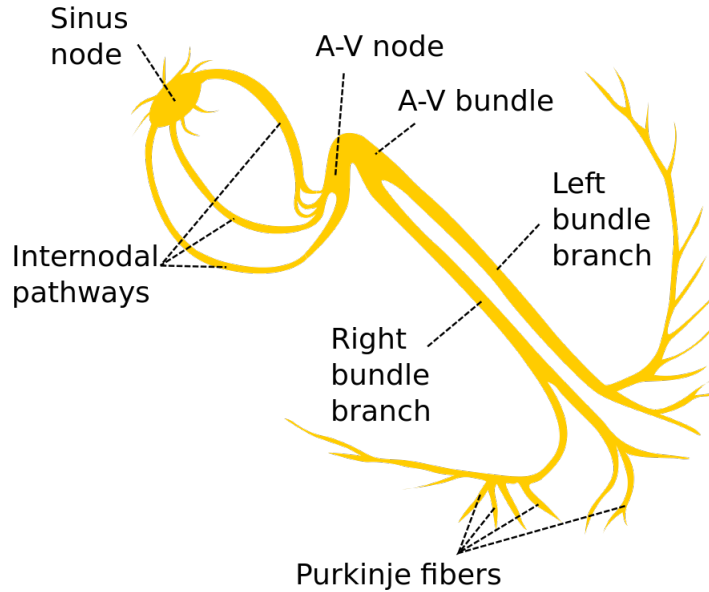


Figure 2.4: Electrical conduction in a heart from [4]

by the somatic nervous system, but by the autonomic nervous system [4]. This means it is not something you could control, but a process that is going on automatically without your attention. The heart muscle always responds with maximum response, given that the electric impulse exceeds the heart muscle's excitation threshold, this is different from many other muscles where there is a relation between the strength of the impulse and the contraction. The cardiac muscle also has the possibility to initiate a contraction, without any external stimulus.

The *sinoatrial node* (SA) commonly called the sinus node, generates the electrical impulse, which eventually makes the heart contract and makes a heartbeat [12]. When the SA node generates an impulse it instantly triggers the atrium to contract. The impulse then travels like a pebble into a pool of water through the atria. After fully contracting the atria the signal is reaching the *atrioventricular node* (AV). The AV node is located in the internal septum, this is what separates the left and right atria of the heart. The atria are electrically isolated from the ventricles, only connected through the AV node. After a delay for allowing the atria to completely empty and filling the ventricles. The electrical signal is then propagating through the bundle of His (AV bundle) and splitting into right and left bundle branch that run along the interventricular septum. This brings the electrical signal to the apex of the heart, this is where the contraction of the ventricles starts. The electrical signal propagates through *Purkinje fibres* and the cardiac muscle very rapidly, this makes the ventricles contract efficiently.

There are several places in the heart that could generate action potentials, but this is at a slower rate than the SA node and would be overridden by the SA node normally because of the higher frequency of SA node. This works as a safety mechanism. The normal rate of the SA node is 60-80 beats per minute (bpm). Other places that could produce action potentials in the heart's conduction system is the AV node with 40-60 bpm. Also the bundle of His and the Purkinje fibres could generate action potentials with 30-40 and 20-30 bpm respectively if not overridden. If any other than the SA node is triggering a contraction this is called an ectopic beat.

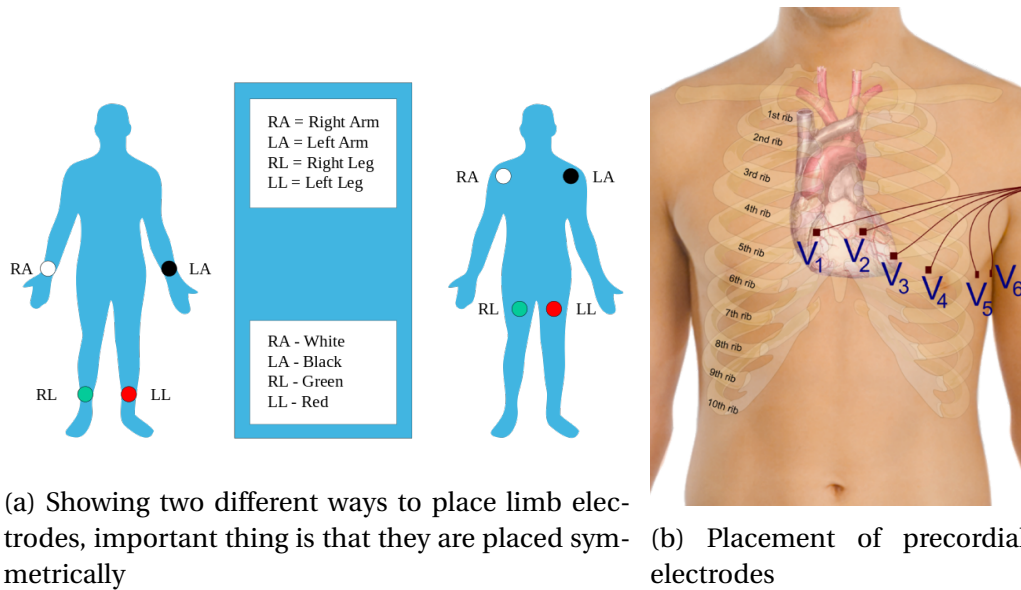


Figure 2.5: Placement for a 12 lead ECG. A 12 lead ECG using only 10 electrodes figures from [5]

Figure 2.4 shows the hearts electrical conduction system [4].

2.2 ECG signal

Electrocardiogram(ECG) is the recording of the electrical activity of the heart [12]. The ECG recording is very helpful as being a non invasive measurement of the heart activity. The recordings is done only using electrodes placed on the skin.

The recoding of ECG is done by electrodes placed on the skin, but it necessary with two or more electrodes to have one as reference. The electrodes is divided into two groups the limb (figure 2.5a) and precordial (figure 2.5b) electrodes these could be placed as shown in figure 2.5.

A *lead* in ECG could be seen as a measurement of electrical potential in a certain angle this is what gives a signal. There are two types of leads; bipolar and unipolar leads. Bipolar leads is the measurement of the electrical potential between two electrodes, usually between the lime electrodes. The unipolar leads are then a measurement between an electrode and an group of others making a common lead, usually the Wilson's central terminal which will be described below.

The Wilson's central terminal V_w is produced from the three limb electrodes RA, LA and LL this gives an average potential across the body [12], [5].

$$V_w = \frac{1}{3}(RA + La + LL) \quad (2.1)$$

Lead I, II and III are bipolar leads, these leads are also called limb leads, this is because the are coming from the the limb electrodes.

- Lead I, is the lead between the left arm and the right arm, with the left arm as the positive.

$$I = LA - RA \quad (2.2)$$

Table 2.1: Electrode names and placement for 12 lead ECG

Electrode name	Electrode placement
RA	Right arm
LA	Left arm
RL	Right leg
LL	Left leg
V_1	In the fourth intercostal space(between ribs 4 and 5) just to the right of the sternum
V_2	In the fourth intercostal space(between ribs 4 and 5) just to the left of the sternum
V_3	Between V_2 and V_4
V_4	In the fifth intercostal space(between ribs 5 and 6) in the mid-clavicular line
V_5	Horizontally even with V_4 in the left anterior axillary line
V_6	Horizontally even with V_4 and V_5 in the midaxillary line

- Lead II, is the lead between the left leg and the right arm, with the left leg as the positive.

$$II = LL - RA \quad (2.3)$$

- Lead III, is the lead between the left leg and the left arm, with the left leg as the positive.

$$III = LL - LA \quad (2.4)$$

There is also three other leads generated from the limb electrodes, this is the augmented limb leads, aVR, aVL and aVF. These leads is unipolar as there references is from multiple leads.

$$aVR = RA - \frac{1}{2}(LA + LL) = \frac{3}{2}(RA - V_w) \quad (2.5)$$

$$aVL = LA - \frac{1}{2}(RA + LL) = \frac{3}{2}(LA - V_w) \quad (2.6)$$

$$aVF = LL - \frac{1}{2}(RA + LA) = \frac{3}{2}(LL - V_w) \quad (2.7)$$

The precordial leads are generated from the precordial electrodes and they all are having the Wilson's central terminal as their reference(negative pole). This makes the precordial leads unipolar.

An illustration of the limb leads and the augmented limb leads could be seen in figure 2.6.

To understand the ECG signal it is important to know what it represents. There is four main points:

- depolarization of the heart toward the positive electrode produces a positive fluctuation.
- depolarization of the heart away from the positive electrode produces a negative fluctuations.
- repolarization of the heart toward the positive electrode produces a negative fluctuations.

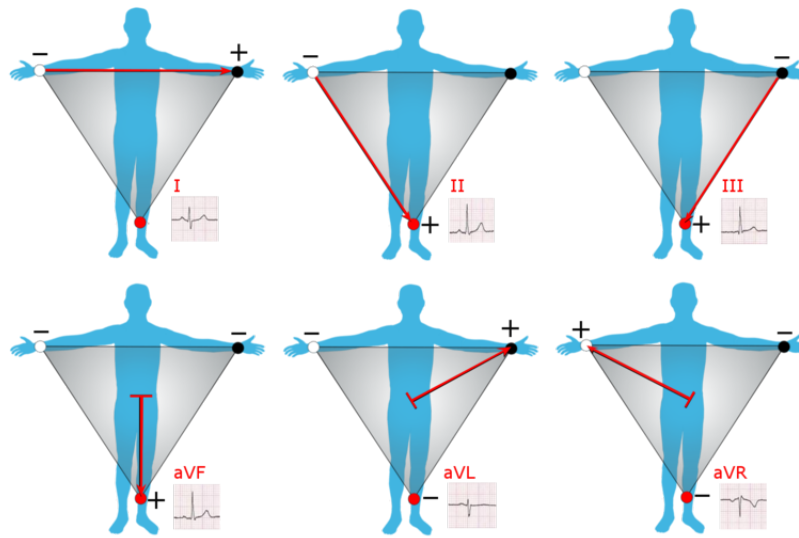


Figure 2.6: Limb leads and augmented limb leads, captured from [5]

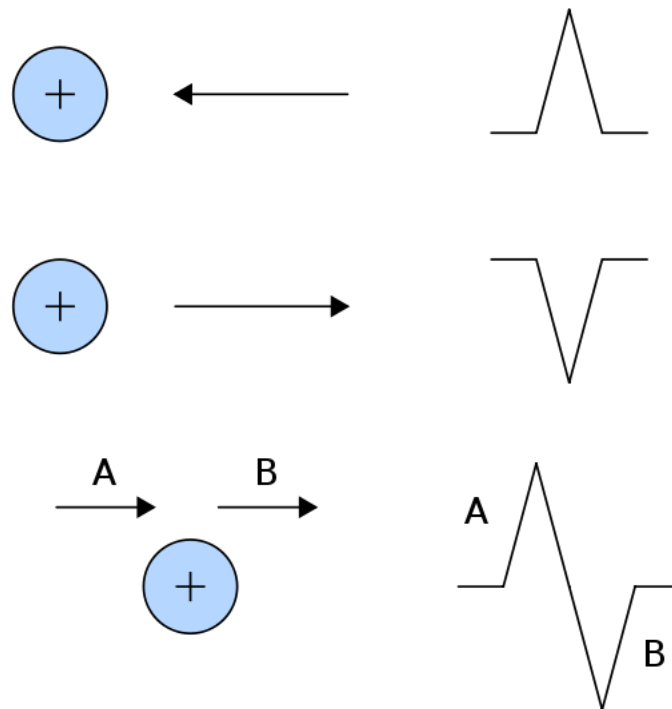


Figure 2.7: Illustration of recorded signal by an electrode, captured from [5]

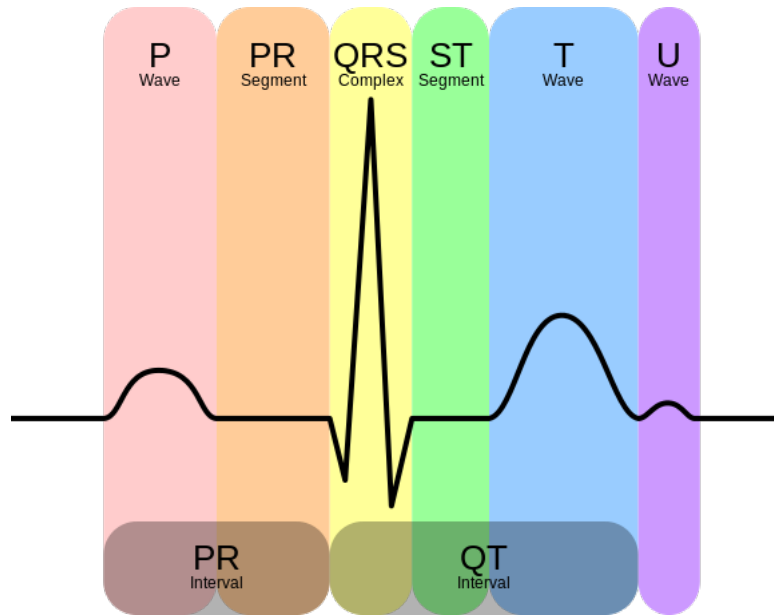


Figure 2.8: Typical ECG waveform from a healthy person, captured from [5]

- repolarization of the heart away from the negative electrode produces a positive fluctuations.

The ECG complex is a very characteristic signal. The waveform from a healthy heart is shown in figure 2.8.

Three major waves appear in the normal ECG signal, each one showing different part of the heartbeat. The first wave is called the P wave, this shows the electric activity of atria. Then follows the QRS complex, which is the largest wave. The QRS complex shows the electric activity of the ventricles. The third wave is the T wave shows the hearts relaxation phase.

- The P wave represents atrial depolarization
- The QRS complex represents ventricular depolarization
- The T wave represents ventricular repolarization

In some cases a fourth wave could be visible, the U wave. The U wave represents the repolarization of the papillary muscles.

2.2.1 Noise sources in ECG

In the ECG signal as any other real signal it is common with some noise or artifacts. These ECG artifacts could be divided in two groups, Physiologic noise sources and External noises. A short list of these artifacts or sources of noise follows[12][13]:

Physiological noise sources

Muscular activity, the muscles is as the heart triggered by electric impulses. Muscle activity close to an electrode could damage the signal. EMG usually has frequency content in the range 50-500 Hz [12].

Movement of electrodes, If the electrodes is not properly fixed or the patient moves it will give a motion artifact.

External noise

Power supply, in Europe this mains component is 50Hz.

Electronic noise, this is usually a high frequency component introduced by the acquisition equipment itself.

2.3 Blood Pressure

Blood pressure(BP) is the pressure exerted by the circulating blood upon the walls of blood vessels [14]. The blood pressure is one of the vital signs of the body, commonly it refers to arterial blood pressure.

The blood pressure is a direct response from the pumping action of the heart. This means that the blood pressure will vary with the different phases of the heart beat. This gives the systolic and diastolic pressure, which is the normal way to present the blood pressure. The systolic pressure corresponds to the pumping(systole) phase of the heart and the diastolic pressure corresponds to the filling(diastole) phase of the heart. The mean pressure is affected by the blood pressure and resistance of the blood vessels.

The pressure is the cardiac output(Q) times the peripheral resistance(R). Cardiac output is then again stroke volume(SV) times heart rate(HR). These process are complex and driven by the autonomous nervous system to control the blood pressure [14] [3].

$$\begin{aligned}\Delta P &= Q \times R \\ Q &= SV \times HR\end{aligned}\tag{2.8}$$

The cardiac output is the blood flow out of the heart, this is depending on how much blood being in the heart chambers(volume) times how often this is pumped out. Average cardiac output for a human is 4.0-8.0 L/min depending on the person[15].

The peripheral resistance also known as the systemic vascular resistance(SVR) is the resistance that must be overcome to push blood through the circulatory system [16]. Vasconstriction, i.e constriction in blood vessels increases SVR and opposite vasodilation increases the diameter of the vessels and decreases the SVR. This is also controlled by the autonomous nervous system and a way of controlling the blood pressure.

The recording of blood pressure is done by cannula in a chosen blood vessel, the cannula is then connected to a infusion tubing set. This is often filled with sodium chloride. This liquid is in contact with a diaphragm that moves in response to the transmitted pressure waveform. The movement is then converted to an electrical signal by a transducer [17].

The invasive blood pressure technique is very robust against noise, but some equipment need calibration to get correct values. This would though not distort the frequencies in the

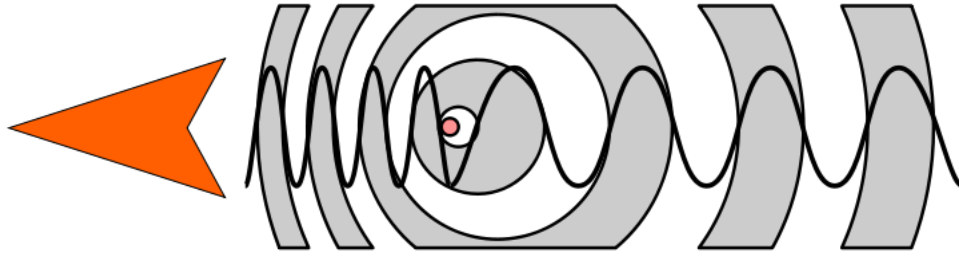


Figure 2.9: Change in frequency due to a moving source, from [6]

signal. A important thing is that the transducer have to be kept at a horizontally level with the heart, raising or lowering the transducer relative to the patients heart will alter the signal.

2.4 Laser Doppler flowmetry

Laser doppler flowmetry(LDF) is a noninvasive technique for continuous measuring microcirculatory blood flow [18]. As the names says LDF is using the the principle discovered by Christian Doppler, i.e. that sound waves from a moving source would increase in frequency as the source moves toward the observer and decrease as the source moves away from the observer[6].

The signal is obtained by sending a monochromatic coherent laser light towards the area of interest, the laser light is shifted in frequency when it is scattered by an moving object. This means when the laser light are scattered of the blood cells flowing in a vessel it is shifted according to the speed of the cells. The relationship between the velocity and observed frequency is shown in eq. 2.9.

$$\Delta f = \frac{2\Delta v}{c} f_0 \quad (2.9)$$

In eq. 2.9 $\Delta f = f - f_0$ and $\Delta v = v_r - v_s$. f is received frequency and f_0 is transmitted frequency, v_r is the velocity of the receiver relative to the medium and v_s is the velocity to the source relative to the medium. The equation is multiplied with 2 because the incident wave is affect as well as the wave reflected back to the probe [6].

The advantage with LDF is that you could measure the blood flow in the microcirculation. The strength of the technique is to continuously looking at at changes in blood flow.

A problem with the LDF technique is it's sensitivity for motion artifacts [19]. Motion artifacts will give a huge doppler shift and gives huge spikes in the signal. This motion artifact makes it hard collecting a long noise free signals from patients which are awake.

2.5 Heart rate and HRV

The heart rate is the rate of how often the heart beats, this is often measured in beats per minute(bpm). The heart is controlled by the the autonomous nervous system to change as the body's need of oxygen changes [20] [21].

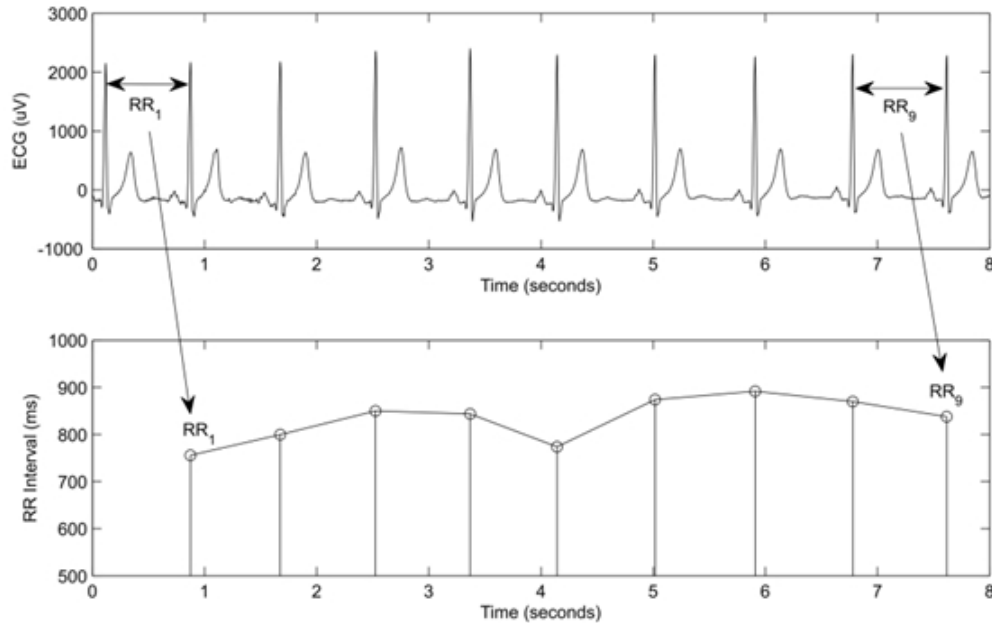


Figure 2.10: The upper plot shows the ECG signal and how the R-R interval is extracted, the lower plot shows the R-R intervals, from [7]

The heart rate could be extracted from several signals, by measuring the instant an event occurs. The easiest way for measuring the heart rate is using the ECG signal and measuring the time between one R wave and the next. This is called for the R-R interval, i.e. time interval between two subsequent R peaks[13]. The HR is calculated from the R-R interval, by taking one over the R-R interval the heart frequency is found as described in eq. 2.10

$$\Delta HR = \frac{1}{R - R \text{ interval} [\text{sec}]} \quad (2.10)$$

The Heart rate variability is the signal composed of the all the R-R intervals[22]. It is an interesting signal as it shows that the heart rate changes slightly from beat to beat, even during similar conditions.

There are several reasons for change in HR from [21]:

1. Respiratory Sinus Arrhythmia (RSA) mediated by respiration is responsible for changes of the heart-rate in 2-5 seconds intervals and is controlled by parasympathetic activity. The sympathetic system is too slow to influence this frequency band
2. Blood pressure regulation contributes to HRV in 10 second rhythms
3. Changes with a periodic length above 20 seconds are mediated by the sympathetic system
4. Changes in the range of minutes and hours are influenced by the neurohumoral oscillations in the circulating blood, by circadian rhythms or rapid eye movement phases during sleep

2.6 Analysis methods

In this section some methods for analysis of biomedical signals will be described. Starting with some frequency analysis methods and then describing a time domain analysis named Poincaré analysis.

2.6.1 Frequency analysis

Any signal that varies over time has a corresponding frequency spectrum [23]. Viewing these signals in the frequency domain certain aspects not seen in the time domain and the underlying reasons producing the signal might be revealed.

To convert a signal from time domain to frequency domain a mathematical transform is applied, this could be a Fourier transform. By using the inverse transform the original time domain signal could be obtained.

The frequency spectrum could shows which frequencies that are prominent and important for keeping the general shape of the signal. This makes the it a very useful tool for finding frequencies that is not suppose to be in the signal or maybe are redundant. By knowing this it is possible to design filters to remove these frequencies.

Fourier

The Fourier transform(FT) is used to transform a signal from time domain to frequency domain[24], seen in equation 2.11. The FT decomposes the signal in to the frequencies that make it up using a complex sinusoid. The inverse Fourier transforms converts the signal back to time domain(2.12).

$$G(\omega) = \int_{-\infty}^{\infty} g(x) e^{-i\omega x} dx \quad (2.11)$$

$$\omega = 2\pi f$$

$$g(x) = \int_{-\infty}^{\infty} G(\omega) e^{i\omega x} d\omega \quad (2.12)$$

As found out by Parseval the energy is preserved in the Fourier transform[25]. This is shown in Parsevals theorem in equation 2.13.

$$\int_{-\infty}^{\infty} |g(x)|^2 dx = \int_{-\infty}^{\infty} |G(\omega)|^2 d\omega \quad (2.13)$$

Fast Fourier Transform

The Fast Fourier Transform(FFT) is a algorithm that computes the discreet Fourier transform or the the inverse transform of a sequence[26]. As the original DFT has a complexity of $O(n^2)$, the FFT algorithm has a complexity of $O(n \log(n))$, where n is the data size. This gives a much faster computation of the Fourier transform.

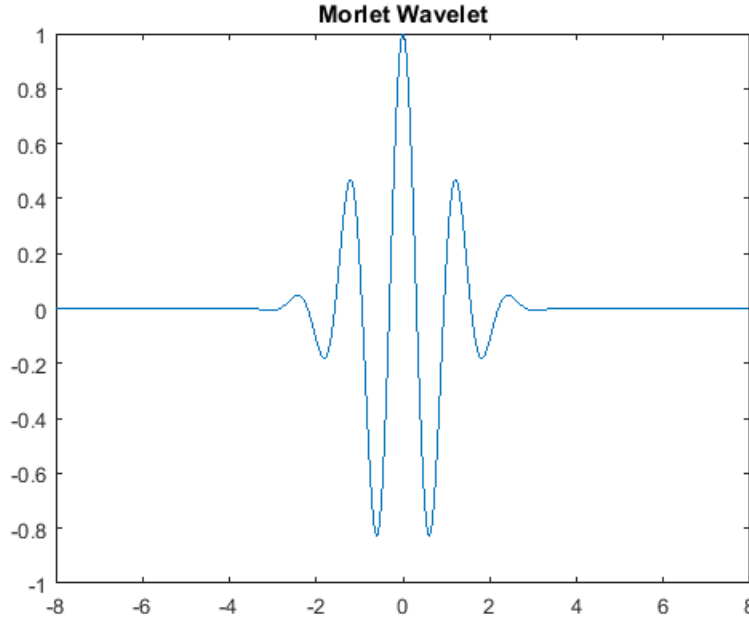


Figure 2.11: Continuous wavelet, Morlet

Wavelet

A wavelet is a short wave-like oscillation that starts at zero, has some oscillation and goes back to zero. An example of a continuous wavelet is shown in figure 2.11.

The continuous wavelet transform(CWT) differ from the Fourier transform in that way that is using any chosen wavelet as basis function instead of the sinusoid [12]. It does not relate to frequency in the same way. By warping the time axis "t" allows us to obtain the harmonics from the original signal. By replacing the time axis with a multiple n of the time axis produces the n -th harmonic. This is essentially scaling the signal. By doing this "scaling" with the basis function or the wavelet it would produce a new version of the wavelet. A scaling of a Mother wavelet(the original wavelet) is often called a child wavelet. The claim is that the main characteristics of harmonic frequencies can be drawn from a more general concept called a "scale" [27]. The interesting part is that unlike frequency that only is defined for periodic signals, a scale works equally fine for a non periodic signal. A relation between a scale and a pseudo-frequency exist and is shown in equation 2.14. This relation is based on the center frequency of the wavelet, F_c . The idea is to associate a given wavelet with purly periodic signal with frequency, F_c [28]. The frequency maximizing the FFT of the wavelet modulus is F_c .

$$F_a = \frac{F_c}{a \times \Delta} \quad (2.14)$$

where

- Δ is the sampling period
- F_c is the center frequency

- F_a is the pseudo-frequency corresponding to the scale a

The continuous wavelet transform could then be seen in the equation 2.15.

$$W_{\Psi,x}(a,b) = \frac{1}{\sqrt{|a|}} \int_{-\infty}^{\infty} x(t) \Psi^*\left(\frac{t-b}{a}\right) dt, \quad a \neq 0 \quad (2.15)$$

In the continuous wavelet transform equation 2.15 the $\Psi(t)$ is the mother wavelet function, b is the shifting parameter and a is the scaling parameter (replacing the frequency). $\Psi\left(\frac{t-b}{a}\right)$ is a shifted and scaled version of the mother wavelet called often called a child wavelet. Just like the Fourier transform the CWT also has an inverse transform for returning back to time domain. The inverse continuous wavelet transform is seen in equation 2.16.

$$x(t) = \frac{C_{\Psi}^{-1}}{a^2} \int_{-\infty}^{\infty} \int_{-\infty}^{\infty} W_{\Psi,x}(a,b) \Psi\left(\frac{t-b}{a}\right) da db, \quad a \neq 0 \quad (2.16)$$

In the inverse transform the C_{Ψ}^{-1} is a constant depending on the choice of mother wavelet.

As choosing different mother wavelet gives a unique CWT, there is an infinite number of transformations that all are called CWT. This makes CWT suitable for a variety of tasks.

To choose the right mother wavelet is difficult and there is no right answer, but there are two rules of thumb[12]:

1. Complex signals need complex mother wavelets
2. The mother wavelet that resembles the general shape of the signal to be analyzed

2.6.2 Poincarè analysis

An Poincare analysis is based on a Poincare plot. The Poincare plot is a plot which is used to quantify self similarity in a process. A Poincare plot is also known as return map. The plot is a graph where each samples is plotted against the next. If there is a time series $x_t, x_{t+1}, x_{t+2}, \dots$, the process is plotted as $(x_t, x_{t+1}), (x_{t+1}, x_{t+2}), (x_{t+2}, x_{t+3}), \dots$. This gives a plot that varies around a line of identity, this is where the samples have similar value ($x_t = x_{t+1}$).

Poincare plots are helpful to visually analyse the process[29]. The normal way of quantitatively analysing a Poincare plot is using an ellipse fitting technique. This technique entails fitting an ellipse to the plot with the center coinciding with the center point of the process ((x_{avg}, x_{avg})). The line defined as axis 2 describes the slope of the longitudinal axis, while axis 1 defines the transverse slope, which is perpendicular in direction to axis 2. Axis 2 has the same direction as the line of identity. The length of the axis making the ellipse is defined by the standard deviation in the direction of the axis, this gives the variables SD1 and SD2, as seen in figure 2.12. SD2 gives the continuous long-term variability of the process. SD1 gives the sample to sample variations of the data, this is short-term variability. It is common to use the ratio $SDR = SD1/SD2$ to relate to only one variable.

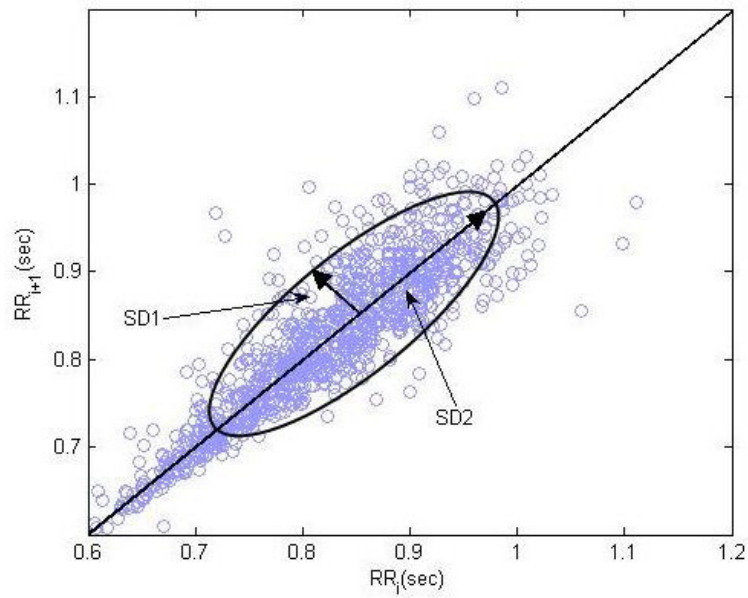


Figure 2.12: Poincaré plot showing the fitted ellipse and the variables SD1 and SD2, figure from [8]

Chapter 3

Methods and Implementation

This chapter will describe what's been done in this thesis and describe how it has been done. It will start with how the signals are collected, it will then go on to how the signals look and how to process them. Thereafter a description on how the application for the signal analysis was done.

Some results will be shown and discussed for the different parts as further work is dependent on these results.

3.1 Signal acquisition

Every patient is monitored in approximately one hour before surgery, they are then brought to surgery and some kind of cardiac innervation is performed. After surgery the patient is monitored all the time to the next morning. The first period after surgery the patient is connected to the ventilator. The signals recorded is the ECG, invasive Blood Pressure(BP) and Laser Doppler flow(LDF). These signals are collected by the medical students Bjørn Gardsjord Lio and Fredrik Axelsson supervised by their supervisor and anesthesiologist Nils Kristian Skjærvold. A description of how these signals are acquired will follow.

Hardware used in the signal acquisition is from ADInstruments.

- PowerLab 16/35 DAQ
- Blood FlowMeter, LDF input
 - LDF probe, MNP100XP
- BP Amp
 - Disposable BP transducer, MLT0670
 - Cable from transducer to BP Amp, MLAC05
- Bio Amp, used for ECG recordings
 - Bio amp cable, MLA2340

All the equipment is connected to the PowerLab and each signal has their own amplifier as described in the list above. The PowerLab is connected to a computer where ADInstruments software, LabChart has been used to view and export the signals to MatLab files. All the signals is recorded with a sampling frequency of 400Hz. This was chosen as appropriate after testing some different sampling frequencies as high as 1000Hz and as low as 200Hz. 400 Hz is way higher than needed for looking at the low frequency's in this thesis, but where chosen to keep the original form of the signal if the recorded signal was going to be used in any other study.

3.1.1 ECG recordings

The ECG recordings are done with 3 electrodes, where one electrode is placed on each shoulder and one at the left hip, this is the limb electrodes as described earlier. The extracted signal is from lead II.

3.1.2 Blood pressure recordings

An anesthesiologist is inserting an arterial cannula in a artery in the wrist(usually the radial artery). The cannula is connected to a infusion set which again is connected to the BP amplifier from AdInstruments. To do the Blood pressure recordings in LabChart the system have to be calibrated by opening a valve on the transducer, this calibrates the pressure against the atmospheric pressure.

3.1.3 Laser Doppler Flow

The Laser Doppler Flow probe register cutaneous perfusion and could be placed any place on the body. In this case the probe is connected to the calf of the patient. This is chosen as place most likely to get the least noise from motion artifacts. The probe is then connected straight to the Blood FlowMeter amplifier.

3.2 Noise analysis

To study the noise and artifacts seen in the signal, some which is know from the theory it was made a program to investigated these noises and try to remove them in any manner.

3.2.1 ECG

As there was seen some motion artifacts and some high frequency noise when inspecting the signals it was decided to look closer into this. An example of these noises is shown in figure 3.1, this shows the same patient in different time segments. The high frequency's oscillations where not that important as the scope of the thesis was to look at the low frequency oscillations(2Hz and lower), but was just briefly looked at.

To find the noise sources there where done some frequency analysis using FFT and spectrogram's showing the time frequency relation.

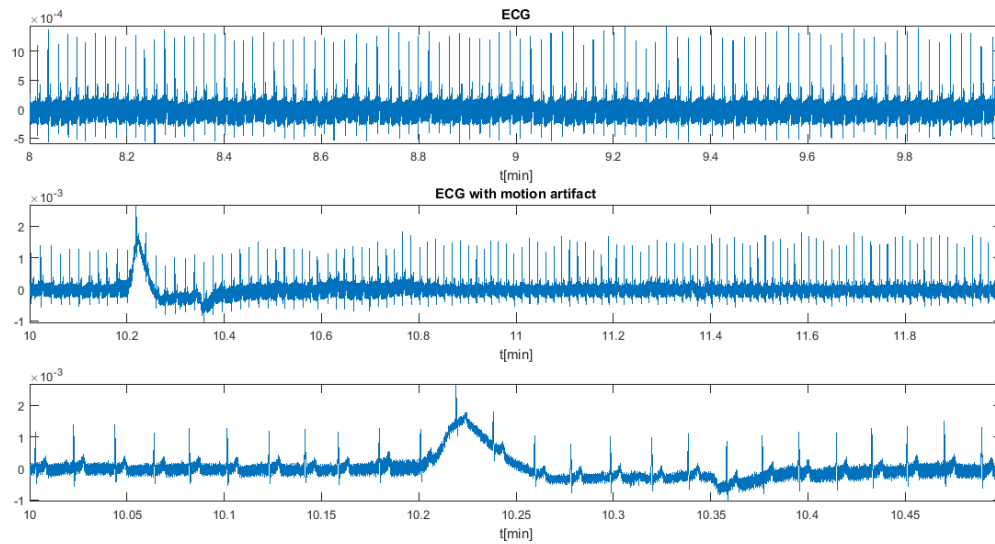


Figure 3.1: A raw ECG signal where the upper one showing a period without any motion artifact and the two lower plots show the same motion artifact

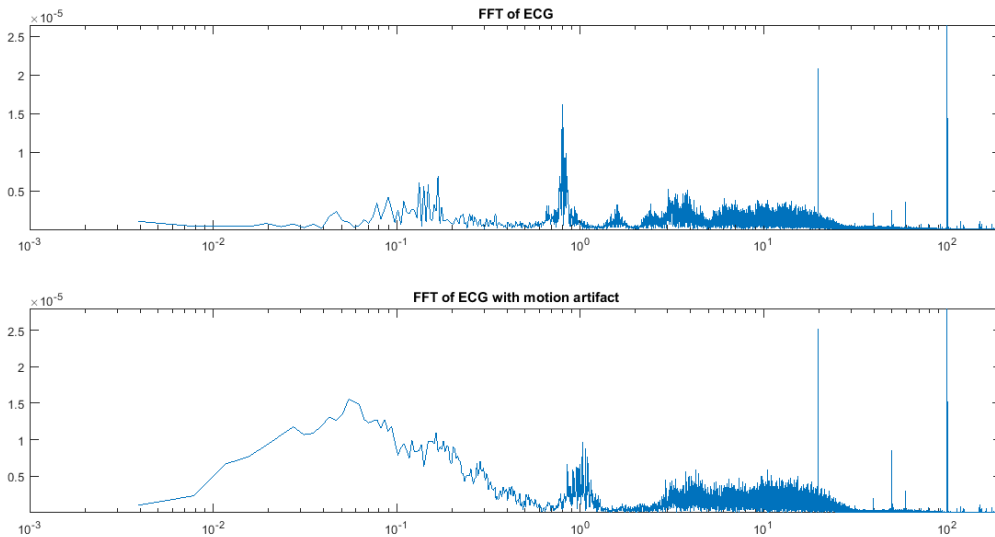


Figure 3.2: Showing the frequency spectrum of ECG signal where the upper one showing a period without any motion artifact and the lower plot shows with motion artifact

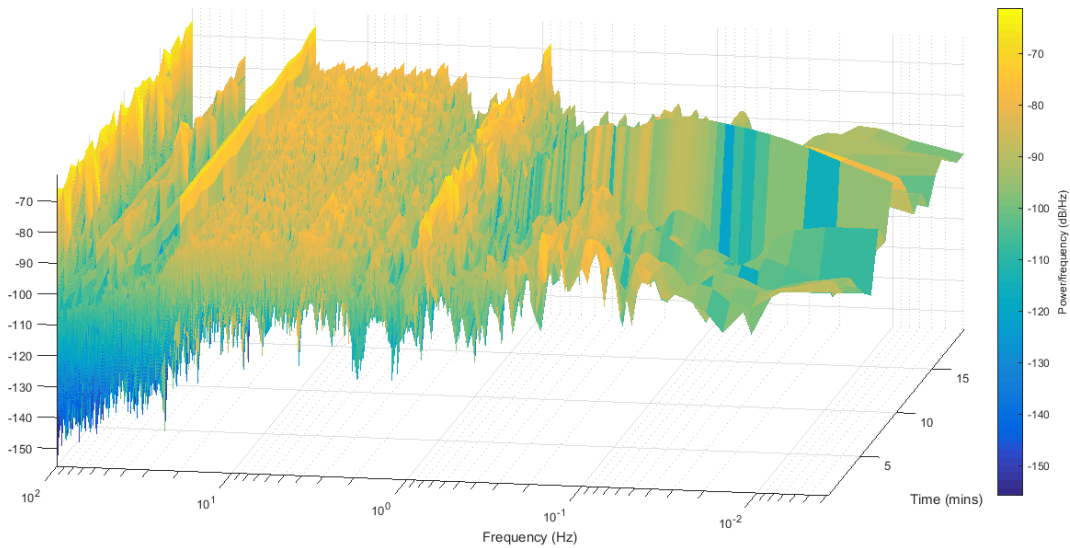


Figure 3.3: Showing the time-frequency spectrum of ECG signal

By inspecting the FFT without the motion artifact it was seen that there were some very distinct peaks around the frequencies 20Hz, something around 50Hz and 100Hz. The 50Hz component is known as the mains frequency. The 100 Hz component could be a harmonic, but should then have a lower power than the 50Hz component.

After looking at a spectrogram and seeing how stationary the higher frequency noises were, it was concluded that it most likely is coming from internal or other external sources in the room. As mentioned earlier this is not that important as the interesting thing in this thesis is the low frequencies. It was therefore decided not to do any filtering of these frequencies. If a low-pass filter could be applied to remove this noise [13].

The FFT of the time segment with the motion artifact shows a clear increase of frequencies in the low frequency range compared to the FFT of the segment without the motion artifact. It is also spread out over a great range of frequencies, this makes it harder to remove without distorting the signal of interest.

To remove unwanted frequencies and motion artifacts there were looked at two methods; filtering [13] and trend removal.

- **Filtering**, there were tested different types of filter for removing two types of noise:
 - **Motion artifact**, looks like quick variations in baseline with an exponential decay. This could be removed with a high-pass filter.
 - **High frequency noise**, such as from the power supply and the acquisition hardware itself, which could be removed with a low-pass filter.
- **Trend removal**, it was tried to fit a low order polynomial to a segment of motion artifact and subtract it from the original signal.

Filtering of the signal is effective for removing specific frequencies or frequency bands from the time signal. As the motion artifacts distort the interesting low frequency band it was de-

decided that it was not wise to filter the entire signal as this would also remove the interesting part of the signal. The idea was to only filter the part in time domain that is affected by the motion artifact. There was chosen a high pass FIR filter with start cutoff at 0.7Hz and start stopband at 0.5Hz. This gives the result shown in figure 3.4.

The time domain results from figure 3.4 is quite good, the problem is that the frequency domain is completely distorted in the interesting region.

An other idea was to fit a low order polynomial to the time region of the motion artifact, subtract this polynomial from the curve and add a constant to the hopefully artifact free signal to get it back to baseline.

By inspection it looked like a 10th order polynomial was a good fit for removing the motion artifact.

The method of subtracting a low order polynomial fitted to the motion artifact, looks in time domain to work well as seen in figure 3.5a. In frequency domain it has clearly also removed some of the low frequencies, the problem is to know if this is a true representation or an adequately good representation. Time and frequency plots of the motion artifact signal are shown in figure 3.5

Problem with these techniques are that there had to be developed an algorithm for detecting a motion artifact and decide where to start the wanted technique for removing the artifact. Since these techniques distorts the interesting low frequencies it is not advantageous to do this over the entire signal. This algorithm was never started on as it was decided in collaboration with other parties to the project that we were going to try to use only time segments mostly without these artifacts in the further work.

3.2.2 Laser Doppler Flow

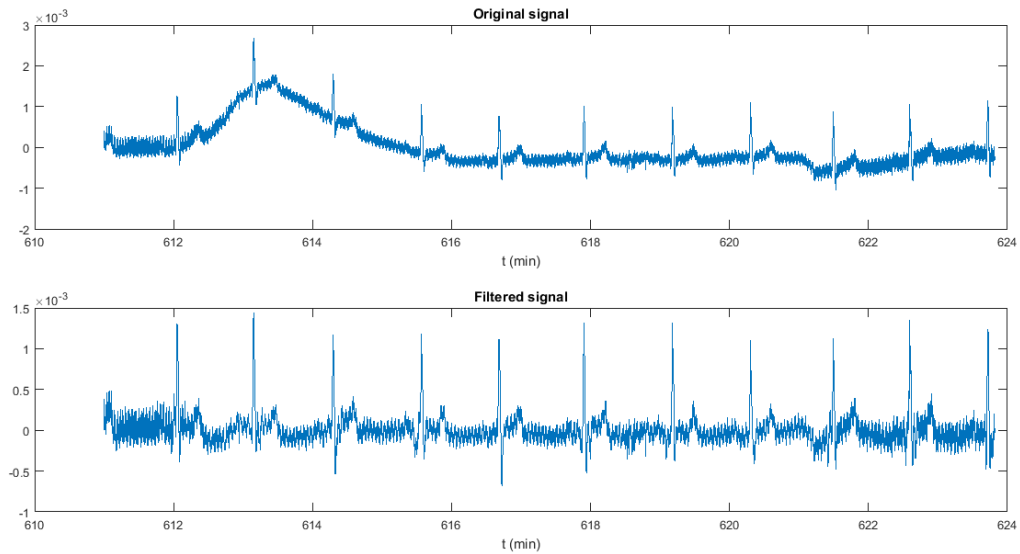
As mentioned in the theory part the laser doppler flow signal is very prone to motion artifacts. These artifacts looks like high spikes in the signal as shown in figure 3.6. These artifacts are easy to recognize as they are much greater than the rest of the signal. To find out how to remove these artifacts there were done some frequency analysis as seen in figure 3.7

As seen in figure 3.7b the motion artifact is composed by many low frequency components. This gives the same challenge as for the ECG signal, i.e. the noise and the interesting information is in the same frequency band. This makes it difficult to remove without losing or distorting valuable information.

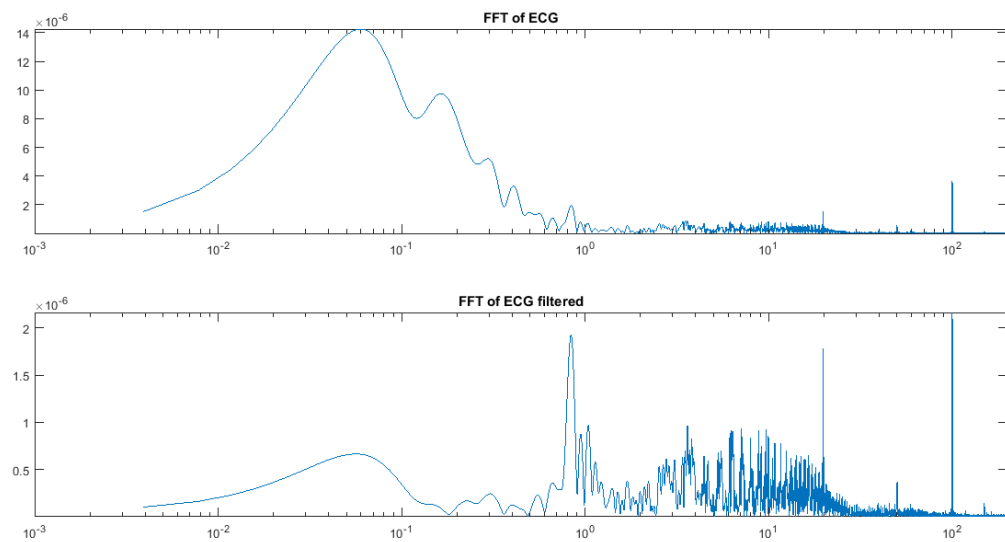
Applying a filter was tested but without success. This has the same disadvantages as all ready discussed, as it would remove or distort the valuable low frequency information.

An idea came since the noise is so much greater than the signal it should be easy to detect and then just replace with something appropriate.

For detecting the outliers this was done in two ways; one adaptive and one hard threshold. The adaptive threshold algorithm was chosen as three times of the standard deviation from the median of a 10000 samples window of the signal for every sample of the signal. If a sample was greater than the outlier threshold it was replaced with the median of the corresponding window. The results from the adaptive threshold is shown in figure 3.8. Problem with the adaptive threshold is that it adapts to the noise as well. This was tried to avoid by having a fairly large window size.

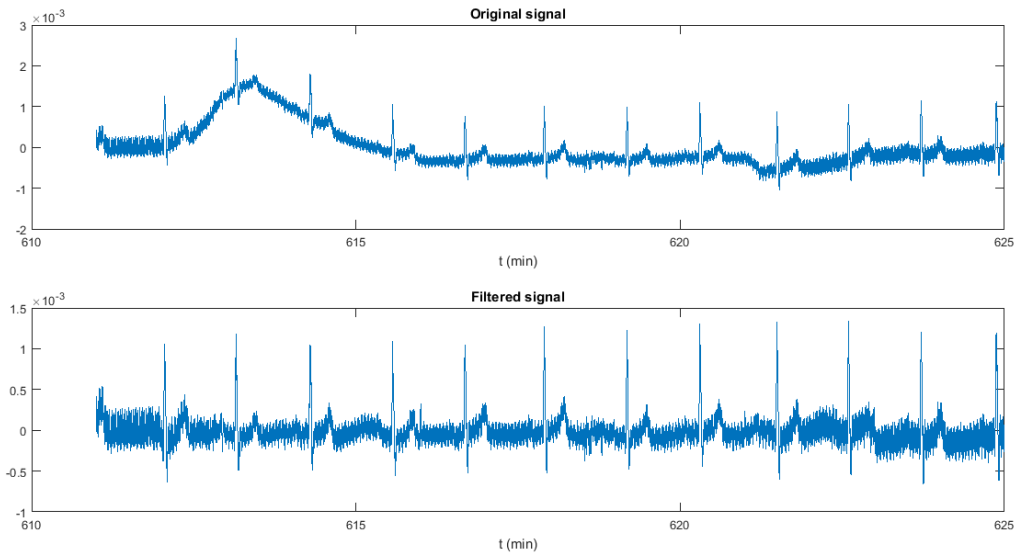


(a) Time domain

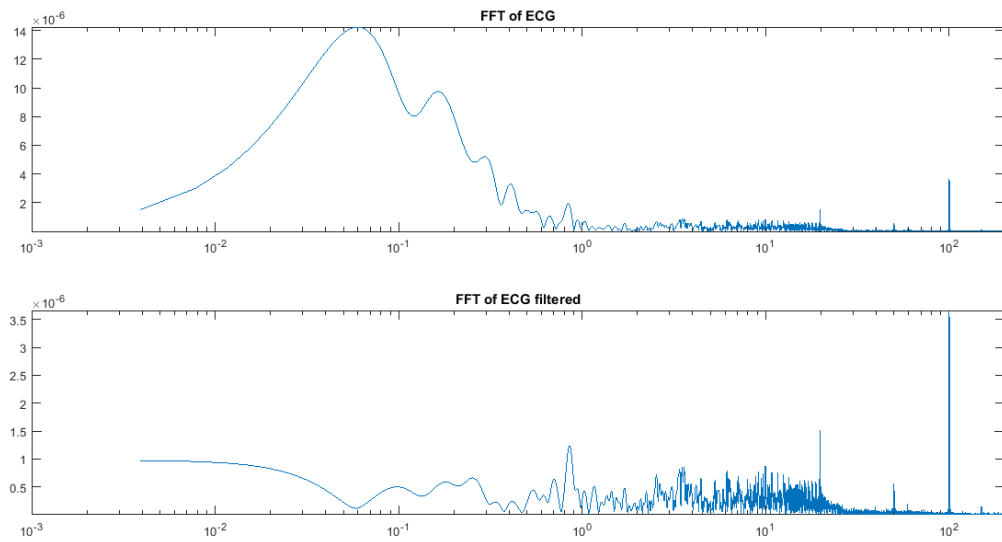


(b) Frequency domain

Figure 3.4: Top plot's shows original signal with motion artifact, lower plots show the original signals filtered.



(a) Time domain



(b) Frequency domain

Figure 3.5: Top plot's shows original signal with motion artifact, lower plots show the original signal after removing the motion artifact using the polyfit technique.

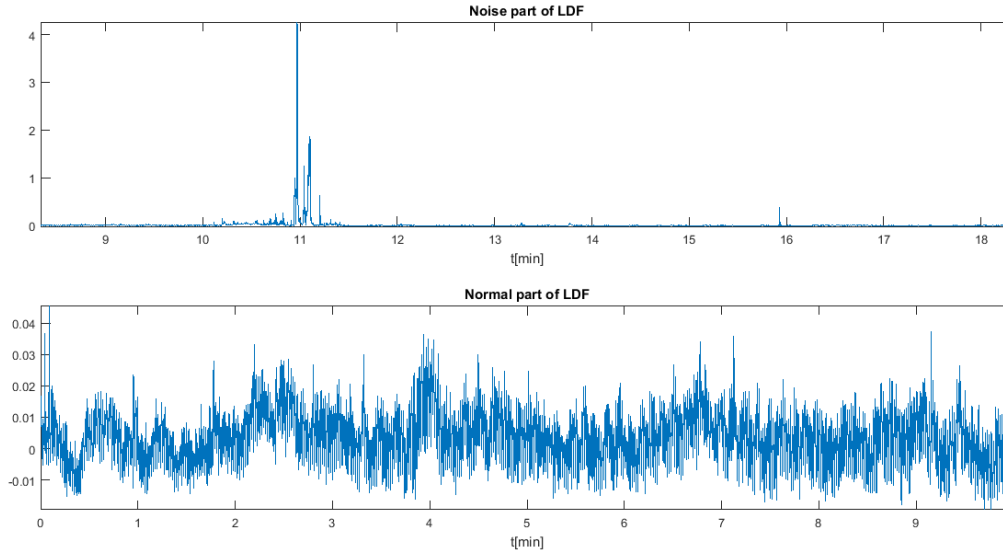


Figure 3.6: Upper plot shows a noisy part of a LDF signal the lower plot shows a noise free LDF signal, , both are from the same patient with some overlap at 8-10min.

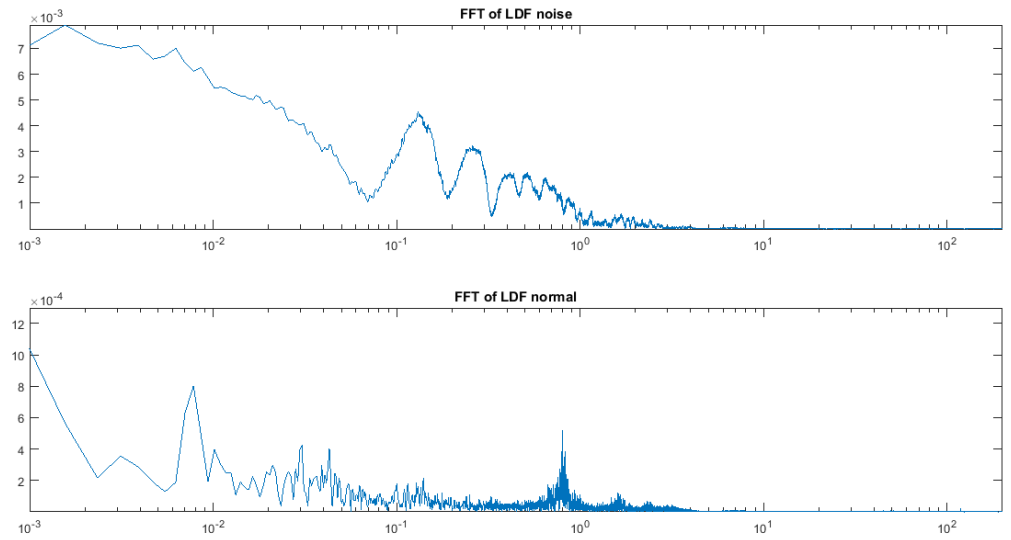
The problem with the adaptive threshold gave the idea for a much easier solution just to have one hard threshold defined from a noise free signal segment. This threshold was chosen as four times the standard deviation from the mean, this was to be safe not to remove more than the noise. The outliers was then replaced with the mean from the a window of 500 samples around the actual sample. Results from hard threshold testing could be seen in figure 3.10 and 3.11.

The problem with these outlier techniques is what to replace the outlier value with. What ever you put in instead of the outlier value is not the correct value and will give a change in the frequency spectrum. By looking at the spectrum's in figure 3.12 it is clearly that is actually might have been useful to use on of these techniques as there is possible to distinguish the known to be present heart rate peak at around 1 Hz in the spectrum's after removing the outliers. It is also worth noticing how much more similar the spectrum after removing the outliers are to the noise free spectrum shown in figure 3.7a.

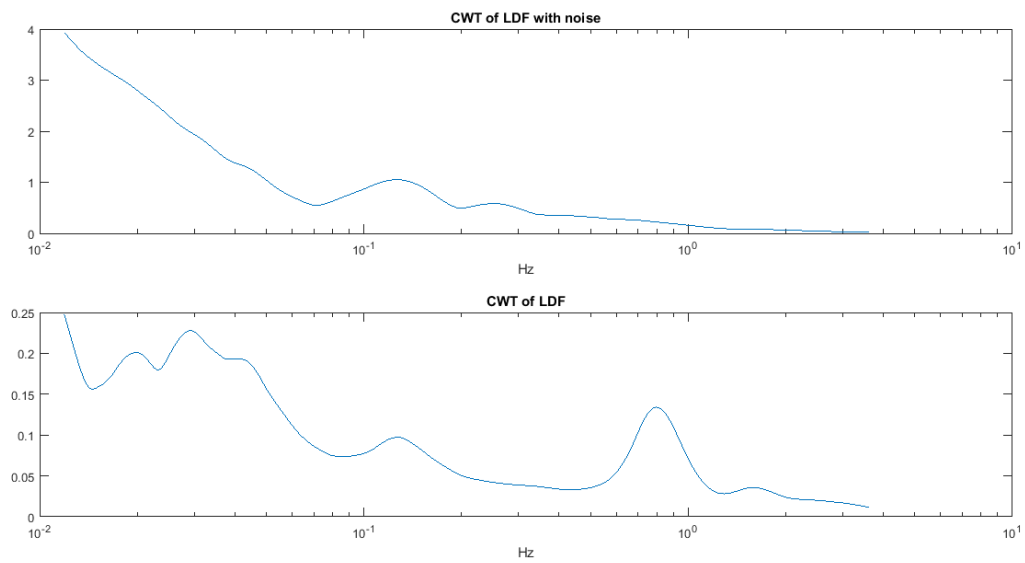
It was decided in collaboration with other parties of the project to try to avoid these artifacts in best possible way when choosing time segments for analysis later on. This way there would be no introduced samples in the signal that might give false information.

3.2.3 Blood Pressure

The blood pressure signal is very robust to noise. There is a possibility of getting wrong pressure values if the calibrations was not done or not done correctly. This would not affect the frequency's but might affect the power of the frequency's.



(a) FFT



(b) Continuous Wavelet analysis

Figure 3.7: Frequency analysis of the laser doppler flow signal from FFT and CWT. Top plot's is of the noisy LDF and bottom is of the normal LDF

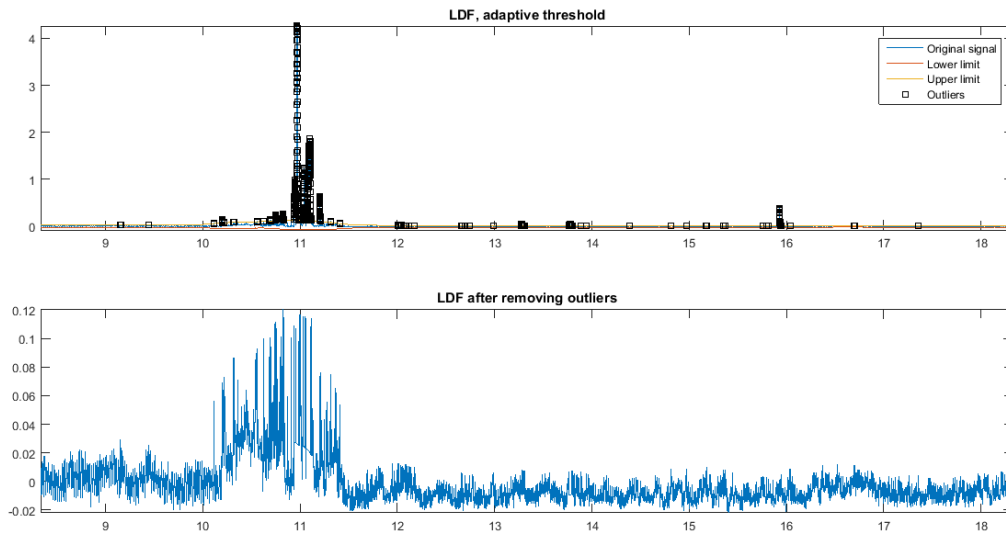


Figure 3.8: Using the LDF signal with motion artifact from figure 3.6, the black boxes shows the outliers and the red and orange lines shows the thresholds

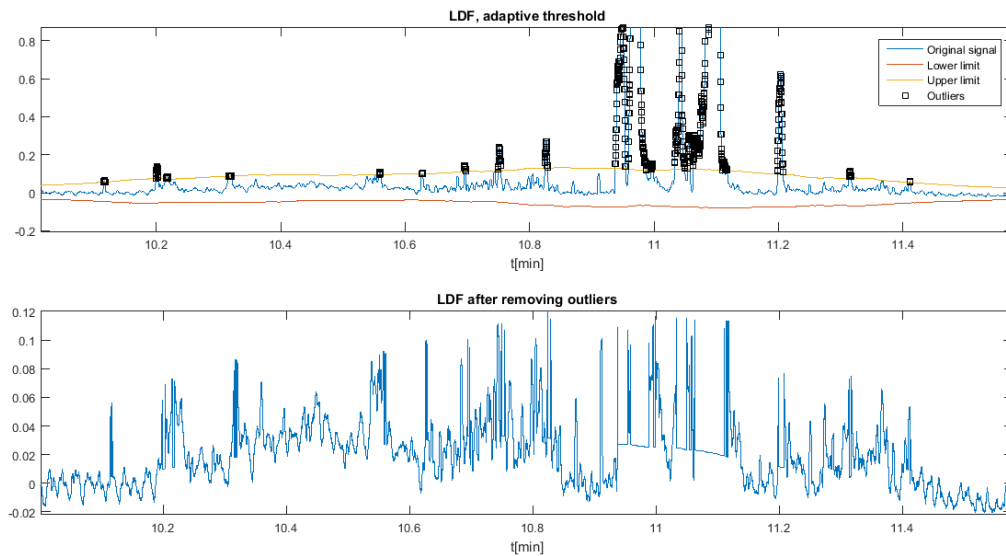


Figure 3.9: Using the LDF signal with motion artifact from figure 3.6, zoomed into a segment, the black boxes shows the outliers and the red and orange lines shows the thresholds

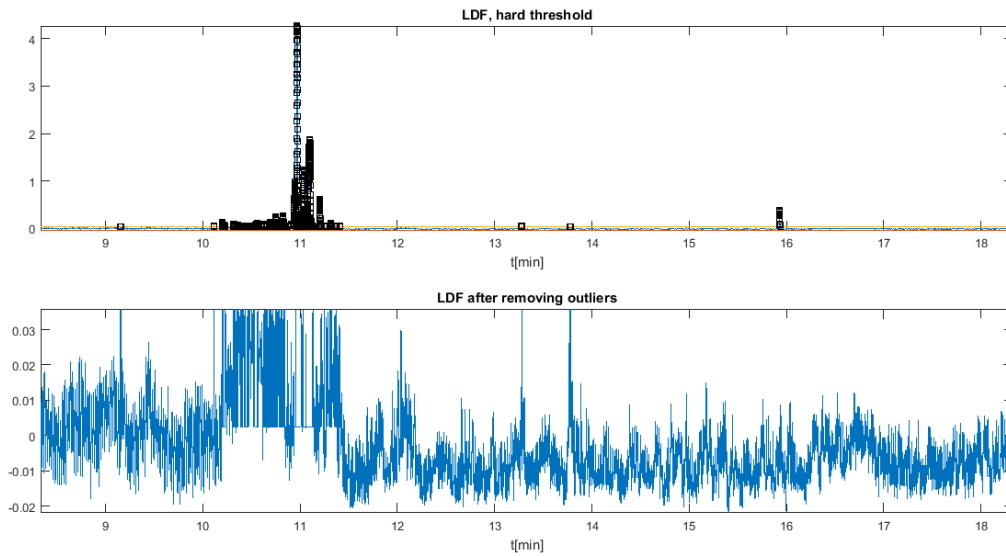


Figure 3.10: Using the LDF signal with motion artifact from figure 3.6, the black boxes shows the outliers and the red and orange lines shows the thresholds

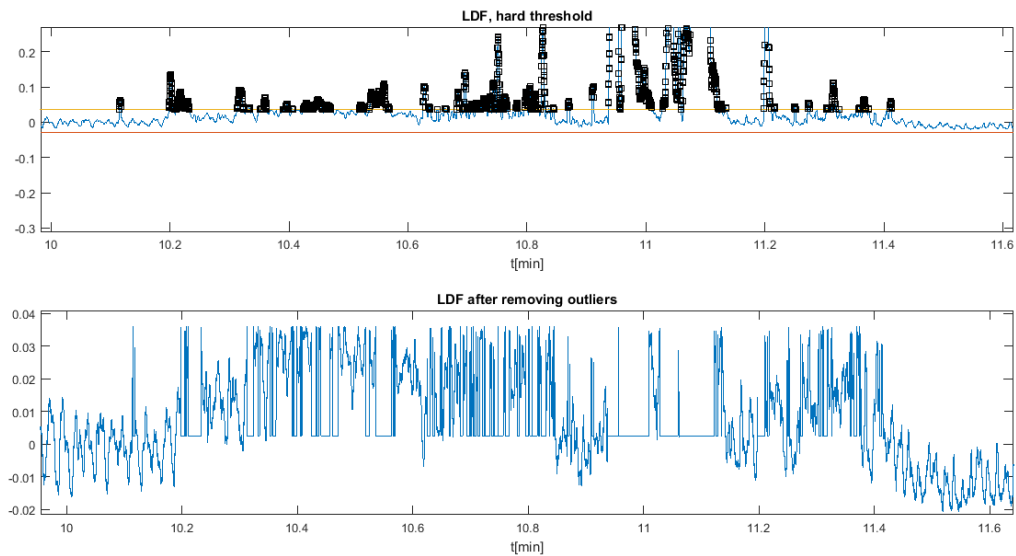


Figure 3.11: Using the LDF signal with motion artifact from figure 3.6, zoomed into a segment, the black boxes shows the outliers and the red and orange lines shows the thresholds

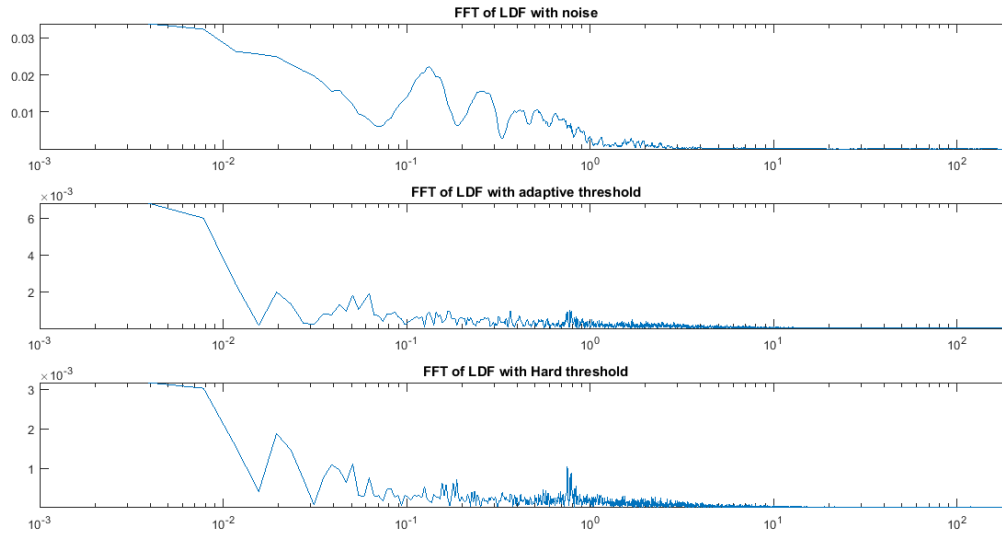


Figure 3.12: FFT of the LDF signal with motion artifact from figure 3.6, on top with the outlier techniques adaptive and hard threshold following

3.3 The application

To make analysis faster and easier there was made an application to do the analysis of the chosen biomedical signals. This would make it possible for the physicians and other personnel without technical background to easier do frequency analysis of a wanted signal.

The application was made with a graphical user interface (GUI). The GUI's were made using Matlab's Guide layout editor. The rest of the application was made as functions in Matlab.

It was decided to split the task into two programs. A pre program to extract time segments and set up a file in standard format for a second program. The second program is the analysis program and does different kinds of frequency analysis of the chosen signals.

3.3.1 Pre program

Since some of the files were extremely large (17 hours of data) there was decided to have a pre program to extract smaller interesting time segments which would make the analysis easier and faster. The pre program is named `data_exc_GUI.m` in the file folder. The pre program also serves two other features; this is setting up the files in a standardised way and extract some underlying signals.

The pre program extracts underlying signals as the HRV signal from the ECG and systolic and diastolic pressure from the blood pressure signal. This is done by using a function called `findpeaks` in Matlab. This finds the local peaks in a signal. By setting some constraints this makes it fairly easy to detect the R peaks of the ECG signal. The constraints used for finding the HRV is:

- Minimum distance between peaks is 200 samples. With a sampling frequency of 400Hz this gives a minimum distance of half a second which is 120 beats in minute. Anything

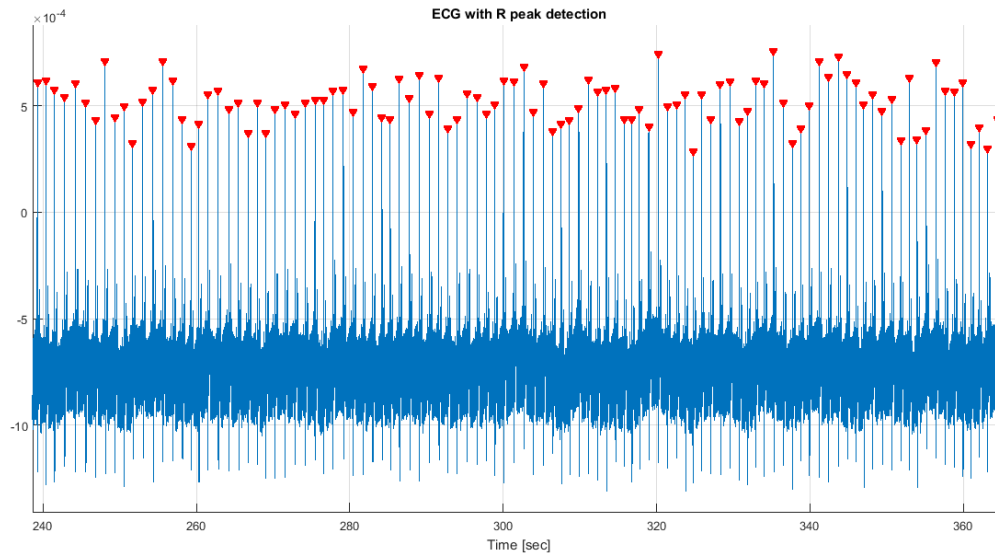


Figure 3.13: The plot shows a ECG signal with R peaks detected buy the function used in the pre program

higher than this is not likely when patient is lying in bed.

- Minimum peak height was chosen as:

$$- \text{minPeakHeight} = \text{mean}(x) + 1.5\text{std}$$

The R peak detection is shown in figure 3.13. When the R peaks are found the HRV signal is found as the time difference between two R peaks often called an R-R interval. The HRV could also be interpreted as a frequency, then as one over the R-R interval.

$$\text{HRV}(i) = t(R_{i+1}) - t(R_i) \quad (3.1)$$

The systolic and diastolic blood pressure was also found using the same function, but with some other constraints. The systolic pressure which is the peak pressure over a heart beat was found using the constraints:

- Minimum distance 200 samples
- Minimum peak height 100 mmHg as this is in the lower range of normal systolic blood pressure

for diastolic the blood pressure signal was simply multiplied with -1 to convert the minimums to maximum. The following constraints to the *findPeaks* function was used:

- Minimum distance 200 samples
- Minimum peak height -100, this means that the diastolic pressure have to be less than 100 mmHg to be detected.

Table 3.1: Standardized way of saving the files from the pre program

Variables	Description
ECG	ECG signal for extracted time segment
BP	BP signal for extracted time segment
LDF	LDF signal for extracted time segment
HRV	HRV signal for extracted time segment
SYS	Systolic signal for extracted time segment
DIA	Diastolic signal for extracted time segment
t_min	Time signal for extracted time segment
fs	The sampling frequency which is equal for all signals*

Detecting these underlying signals, HRV, systolic and diastolic blood pressure depends on finding a specific peak coming from the heartbeat. This means the signal is sampled at various times, as previously mentioned the heart is not beating in perfect rhythm. This is solved by interpolating the signal. The signals was then interpolated using the *interp1* function in Matlab, and using the *spline* method. The HRV, systolic and diastolic signals was then interpolated to have the same number of samples as the original signal.

It is important to remember that these signals originally was sampled at heart rate which approximately is a round 1 Hz for a resting person, even if they now have a theoretical sampling rate at 400Hz as the other signals. This is important to remember when analyzing the frequency spectrum that these signals only would have approximately half the heart rate as highest frequency, i.e. approximately half a hertz.

If the ECG electrodes where placed the wrong way making the ECG signal inverted this program also has an invert button for the ECG signal simply multiplying the signal with minus one.

The pre program also extracts a chosen time segment and saves the chosen time segment in a standardised way. As the files from the LabChart program was not consistent on the way the signals where ordered and the spelling of the signal names, the order depending on what kind of equipment the physicians had connected first and last, or the setup in LabChart. There where a variety from 3 signals to 5 signals where only the ECG,BP and LDF was interesting, other signal could be a respiratory signal or just a blank signal. The pre program loads in all the signals and by choosing the interesting signals the program only saves the interesting signals in a standardized way. The signals are saved as a Matlab file `gui_data_filename_xx_xx.mat` , where *filename* is the name of the file open in the program and *xx_xx* indicates start minute and stop minute of the extracted segment. The standardized way of saving the files from the pre program is shown in table 3.1.

A screen shot of the pre program with the file 160317_01pre chosen, with the R peaks detected from the ECG signal and the systolic and diastolic signals detected from the blood pressure signal is shown in figure 3.14. There is also chosen a time segment from minute 25 to minute 30 from the start. By saving at this point the program would produce the standardized file

`gui_data_160317_01pre_25_30.mat`.

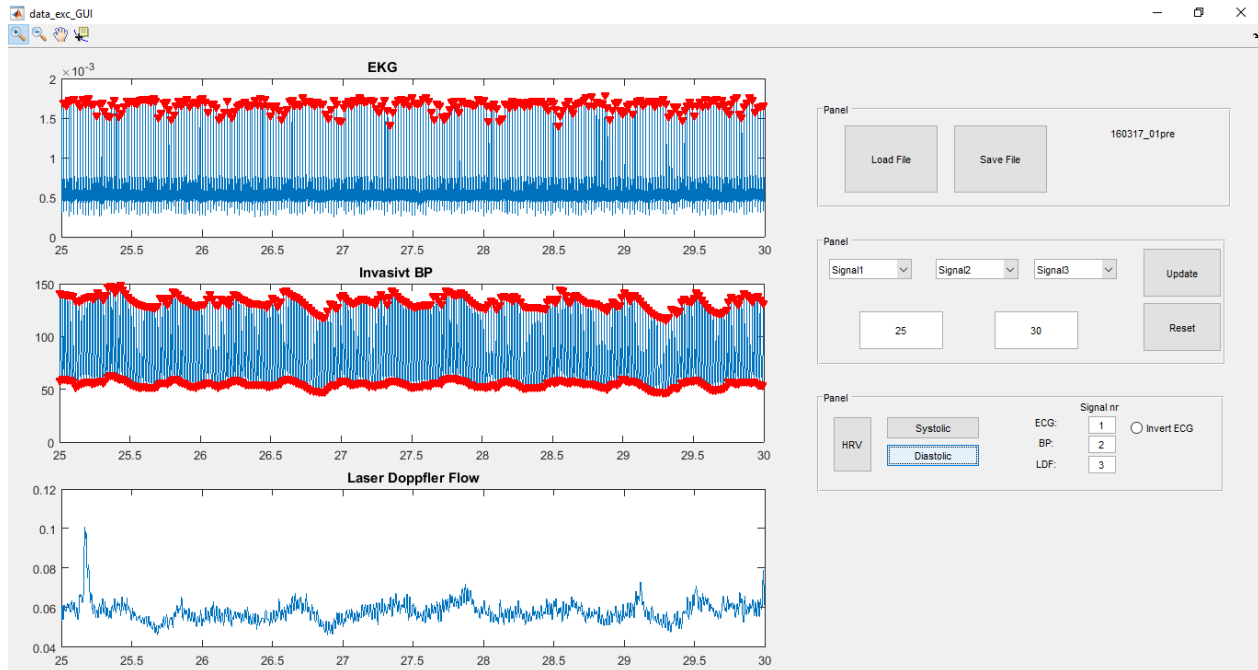


Figure 3.14: Screen shot of the program `data_exc_GUI.m`

3.3.2 Analysis program

The analysis program is the main program in this project. The program is called `master_GUI.m` and is where the frequency analysis is being done. The program is a result after several scripts testing different frequency analysis techniques.

The analysis program takes input from the standardized file from the pre program. The program then have three plots to show any of the loaded signals ECG ,BP, LDF, HRV, SYS or DIA. These signals are chosen by three drop down menus each corresponding to a plot window. By default the program start showing ECG, BP and LDF as shown in figure 3.15. There is also possible to specify a range to look into by typing in chosen start minute and stop minute in the boxes marked with *Start min* and *Stop min* and push the update plots button. Be aware that this is not the same as using the zoom function chosen from top panel as the zoom function only zooms into a segment, while the range selection method clips the signal at the chosen start and stop minute. The range selection is chosen this way to be able to do frequency analysis on a specific shorter segment of the signal. To get back to the full signal simply bush the reset button, and the program will reset to the way it was at start up. In the top panel there is some of the normal features from a standard Matlab figures such as the already discussed zoom function's, pan function, and data cursor function.

The remove outliers button works in the same way as the remove outliers technique discussed in the noise removal chapter. The implemented version uses the hard threshold.

Each plot has a corresponding plot window to the right which shows the chosen frequency analysis method. There are three different analysis buttons, this is the Fast Fourier Transform(FFT button), continuous wavelet transform time-frequency analysis(CWT analysis button) and a continuous wavelet transform frequency analysis(CWT mean button). These buttons and analysis methods will be described next.

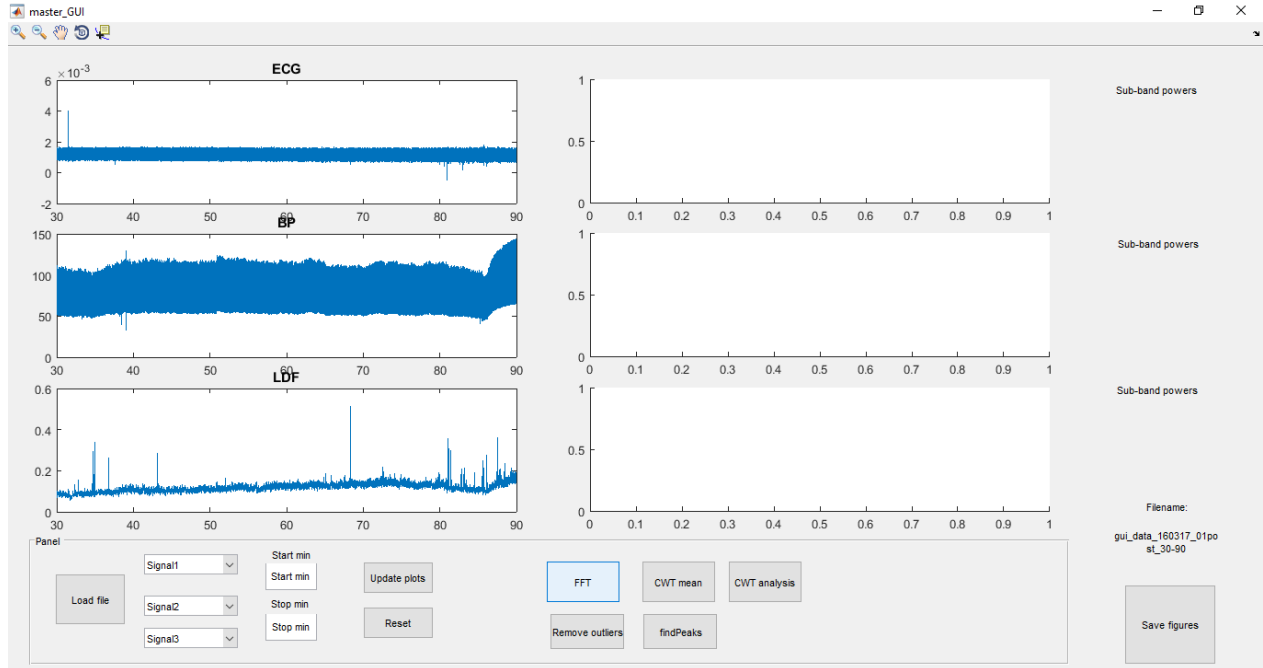


Figure 3.15: Screen shot of the program *master_GUI.m* at start up.

The frequency analysis is restricted by two criteria. The logic one is that the time signal have to be the same length or longer than the longest wave wanted to detect. Second criterion is the Nyquist frequency. The Nyquist frequency tells the highest possible frequency f_{max} detectable with a given sampling frequency.

FFT button

The FFT button uses the fast fourier method. The three chosen signals shown in the plot windows are used and their corresponding frequency spectrum are produced using the FFT algorithm. These spectrum's are plotted in the corresponding frequency analysis windows. The FFT's are produced using $N=204800$, with the sampling frequency of 400 Hz and by Nyquist this gives highest possible frequency as:

$$f_{max} = \frac{f_s}{2} = \frac{400Hz}{2} = 200Hz \quad (3.2)$$

This gives a frequency resolution:

$$f_{resolution} = \frac{f_{max}}{N} = \frac{200}{204800} = 0.000977Hz \quad (3.3)$$

Analysis plots are shown with a logarithmic frequency axis and only up to 10Hz as this covers the the interesting frequencies well.

CWT analysis button

The CWT analysis button gives a time frequency plot using the *cwtft* matlab function. This function returns the continuous wavelet transform of a 1-D signal, using an FFT algorithm to

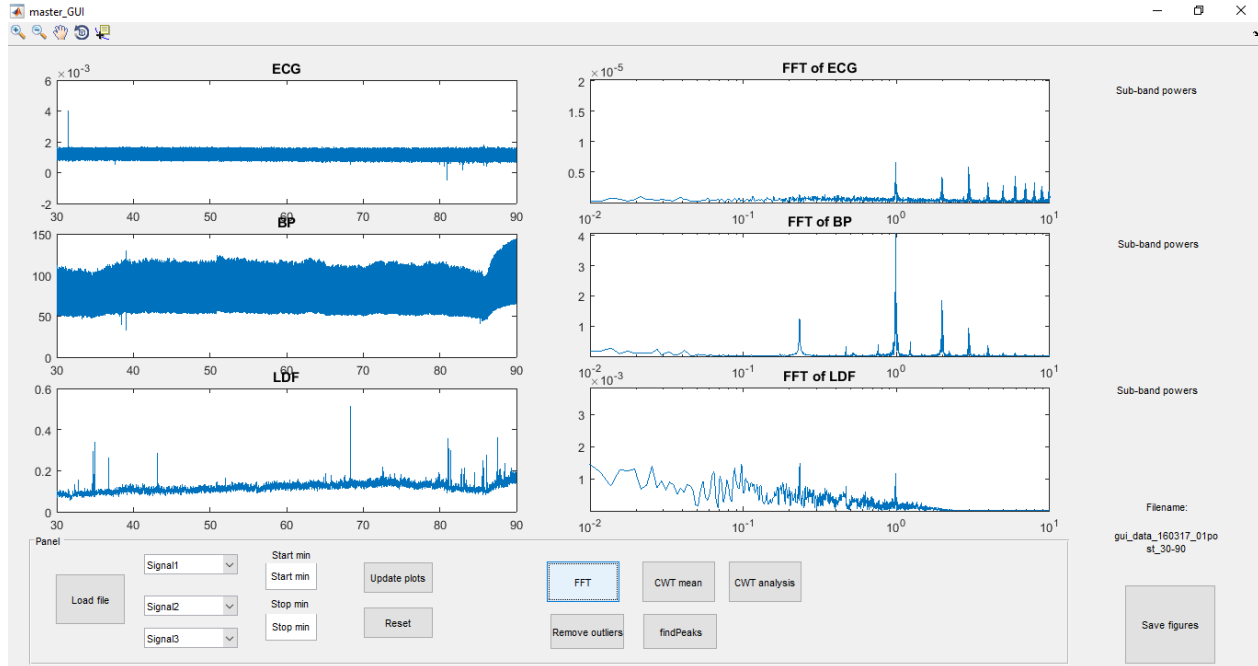


Figure 3.16: Screen shot from *master_GUI.m* with a FFT analysis

compute the CWT.

In the wavelet analysis it is being used an analytic *morlet* wavelet. This is a complex wavelet, which does not separate positive and negative peaks[30]. It was discussed and tested using different wavelets, but the chosen Matlab function gave restrictions in which wavelet's to chose from. Possible analytic wavelets in the *cwftf* function was *morl*, *dog*, *bump* and *paul*. The analytic *morl* and *bump* gave the results thought to be most accurate, as the these shows the clearly known heart rate frequency around 1Hz clearest. It was decided to use the *morl* wavelet in the rest of the analysis as this is a well known and used wavelet for this purpose [10].

Before starting the wavelet analysis the signal was decomposed to remove superfluous information and thus making the signal much smaller in size. This is a way of resampling and filtering the signal. The signal was decomposed five times and reconstructed at this level using the approximation coefficients. This gives a signal only containing the lower frequencies. A five level decomposition gives a sampling frequency of:

$$f_{s_w} = \frac{f_s}{2^{\text{lvl of decomposition}}} = \frac{400}{2^5} = 12.5 \text{ Hz} \quad (3.4)$$

This gives a theoretical detectable frequency of 6.25Hz, which is well within the interesting frequency range of 2 Hz. The computational time of the analysis also drops drastically. The wavelet 'db4' was used in the wavelet decomposition, as this is known as a good wavelet for ECG [31] [32], and seems to work fine for the other biological signals.

The scales of the wavelet was chosen from a wanted frequency range from 0.004 to 2 Hz. This conversion is done as follows:

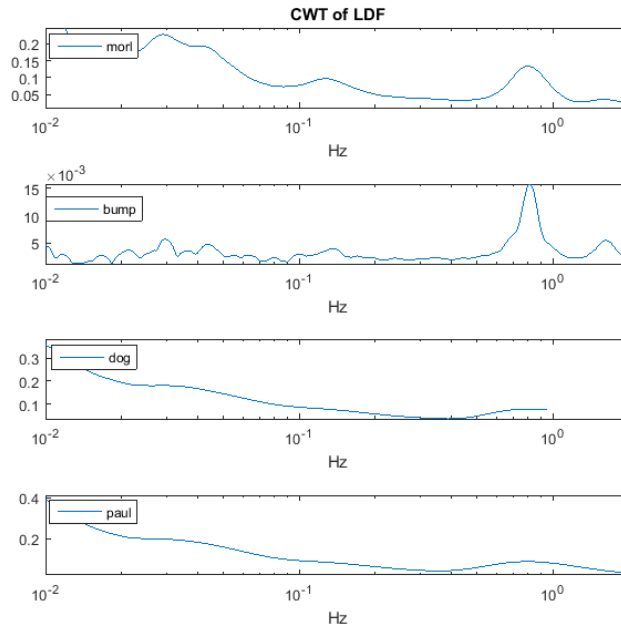


Figure 3.17: CWT using different mother wavelets

$$\begin{aligned}
 a_0 &= 2^{\frac{1}{NumVoices}} \\
 scale_{min} &= \text{floor} \left(NumVoices * \log_2 \left(\frac{wavecenter}{freq_{min} * dt} \right) \right) \\
 scale_{max} &= \text{ceil} \left(NumVoices * \log_2 \left(\frac{wavecenter}{freq_{max} * dt} \right) \right) \\
 scales &= a_0.^{(scale_{min}:scale_{max} * dt)}
 \end{aligned} \tag{3.5}$$

With $NumVoices = 64$ and $wavecenter = \frac{5}{2 * \pi}$.

The CWT analysis button produces time frequency plot's corresponding to the signals shown in the left panels this is shown in figure 3.18

CWT mean button

The CWT mean button uses the same analysis technique as described in the previous section. The difference is that it only show the frequency response of the chosen signal and not the time-frequency response. This is done simply by averaging the CWT coefficients over the time, this could be described as seeing the time-frequency plot with the time axis straight into the screen only showing frequency and power axis. An example of the CWT mean analysis is shown in figure 3.19.

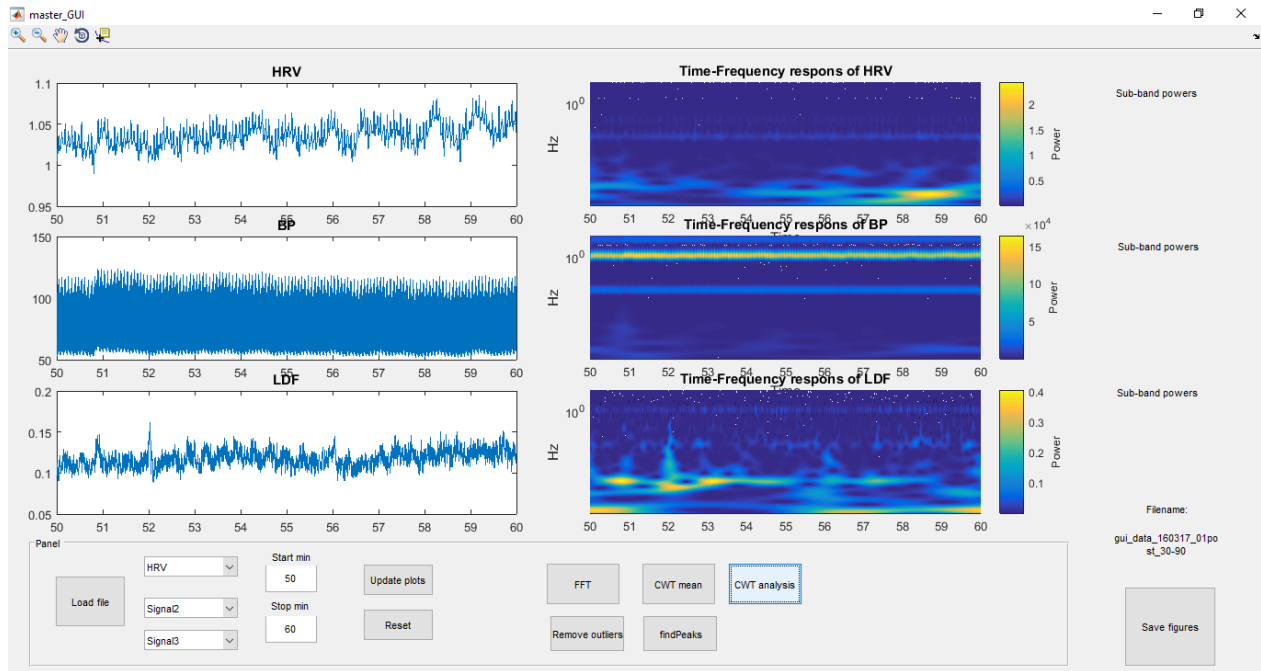


Figure 3.18: Screen shot from `master_GUI.m` with a CWT time frequency analysis

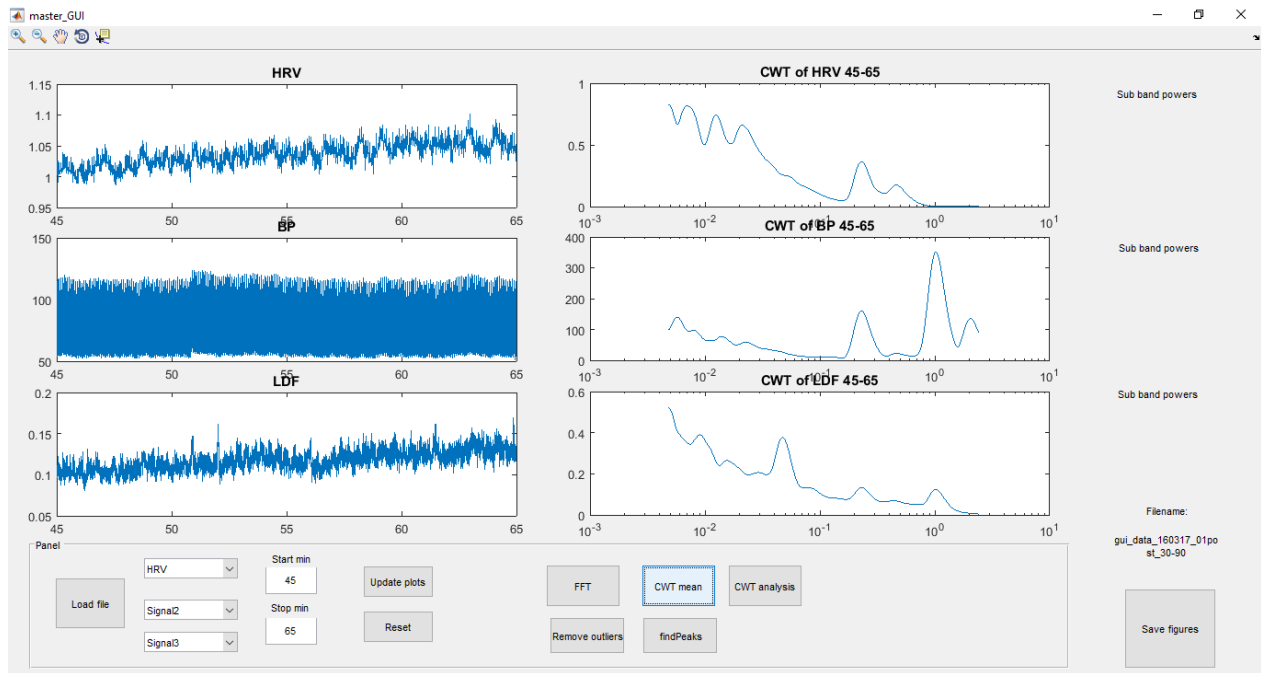


Figure 3.19: Screen shot from `master_GUI.m` with a CWT frequency analysis

findPeaks button

The *findPeaks* button is made to compare the plots from the CWT mean analysis from different time segments. The function extracts 3 variables from 6 different sub-band of CWT frequency spectrum. These sub band will be described later. The three variables extracted from each sub band is:

- *Power*
- *Peak frequency*
- *Peak value*

The power variable is found by taking power of the frequency signal. As shown:

$$P = \frac{1}{N} \sum_{i=1}^N sig(i)^2 \quad (3.6)$$

This produce the average power of the frequency signal.

The *peak frequency* is found as the frequency corresponding to the highest local maxima in the sub-band. The function excludes the end point and start point of the sub-band. The peak frequency gives one frequency as out put. If the sub-band is monotonically increasing or decreasing this means there exsits no local maxima and the peak frequency is set to zero.

The peak value is the value of the highest local maxima corresponding to the peak frequency. Same as for the peak frequency if the sub-band is monotonically increasing or decreasing the peak value is set to zero.

After the function completes, the peak's in each sub-bands are marked with a red triangle and the sub-band powers are displayed to the right of the plots. An example is shown in figure 3.20.

Save figures button

To save the analysis of the current segment worked on the *Save figures* button opens a dialog window where it asks for a folder to save the current work in. It then creates a folder in the chosen folder with the name *gui_data_filename*. Where *filename* is name of the file open in the analysis program. The program then saves each plot window in the analysis program in a separate Matlab figure files. The name of the files specify which signal it is, which time segment it covers and the analysis plots also shows which analysis method that was applied. The *BP_30_90.fig*, contains the time domain signal of the the Blood pressure signal from minute 30 to minute 90 and *LDF_CWT_mean_45_65.fig* means it is the CWT mean analysis on the LDF signal from minute 45 to 65. If the *findPeaks* function has been done the *Save figures* also saves a .mat file containing the variables from this function they are saved as *sub_band_powers_xx_xx.mat*.

3.4 Analysis set up

The analysis set up was decided in collaboration with and on request from the medical students Bjørn and Fredrik and their supervisor Nils Kristian. They collected data from patient real

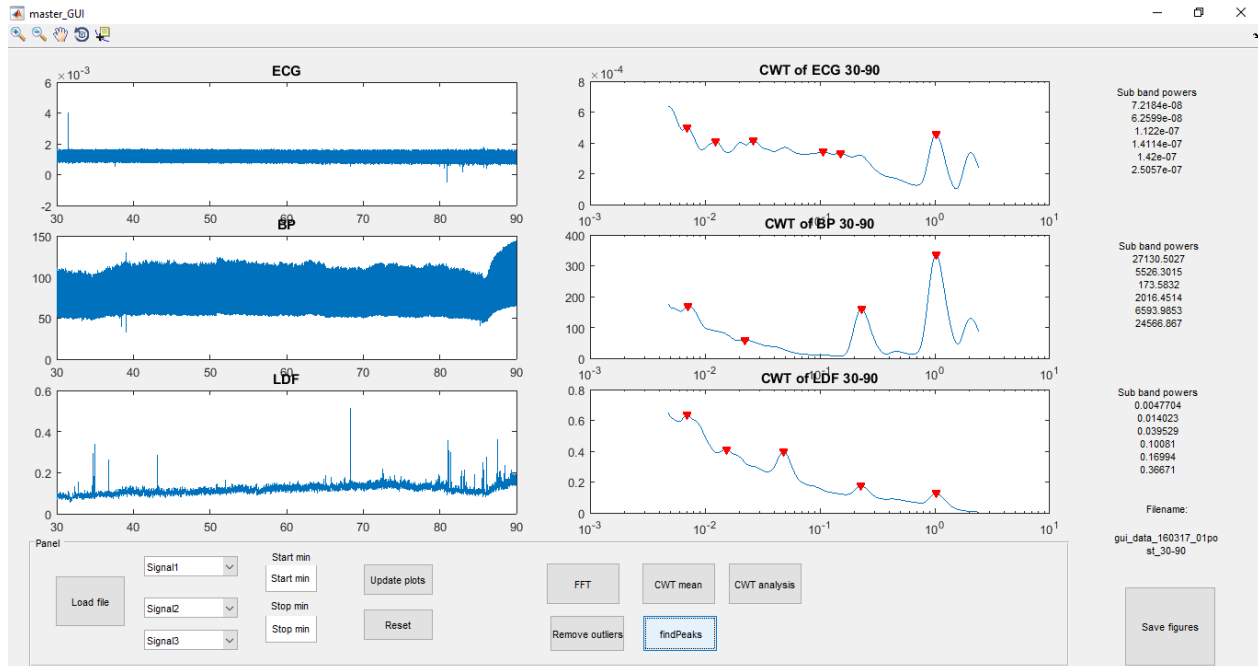


Figure 3.20: Screen shot from *master_GUI.m* with a CWT frequency analysis and *findPeaks* function

time approximately one hour of data before surgery and after the surgery through the night and the next morning this gives approximately 17 hours of data after surgery. It was decided that it was interesting to extract four one hour segments to analyse. One pre surgery and three post surgery (post1, post2 and post3). The post surgery segments were selected by Bjørn and Fredrik. The first post segment is before extubation, where the patient is still on the respirator, next segment Post2 is after extubation and the last segment Post3 is the next morning. Each segment was selected with emphasis on avoiding as much noise as possible. The chosen post segments could be seen in table 3.2.

The chosen segments were extracted and organized with the *data_exc_GUI* program. The standardized files from the *data_exc_GUI* were then opened with the analysis program *msater_GUI*. The analysis was done on the three signals HRV, BP and LDF. The analysis was done with the *CWT mean* analysis. The *findPeaks* function button was then used to give the three variables described earlier: power, peak frequency, and peak value for each sub-band.

The *CWT mean* analysis was chosen, because of the good low frequency resolution, giving a good range for the low frequencies and making a nice representation. The wavelet analysis is also better for non-stationary signals, such as biomedical signals [33]. A comparison of the FFT and CWT mean methods is shown in figure 3.21

The 6 sub-bands were chosen based on the sub-bands from the article [10]. An additional sub-band was added on request from the medical team, this is the VLF sub-band. These sub-bands are shown in table 3.3.

The sub-bands are more or less hypothesized, the heart rate and the respiratory sub-bands are very clear, but the lower sub-bands and their supposed origins are hypothesized.

Bracic and Stefanovska [10], who mostly looked at the LDF signal, has in this paper described

Table 3.2: Time segments chosen for the post segments

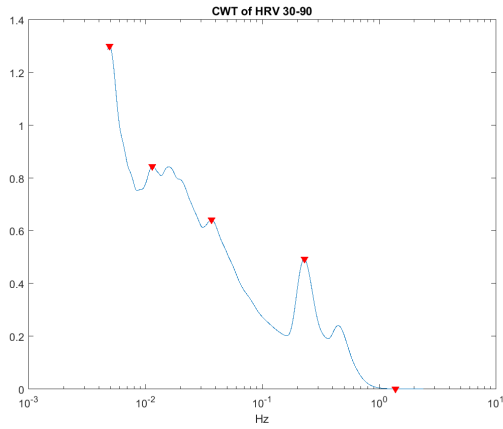
Patient	Post1 [min]	Post2 [min]	Post3 [min]
160317_01	30-90	120-180	945-1005
160329_02	42-102	127-187	915-975
160331_03	52-112	120-180	870-930
160406_04	110-170	180-240	660-720
160407_05	84-144	160-220	1036-1096
160413_06	80-140	160-220	868-928
160416_07	30-90	136-196	750-810
160510_08	30-90	132-192	780-840
160512_09	10-70	270-330	732-792
160524_10	56-116	148-208	720-780

Table 3.3: Frequency sub-bands

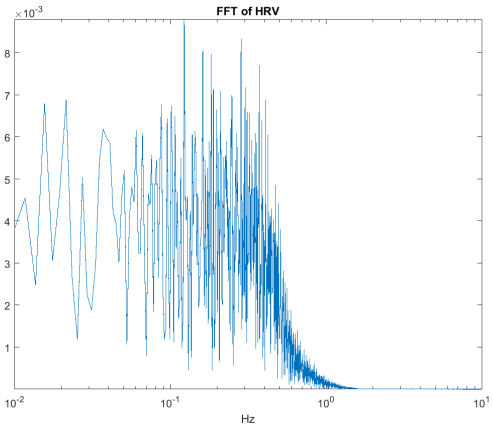
Sub bands [Hz]	Supposed origin of activity	Sub-band name
0.6-2	Heart activity	HR
0.15-0.6	Respiratory activity	resp
0.052-0.15	Myogenic activity	myo
0.021-0.052	Neurogenic activity	neuro
0.0095-0.021	Metabolic activity	eMeta
0.004-0.0095	unknown	VLF

the first five sub bands as:

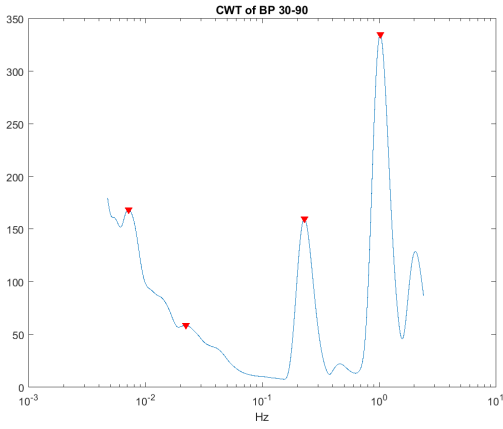
- **The peak around 1Hz.** This peak belongs to the heart rate. This is shown by comparing a scaleogram(time-frequency plot) of the blood flow signal with a scaleogram with a simultaneously recorded signal of the heart.
- **The peak around 0.3Hz.** The peak around 0.3Hz is from respiratory activity, this becomes evident when comparing the scalogram of the blood flow with a simultaneously recording of the respiratory activity.
- **The peak around 0.1Hz.** It has been hypotezised that the peak around 0.1Hz is associated with blood pressure regulation. The smooth-muscle cells in the vessel walls respond continually to the changes in introvascular pressure, which is known as the myogenic response. Therefore, this intrinsic rhythmic activity of the vessels, caused by the pacemaker cells in the smooth muscles of their walls, is called myogenic activity.
- **The peak around 0.04Hz.** A peak a round range from 0.03 to 0.04Hz has been found in blood pressure and HRV signals by several authors [34]. In humans, [35] demonstrated that this peak disappeared completely after denervation, both after local and ganglionic nerve blockade and after sympathectomy. Thus one may conclude that this rhythm results from the neurogenic activity.



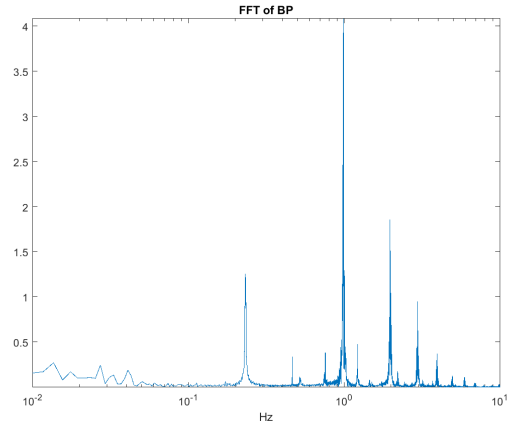
(a) CWT mean HRV



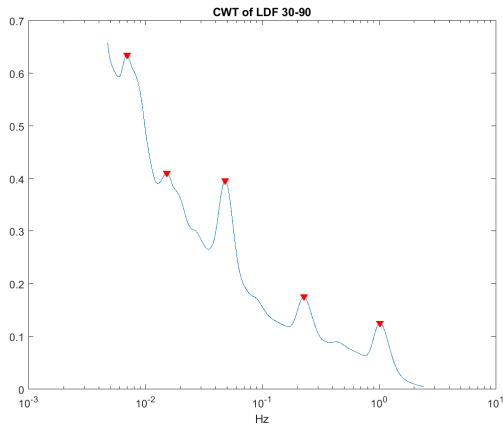
(b) FFT HRV



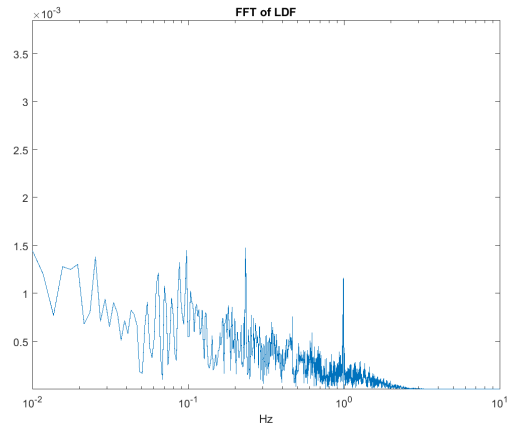
(c) CWT mean BP



(d) FFT BP



(e) CWT mean LDF



(f) FFT LDF

Figure 3.21: Comparing FFT and CWT mean method

- **The peak around 0.01Hz.** This peak is hypothesized that corresponds to metabolic activ-

ity—the rhythmic regulation of vessel resistance to the blood flow initiated by concentrations of metabolic substances in the blood.

This analysis set up gives a frequency spectrum for each of the three signals. Each of the spectrum's are then again divided into 6 sub-bands. From each sub-band there is collected 3 variables. By doing this for each of the four time segments gives:

$$\begin{aligned} \# \text{ data_points} &= 10\text{Patients} \times 4\text{segments} \times 3\text{signals} \times 6\text{sub-bands} \times 3\text{variables} \\ \# \text{ data_points} &= 2160 \end{aligned} \quad (3.7)$$

The data variables and plots where send back to the medical team at St.Olavs hospital, for their medical interpretation of the data.

The variables are also compared for the four segments averaged over the patients. The variables are presented as the evolution over the four segments showing one variable from one segment and one signal.

3.4.1 Poincarè analysis

The Poincarè analysis was applied to the HRV signal, as this is a well used analysis for the HRV signal. It is interesting to see how the data set of relatively few patients works to a well known method and to see if there is some correlation with the frequency analysis. For comparing the quantitative analysis method with fitting an ellipse will be used.

Chapter 4

Results

In this chapter a description and presentation of the results will be given. The results are divided in two parts, the frequency application software and the results from frequency analysis of the patients.

4.1 Frequency analysis application

The frequency analysis application ended up being a working application making it faster and easier to compute the frequency spectrum of a biomedical signal. The application has the possibility of doing two different frequency analysis methods and one time frequency method. The frequency methods are; the FFT and an averaged continuous wavelet method. The time frequency method is the continuous wavelet method.

Computational time for the different methods was tested on a laptop, Lenovo x220 with Intel i7 processor, 4 GB RAM and a SSD disk. The frequency analysis methods had a averaged computational time of 13-14 seconds for the CWT method, 0.5 seconds for the FFT. This is the time it used to compute the three different frequency spectrum's from the three one hour long signals. For the time frequency method this was known to have a very long computational time, it was therefor decided to test computational time for 10 minute time segments. The computational time averaged is 22-23 seconds, but the plots are containing a huge amount of data filling up the memory of the computer and making it extremely slow and unresponsive.

4.2 Patient analysis

Examples of the frequency response for a patient is shown in figures 4.1 and 4.2. This shows the frequencies of the signals HRV, BP and LDF for the patients 160317_01 and 160329_02 respectively. The first row is from the pre segment, on the following rows are the segments post1, post2 and post3. In post1 the patient still is one the ventilator. The heart rate and respiratory frequency are very clear in the BP and LDF signals, also in HRV is respiratory frequency very prominent. The peaks in the lower frequencies does not coincides that well. The frequency response for all the patients are attached in the appendix B.

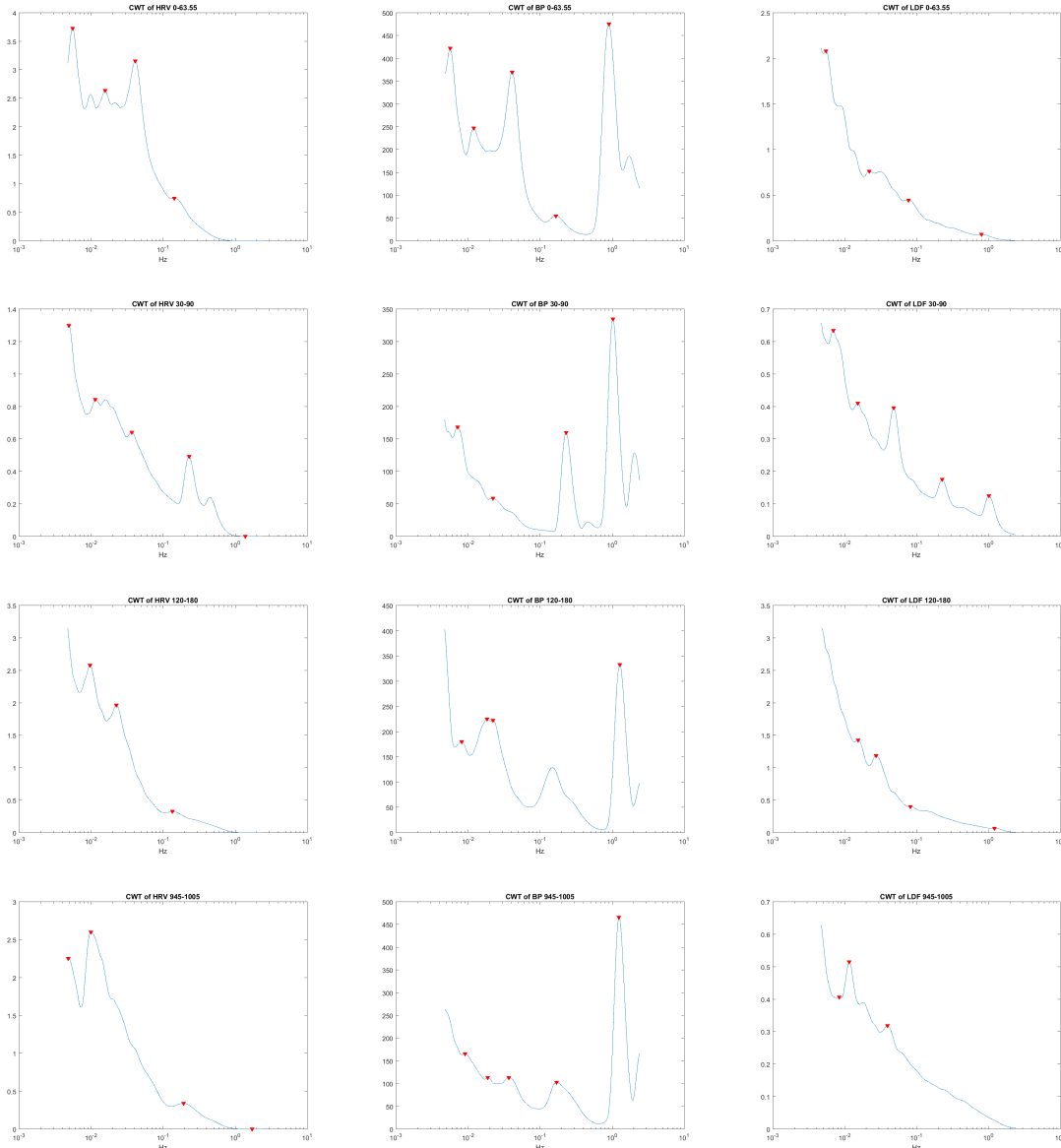


Figure 4.1: CWT mean of 160317 from pre(plot 1:3), post1(plot 4:6), post2(plot 7:9) and post3(plot 10:12)

4.2.1 Averaged evolution

The result shows the four segments pre, post1, post2 and post3 in every box plot for one signal and one variable and one segment. The results will be shown for one sub-band at the time, starting at the HR band and going down to the VLF band. The variable power is collected for all the signals this gives, 10 inputs for every boxplot. For the variables peak frequency and peak value, they are collected only if there is detected a peak in the current sub-band, as described earlier. The number of detections will be presented in each section describing each sub-band. If there is detected 10 peaks for a signal, there is detected a peak for all the patients in the current sub-band.

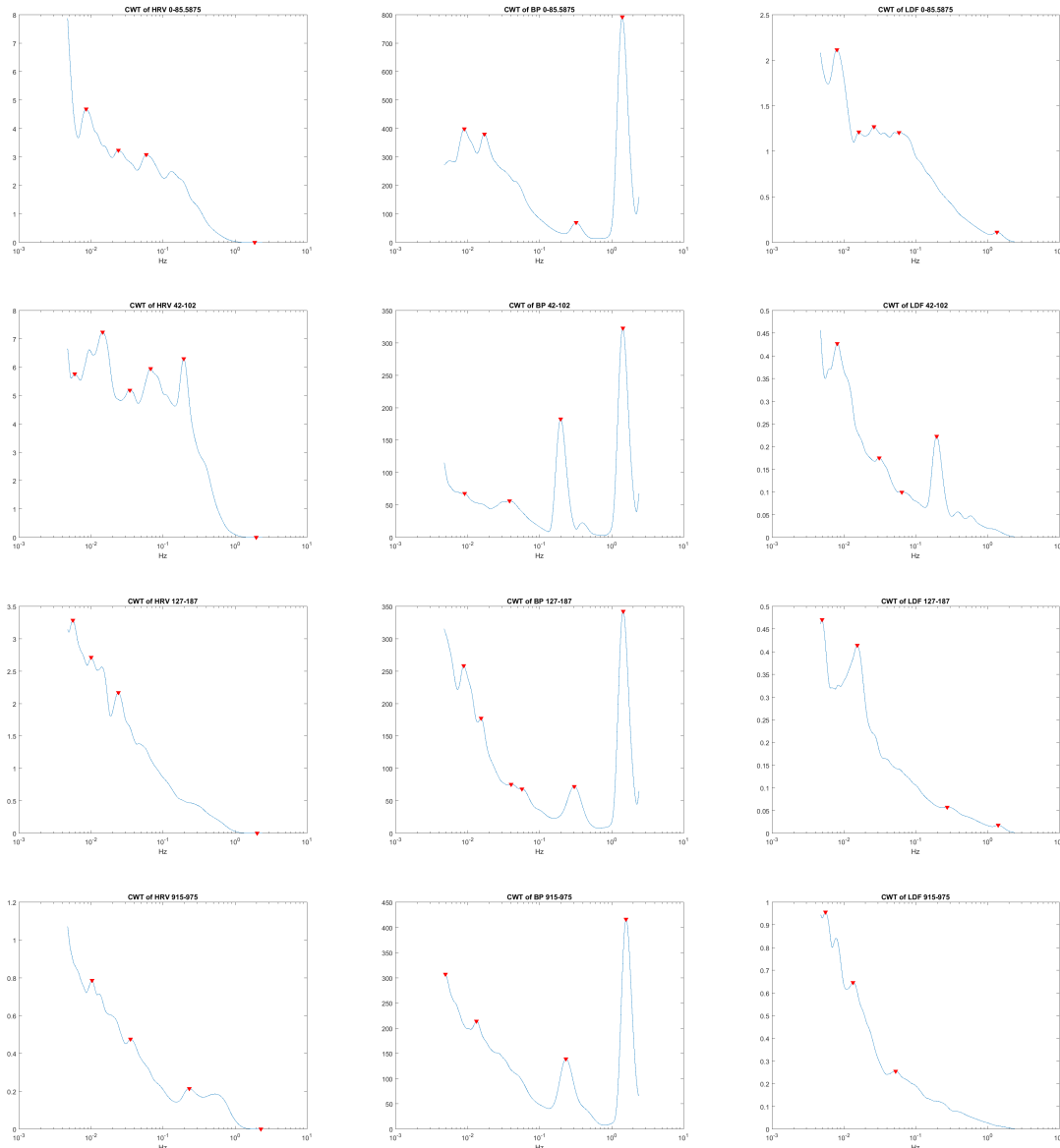


Figure 4.2: CWT mean of 160329 from pre(plot 1:3), post1(plot 4:6), post2(plot 7:9) and post3(plot 10:12)

HR sub-band

As the HRV signal's original sampling rate is the heart rate approximately around 1Hz there is no data from the HRV signal in this sub-band, as seen in table 4.1. The HR frequency peak is always detected in the BP signal, but for the LDF signal it varies from being detected in 9-5 patients in the different segments.

Figure 4.3 shows a very similar data and evolution of the heart rate frequency. The peak values shown in figure 4.4 does not have the same consistency. In figure 4.5 there is a similar trend in the statistics from the LDF signal and BP showing an increase in power after surgery, while dropping down for the last two segments.

Table 4.1: Number of peaks detected for the HR sub-band

	HRV	BP	LDF
Pre	0	10	9
Post1	0	10	8
Post2	0	10	8
Post3	0	10	5

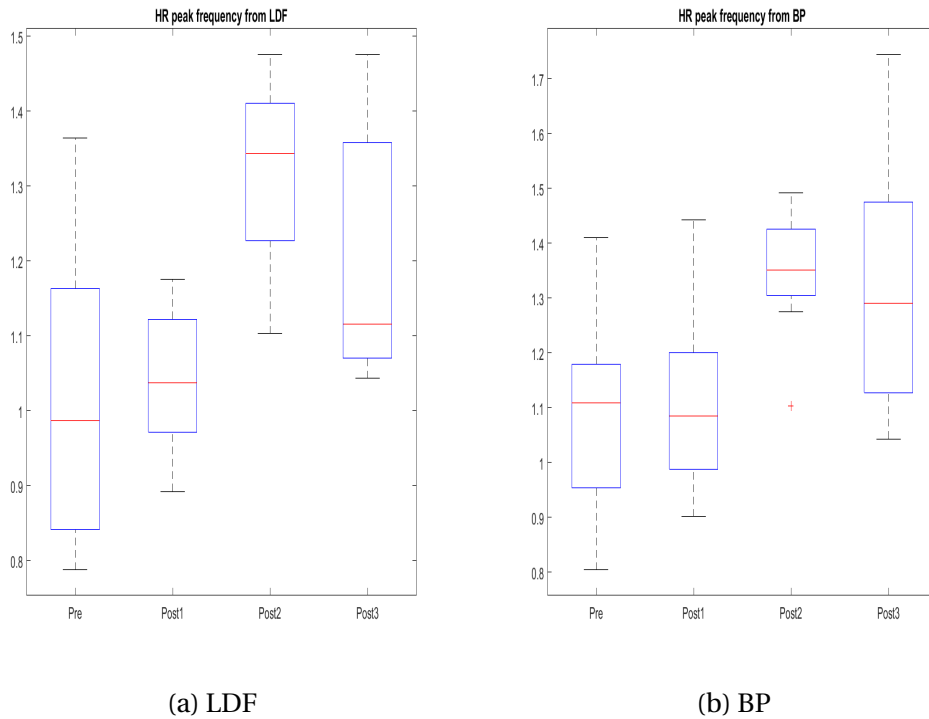


Figure 4.3: Peak frequency's for the HR sub-band

Resp sub-band

The respiratory sub-band from 0.6-0.15 Hz represent the respiratory activity effect on the the cardiovascular system. This becomes very clear when studying a frequency spectrum of a respiratory signal. As shown in figure 4.6 the frequency's from the respiratory signal is clearly shown in the band from 0.15-0.6Hz. This corresponds to 9-36 times a minute this corresponds well with whats known to normal rate, 10-20 breaths per minute [36].

The respiratory frequency is detected in every patient and every signal in segment post1, this is where the patients are connected to the ventilator. For the other segments the respiratory peak is detected in more patients after surgery, and most often in the BP signal with detection in 9 out of 10 patients in segment post2 and 10 out of 10 patients in segment post3.

As mentioned above the patients are connected to a ventilator in the first time segment after the operation. This is very evident in the peak frequency's as this gives much smaller variance in the respiratory rate for the post1 segment compared to the other segments. In all the signals a median of the peak frequency is found at 0.2Hz, this corresponds with a respiratory rate at 12

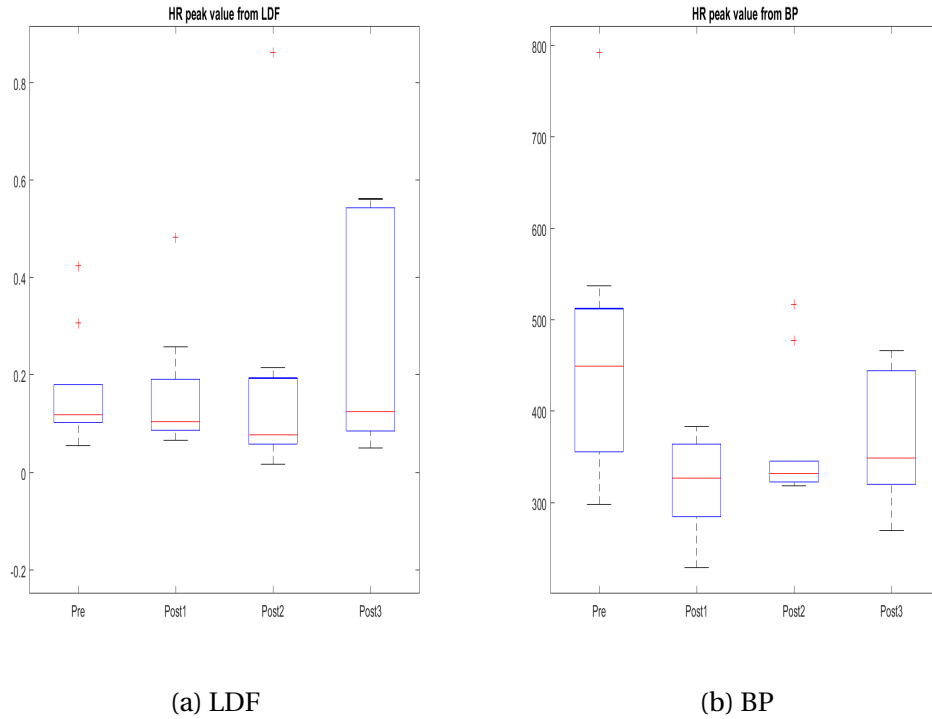


Figure 4.4: Peak value's for the HR sub-band

Table 4.2: Number of peaks detected for the respiratory sub-band

	HRV	BP	LDF
Pre	2	6	3
Post1	10	10	10
Post2	5	9	3
Post3	9	10	4

times a minute. It is also a detectable trend that the rate is higher before surgery, goes down to the ventilator machine rate goes up after extubation, this is a segment with high variance and then goes a bit down for the last segment. The peak frequency is shown in figure 4.7.

The peak values does not show any clear trend, with a great overlap of the interquartile range. The power variables does show a trend quite opposite of the peak frequency, this is with low power in the first segment, increase in power in post1 and decrease in post2 and increase again in the last segment post3. This trend is consistent with all the signals. The peak value and power is shown in figure 4.8 and 4.9.

Myo sub-band

The myo peak is detected on average in 35% of the patients and is most frequently detected from the HRV signal with 47.5% of the patients. This gives very little information to analyse, and introduce a high degree of uncertainty. The number of how many times the myo peak is detected is shown in table 4.3. As seen in table 4.3 the myo peak is not present in the blood

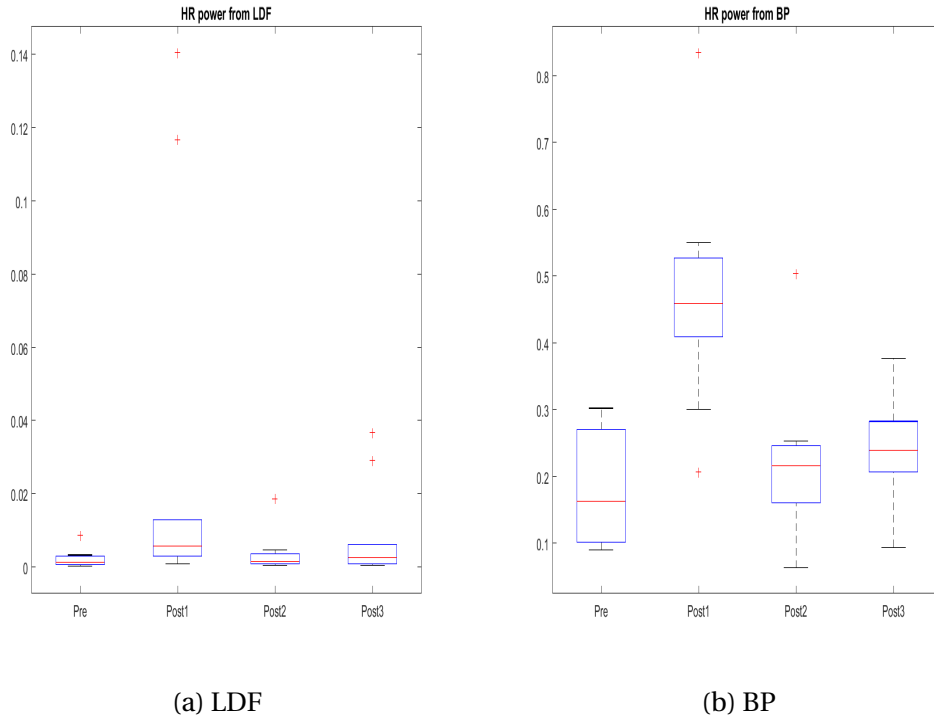


Figure 4.5: Power for the HR sub-band

Table 4.3: Number of peaks detected for the myo sub-band

	HRV	BP	LDF
Pre	6	0	4
Post1	5	2	4
Post2	5	2	2
Post3	3	4	5

pressure signal in the pre segment before surgery.

The peak frequency's does not show any clear trends, the only interesting thing is that it is only possible to detected a peak in the BP signal after surgery. The peak values does not show any clear trends. For the power most of the data has a high degree of overlap of the interquartile range. Peak frequencies, peak value and power is shown in figure 4.10, 4.11 and 4.12 respectively.

Neuro sub-band

The neuro peak is detected 78% of the time averaged over segments and signals, and most with the HRV signal where it is detected in 82.5% of the patients. This is good data for all the segments and signals as seen in table 4.4.

The Peak frequency variable do not show any good trend with all the data almost within the same interquartile range. The peak values are showing a very similar trend for all the signals, with decrease from pre to post1, increase from post1 to post2 and decrease again from post2 to post3. Naturally the power has almost the same trend, but with much higher variance and then

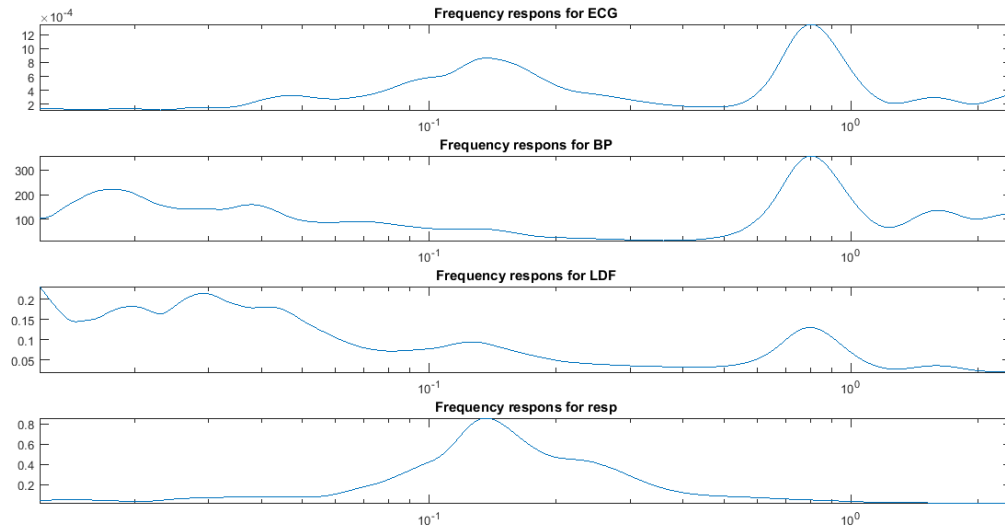


Figure 4.6: Showing frequency content from ECG,BP,LDF and respiratory signal.

Table 4.4: Number of peaks detected for the neuro sub-band

	HRV	BP	LDF
Pre	7	8	9
Post1	10	7	8
Post2	9	8	7
Post3	7	7	7

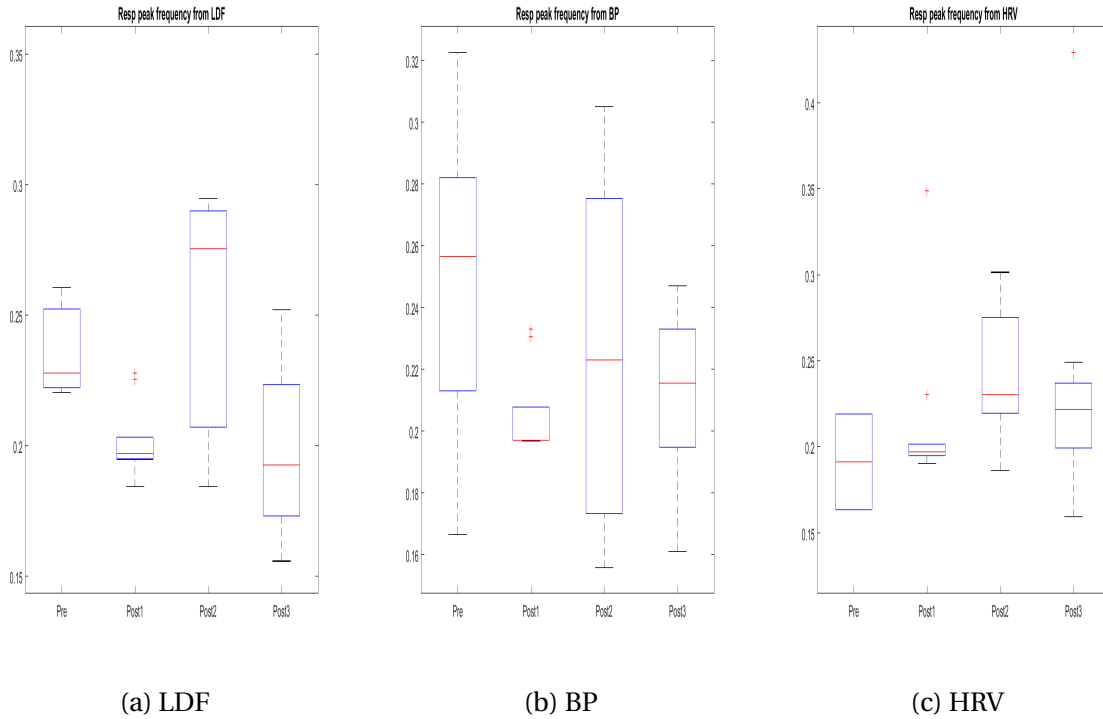


Figure 4.7: Peak frequency's for the resp sub-band

Table 4.5: Number of peaks detected for the eMeta sub-band

	HRV	BP	LDF
Pre	8	10	9
Post1	8	6	9
Post2	9	9	10
Post3	9	9	10

greater overlap of the interquartile range. Peak frequencies, peak value and power is shown in figure 4.13, 4.14 and 4.15 respectively.

As seen in the respiratory sub-band there is possible to see that the power/peak value has an opposite trend from the peak frequency. In this sub-band this is best seen between the peak-value trend and the peak-frequency trend from the HRV signal.

eMeta sub-band

In the eMeta sub-band there is detected a peak in 88% of the patients, with most detections in the LDF signal with 95%. A listing of the number of peak detected for each segment and signal is shown in table 4.5.

For the eMeta sub-band there is a trend where the median of the peak frequency(figure 4.16) in the LDF and BP signal is increasing in the 3 first segments before decreasing in the last segment, but the interquartile range is large and covering the same range, which introduces some uncertainty. In the peak values(figure 4.17) it is seen that there is clearly higher values in

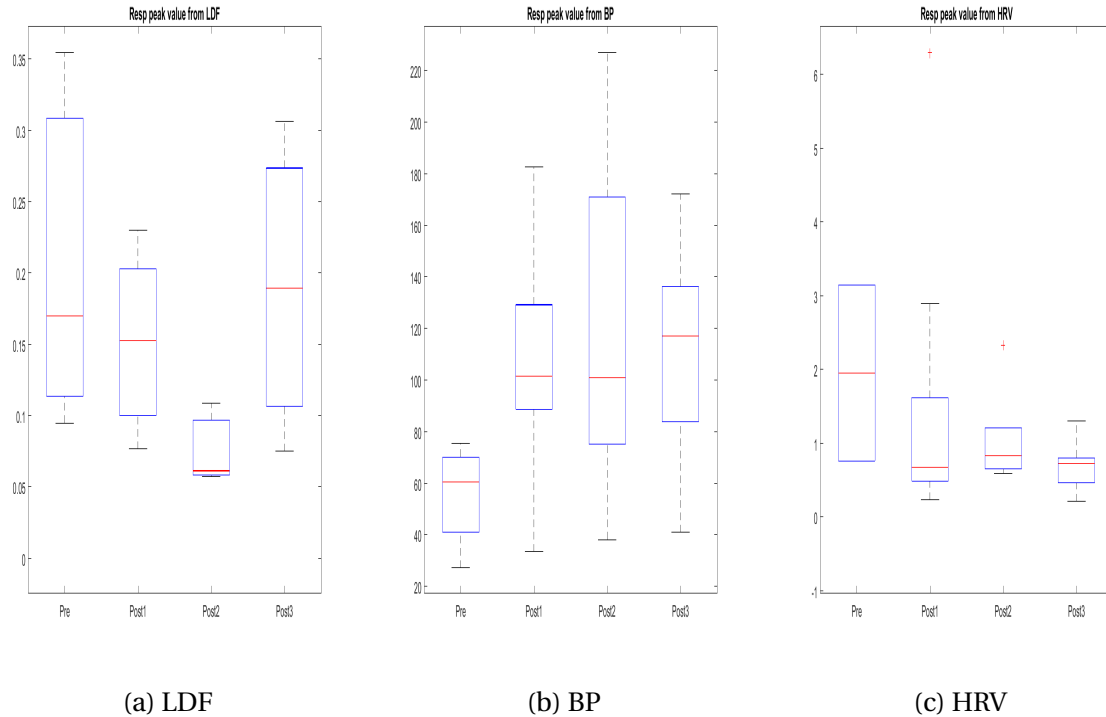


Figure 4.8: Peak value's for the resp sub-band

Table 4.6: Number of peaks detected for the VLF sub-band

	HRV	BP	LDF
Pre	10	8	6
Post1	10	10	9
Post2	9	10	9
Post3	8	10	9

the pre segments than in the post segments after surgery. The power values (figure 4.18) from the LDF and HRV could show some similarity's also when comparing to the trend of the peak frequency.

VLF sub-band

In the VLF sub-band there is detected a peak in 90% of the patients, with most detections in the BP signal with 95%. A listing of the number of peak detected for each segment and signal is shown in table 4.6.

The values from the VLF does not show any clear trends. The interquartile ranges cover mostly the same range. HRV signal peak values has a similarity to the eMeta sub-band. The peak frequency's, peak value and power is shown in the figures, 4.19, 4.20 and 4.21.

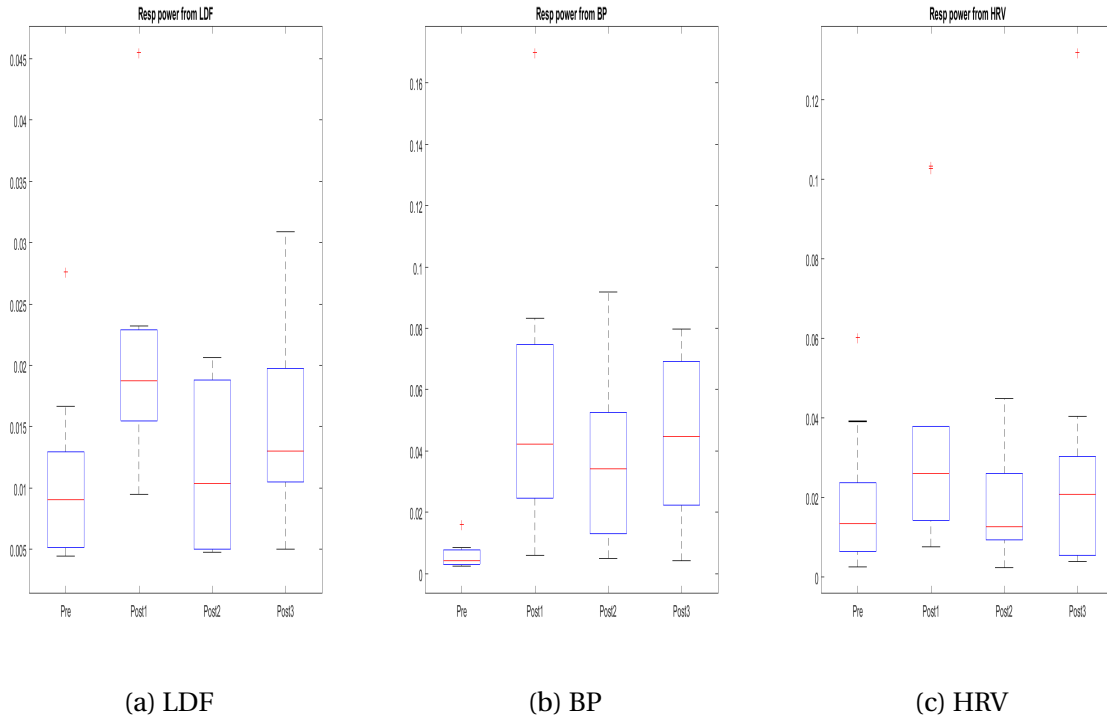


Figure 4.9: Power for the resp sub-band

4.2.2 Peak detection

A summary of the peak detections are presented in the table 4.7. By averaging over both sub-band and time segment it shows that the blood pressure signal has most peak detections with an average of 7.7, then follows LDF with 6.9 detections and HRV with 6.2. This is clear since the HRV can not detect the heart segment, by compensating for this the HRV detects on average 7.1 peaks.

4.2.3 Pre vs Post3

To see if the variables from after surgery has the same mean as after it was preformed a *t test* with a significance level, "alpha" of 0.15. The result from this test is showed in table 4.8. Where h equal 0 indicates that the *t test* does not reject the null hypothesis, where the null hypothesis is that the two data samples are from populations with equal means. The *p-value* for the test is shown in the p column. So if $h = 1$ it has been a significant change in mean in this variable from before to after surgery. The number postfixed to variable name tells which signal the variable is from, in this set up 1 corresponds to HRV, 2 to BP and 3 to LDF as this was the chosen signals in the analysis application. The NaN entries in the table is a result from to little data to do the test.

4.2.4 Poincare analysis

An example of a poincare analysis is shown in figure 4.22. It shows the analysis for each of the time segments. This is only done for the HRV signal.

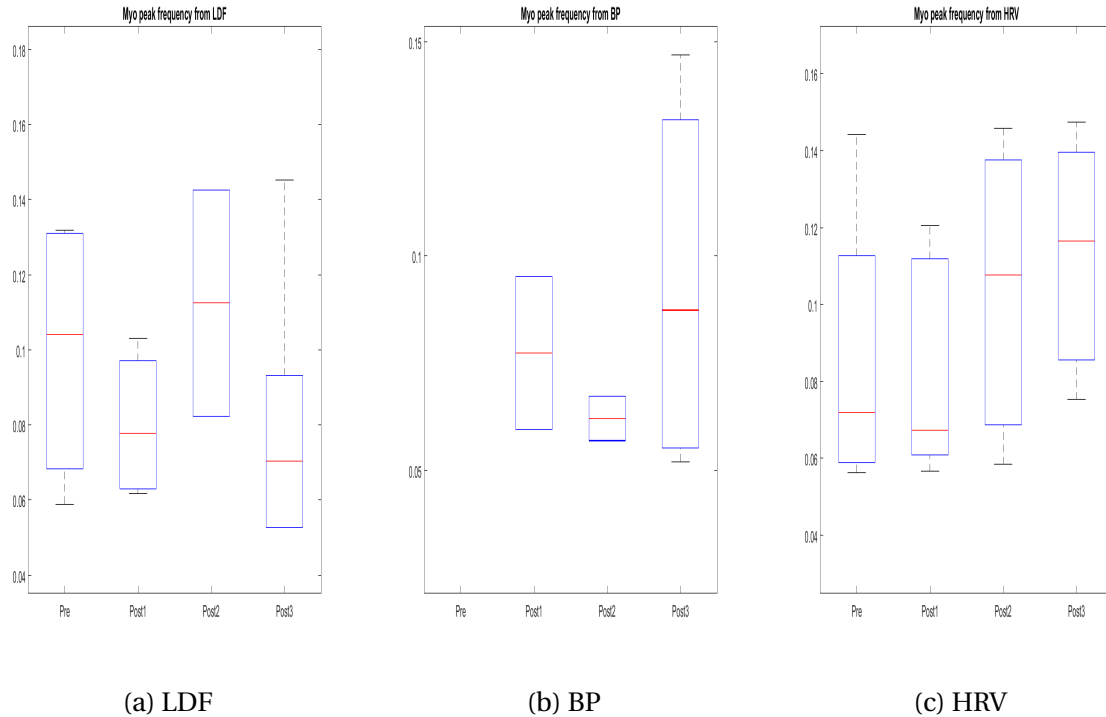


Figure 4.10: Peak frequency's for the myo sub-band

In the table 4.9 the values from the ellipse fitting technique for a quantitative analysis is shown. The er is also been done a *ttest* comparing the different post segments with the pre operative segment, the p-value from this test is shown in the table 4.9. The SD2 variable describes the long term variability of the HRV signal. This is the variation between the different RR values across the entire signal. This might be produced by trend in the signal or a low frequency oscillation. If there is no trend in the signal and the signal is only oscillating between two states this would produce no long term variability and SD2 would equal zero. SD1 equals the short term variability, more precise this represents the beat-to-beat(sample-to-sample) variability. If there where no variations in beat-to-beat, this means a single value through the entire signal the Pointcare plot would produce only a dot, and both SD1 and SD2 would be zero.

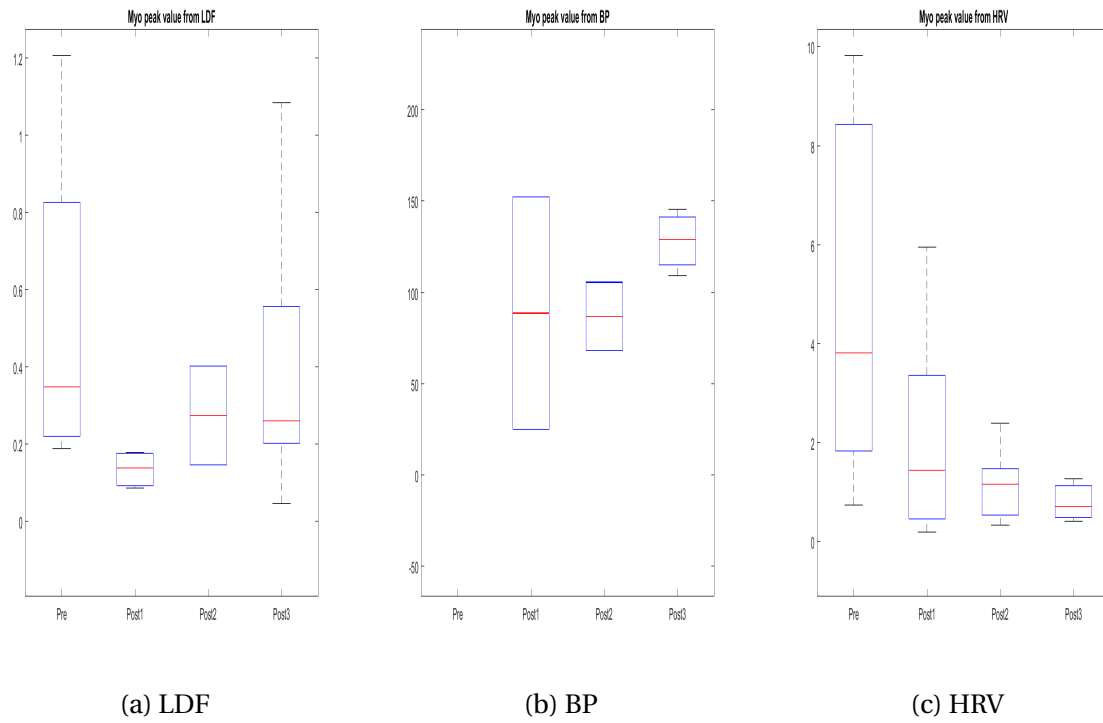


Figure 4.11: Peak value's for the myo sub-band

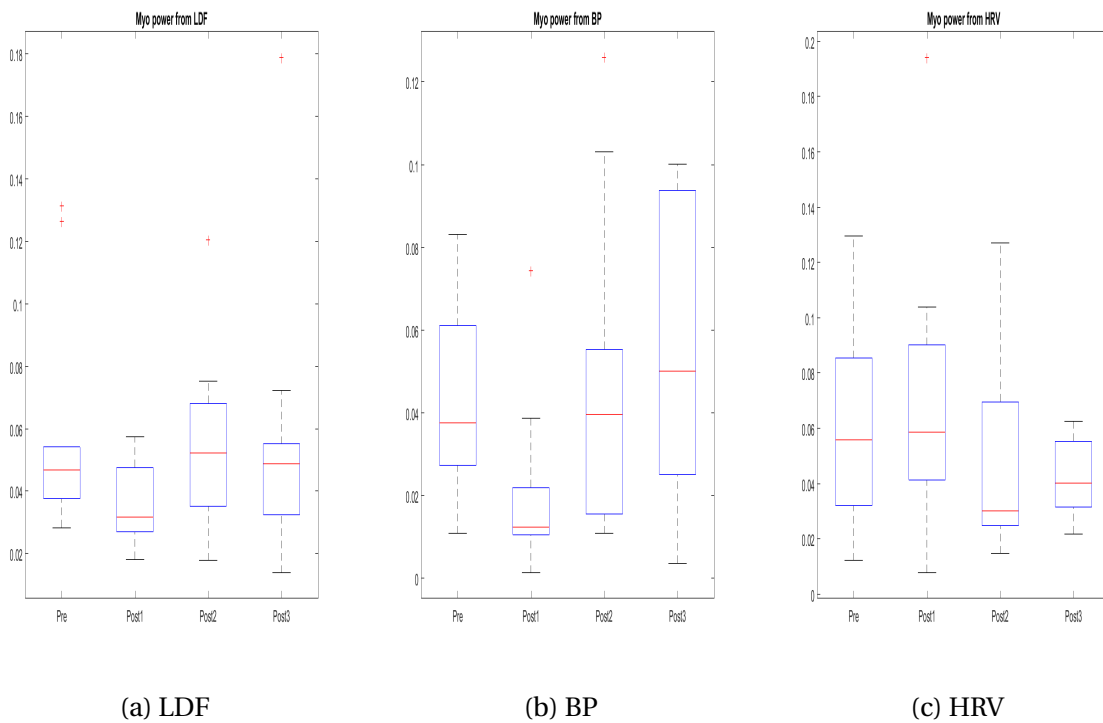


Figure 4.12: Power for the myo sub-band

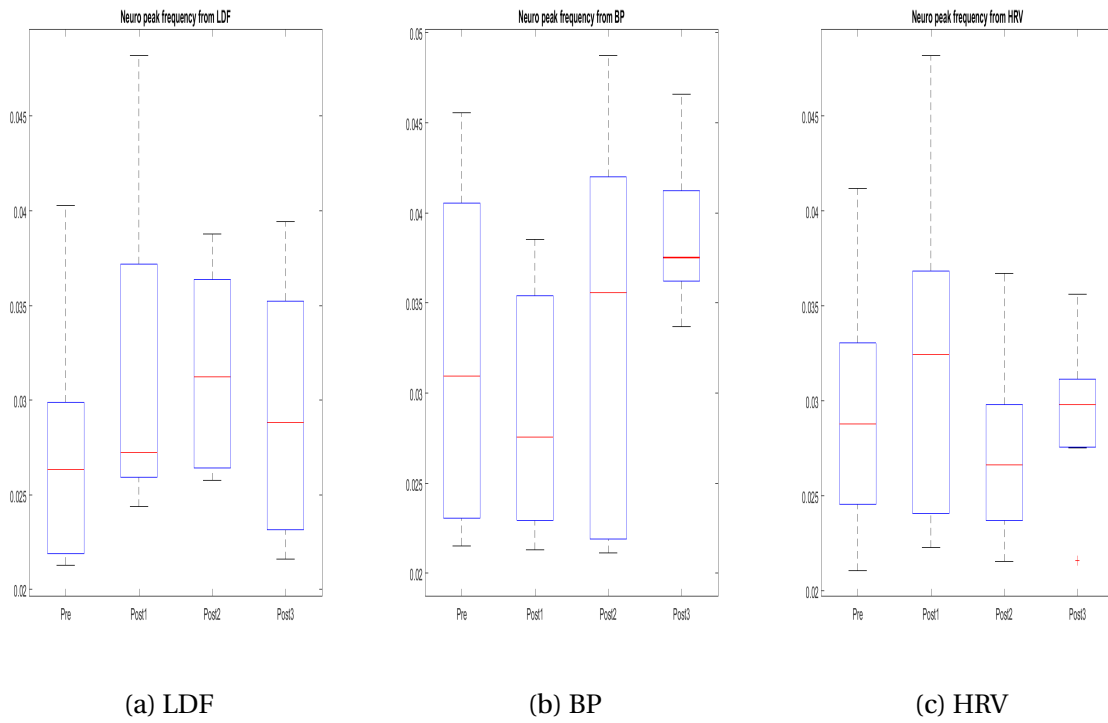


Figure 4.13: Peak frequency's for the neuro sub-band

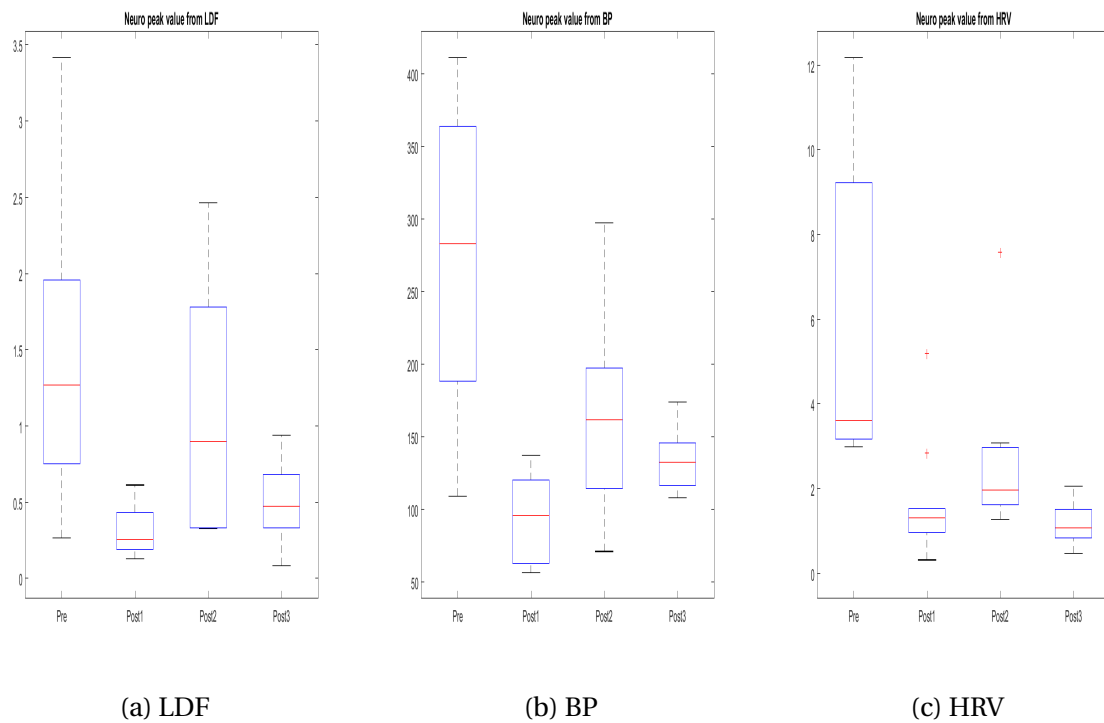


Figure 4.14: Peak value's for the neuro sub-band

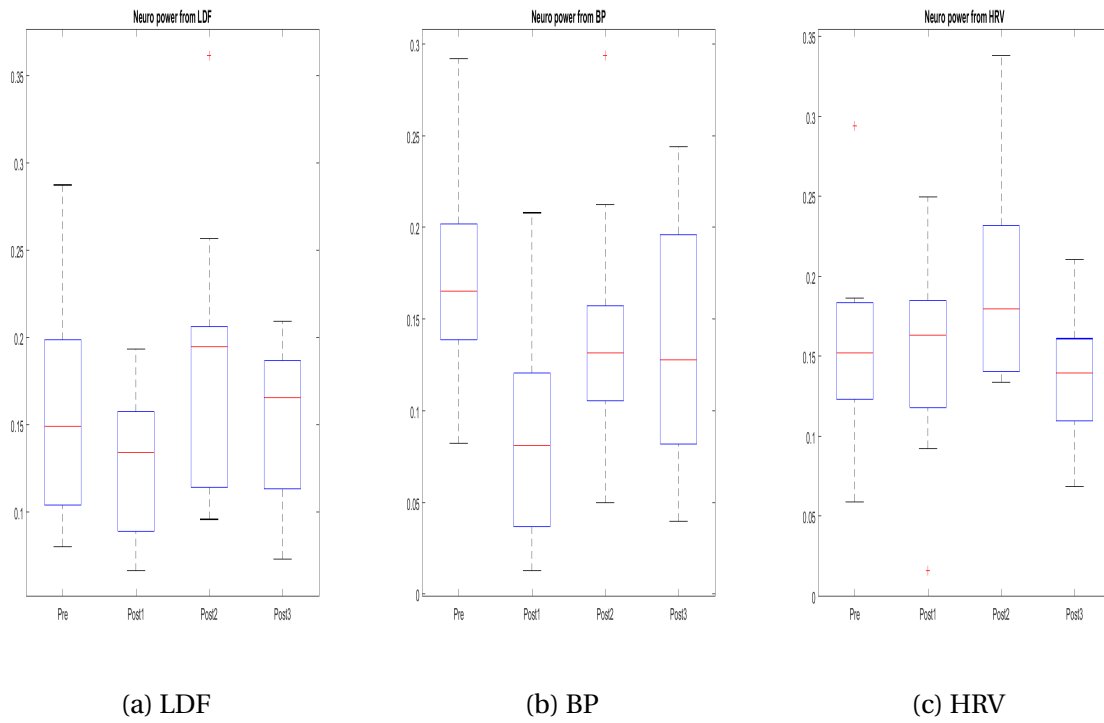


Figure 4.15: Power for the neuro sub-band

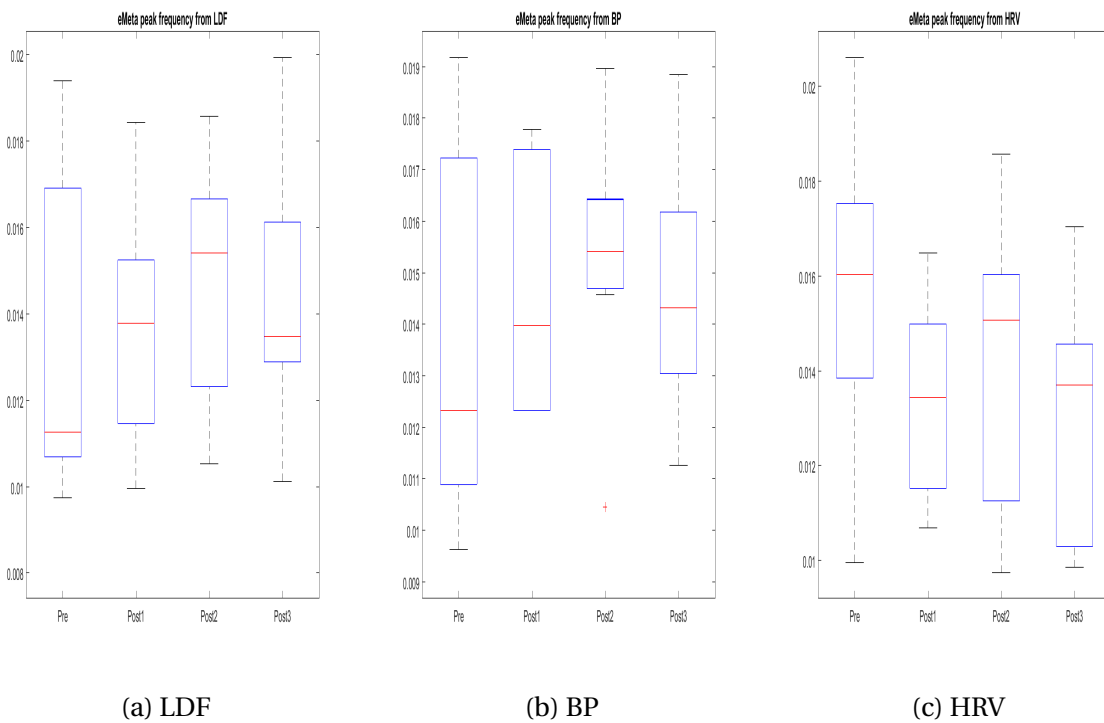


Figure 4.16: Peak frequency's for the eMeta sub-band

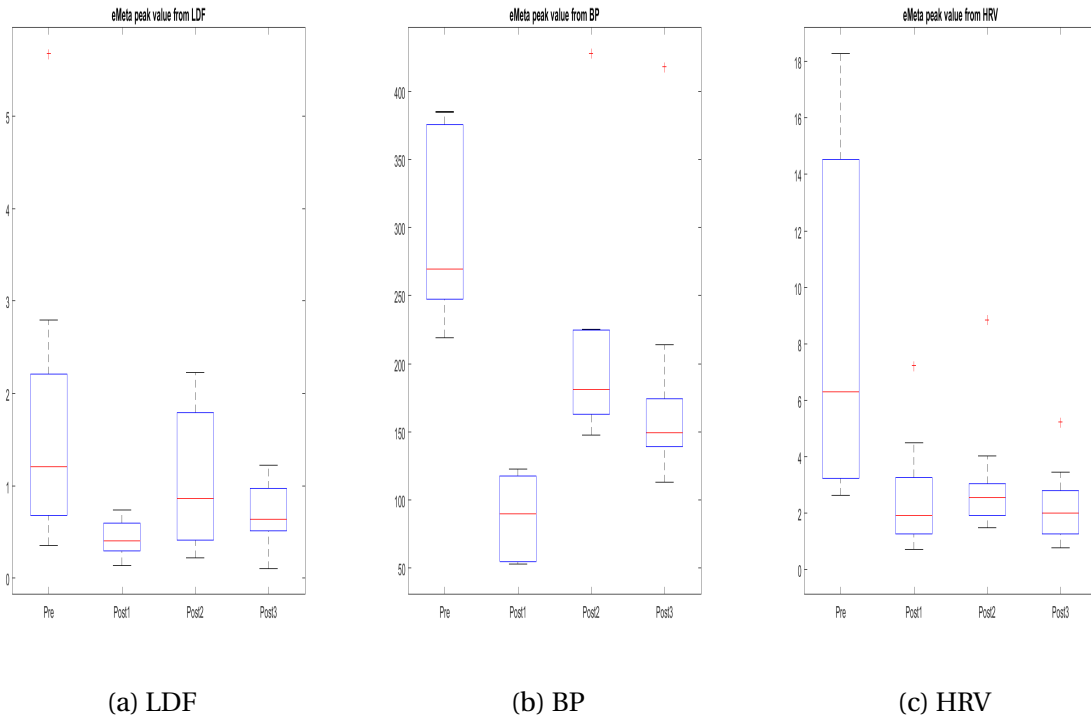


Figure 4.17: Peak value's for the eMeta sub-band

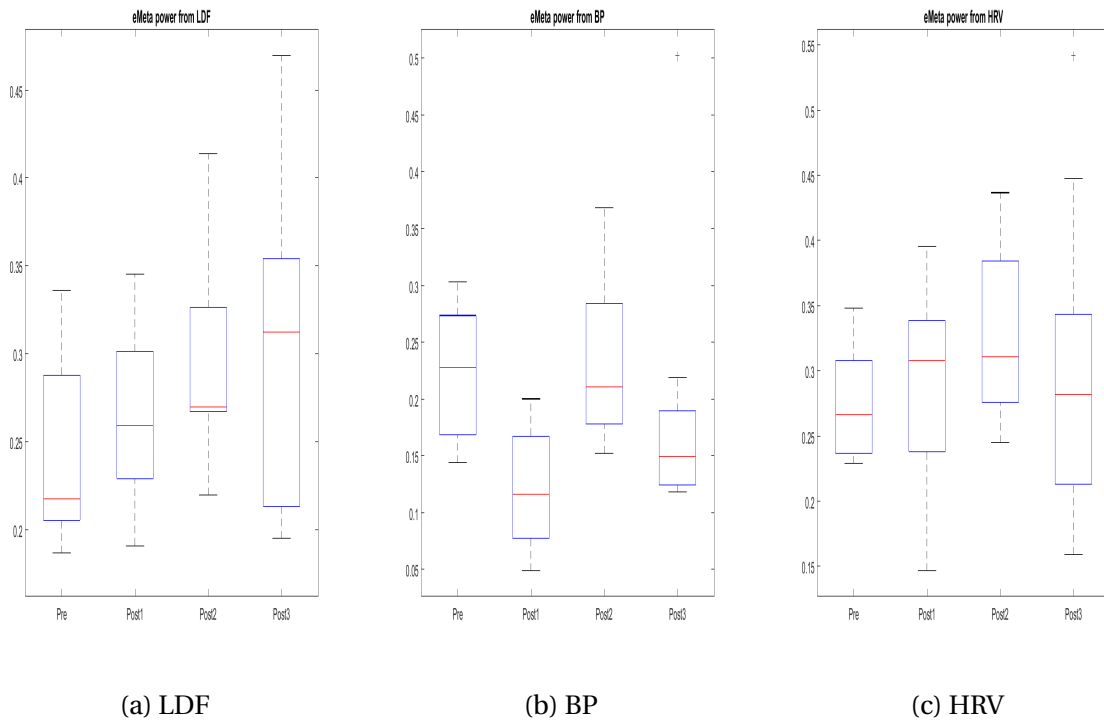


Figure 4.18: Power for the eMeta sub-band

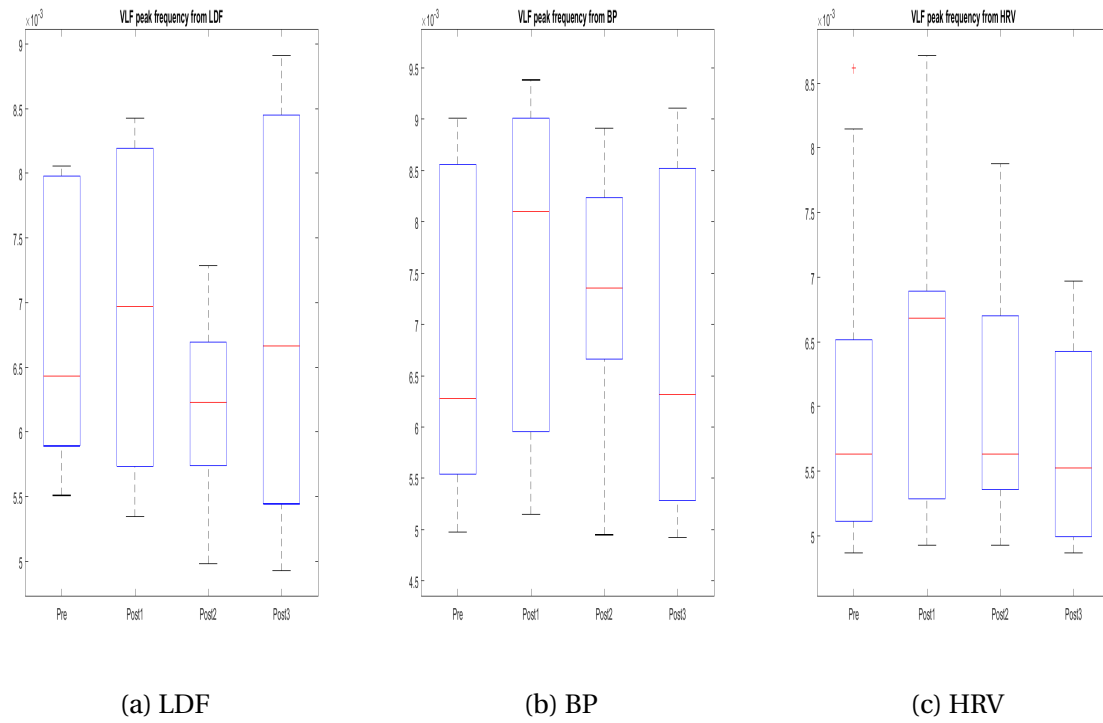


Figure 4.19: Peak frequency's for the VLF sub-band

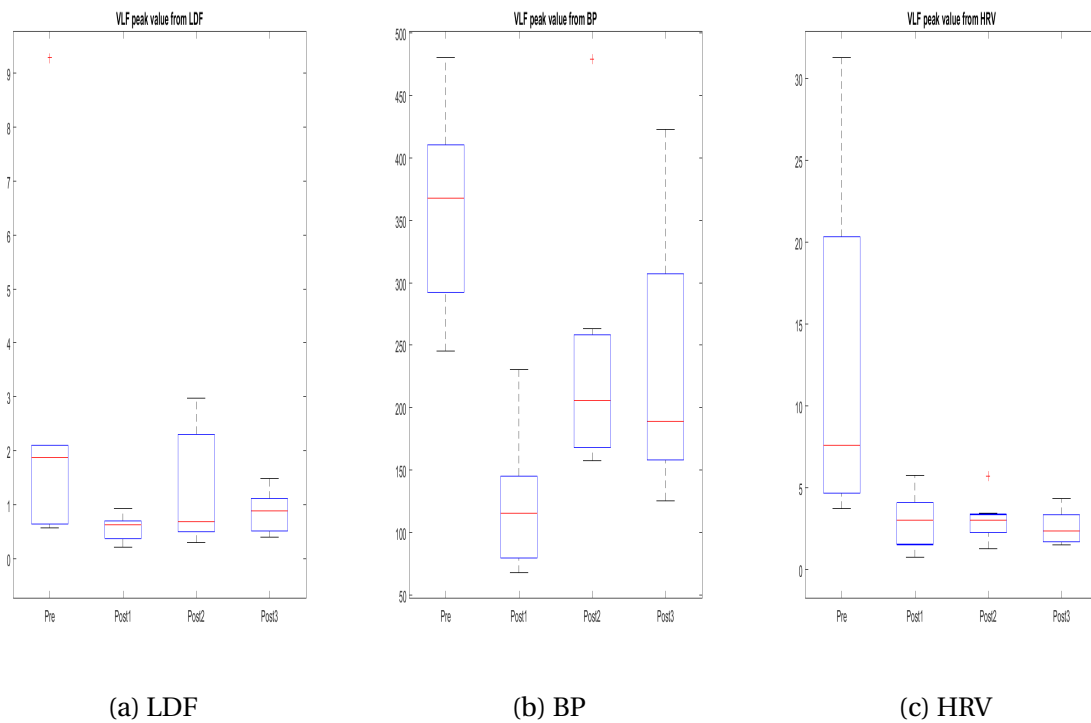


Figure 4.20: Peak value's for the VLF sub-band

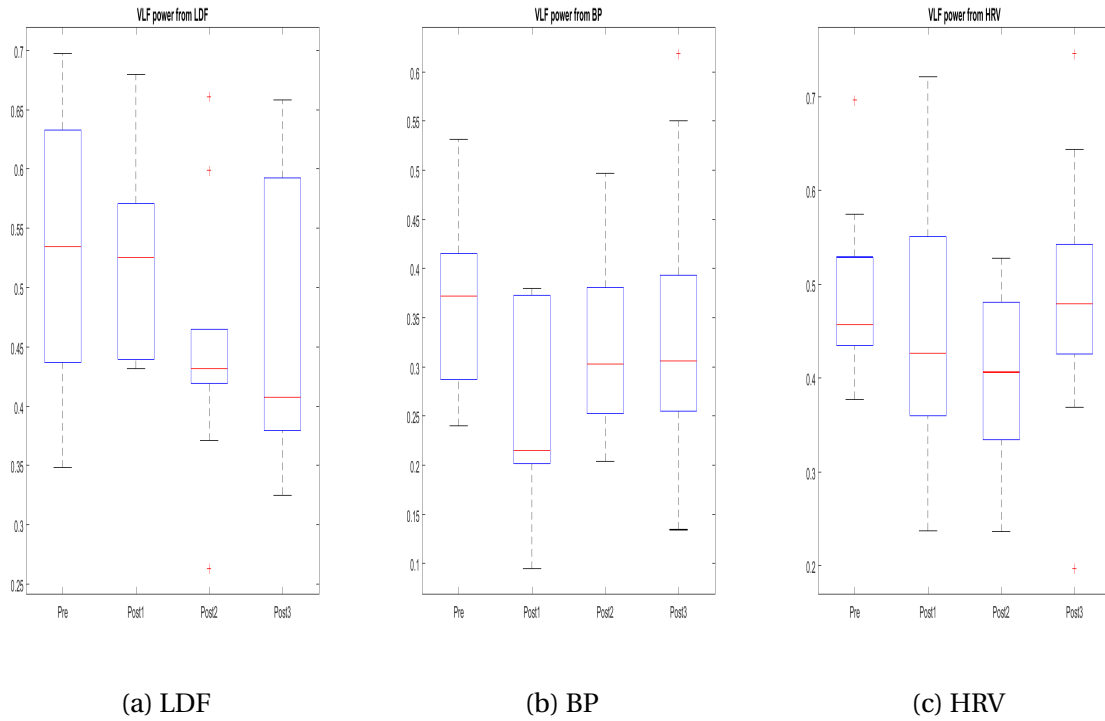


Figure 4.21: Power for the VLF sub-band

Table 4.7: Number of peaks detected for the sub-bands

	HR			Resp			Myo		
	HRV	BP	LDF	HRV	BP	LDF	HRV	BP	LDF
Pre	0	10	9	2	6	3	6	0	4
Post1	0	10	8	10	10	10	5	2	4
Post2	0	10	8	5	9	3	5	2	2
Post3	0	10	5	9	10	4	3	4	5
Avg	0	10	7.5	6.5	8.75	5	4.75	2	3.75

	Neuro			eMeta			VLF		
	HRV	BP	LDF	HRV	BP	LDF	HRV	BP	LDF
Pre	7	8	9	8	10	9	10	8	6
Post1	10	7	8	8	6	9	10	10	9
Post2	9	8	7	9	9	10	9	10	9
Post3	7	7	7	9	9	10	8	10	9
Avg	8.25	7.5	7.75	8.5	8.5	9.5	9.25	9.5	8.25

Table 4.8: T test for variables

Variable	h	p	Variable	h	p
'P1 HR'	NaN	NaN	'P1 neuro'	0	0.46336
'P2 HR'	1	0.14822	'P2 neuro'	0	0.20625
'P3 HR'	0	0.15579	'P3 neuro'	0	0.72839
'Peak sig1 HR'	NaN	NaN	'Peak sig1 neuro'	1	0.0078831
'Peak sig2 HR'	1	0.083472	'Peak sig2 neuro'	1	0.0065841
'Peak sig3 HR'	0	0.28169	'Peak sig3 neuro'	1	0.032807
'Peak freq1 HR'	NaN	NaN	'Peak freq1 neuro'	0	0.99644
'Peak freq2 HR'	1	0.018528	'Peak freq2 neuro'	1	0.1026
'Peak freq3 HR'	1	0.11679	'Peak freq3 neuro'	0	0.55259
'P1 Resp'	0	0.41193	'P1 eMeta'	0	0.4913
'P2 Resp'	1	0.00013616	'P2 eMeta'	0	0.38454
'P3 Resp'	0	0.19563	'P3 eMeta'	1	0.057811
'Peak sig1 Resp'	1	0.033119	'Peak sig1 eMeta'	1	0.0087197
'Peak sig2 Resp'	1	0.005038	'Peak sig2 eMeta'	1	0.0045271
'Peak sig3 Resp'	0	0.86232	'Peak sig3 eMeta'	1	0.076648
'Peak freq1 Resp'	0	0.46678	'Peak freq1 eMeta'	1	0.10575
'Peak freq2 Resp'	1	0.083843	'Peak freq2 eMeta'	0	0.38227
'Peak freq3 Resp'	0	0.19992	'Peak freq3 eMeta'	0	0.47046
'P1 Myo'	1	0.11151	'P1 VLF'	0	0.97459
'P2 Myo'	0	0.5771	'P2 VLF'	0	0.6258
'P3 Myo'	0	0.87251	'P3 VLF'	0	0.23481
'Peak sig1 Myo'	1	0.11408	'Peak sig1 VLF'	1	0.011091
'Peak sig2 Myo'	NaN	NaN	'Peak sig2 VLF'	1	0.015727
'Peak sig3 Myo'	0	0.69612	'Peak sig3 VLF'	1	0.1111
'Peak freq1 Myo'	0	0.31504	'Peak freq1 VLF'	0	0.53449
'Peak freq2 Myo'	NaN	NaN	'Peak freq2 VLF'	0	0.89165
'Peak freq3 Myo'	0	0.44776	'Peak freq3 VLF'	0	0.75467

Table 4.9: Poincare analysis

	Pre	Post1		Post2		Post3	
	Value	Value	p-Value	Value	p-value	Value	p-Value
SD1	0.0767 ± 0.2002	0.0280 ± 0.0344	0.1555	0.0260 ± 0.0144	0.1076	0.0291 ± 0.0175	0.1295
SD2	0.1779 ± 0.2225	0.0543 ± 0.0401	0.0358	0.0515 ± 0.0241	0.0215	0.0545 ± 0.0139	0.0196
SDR	0.4920 ± 0.2296	0.5638 ± 0.2090	0.9009	0.5699 ± 0.2191	0.7778	0.6672 ± 0.3051	0.1756

The values are presented as median ± SD

The p-Values are compared to the baseline(pre segment)

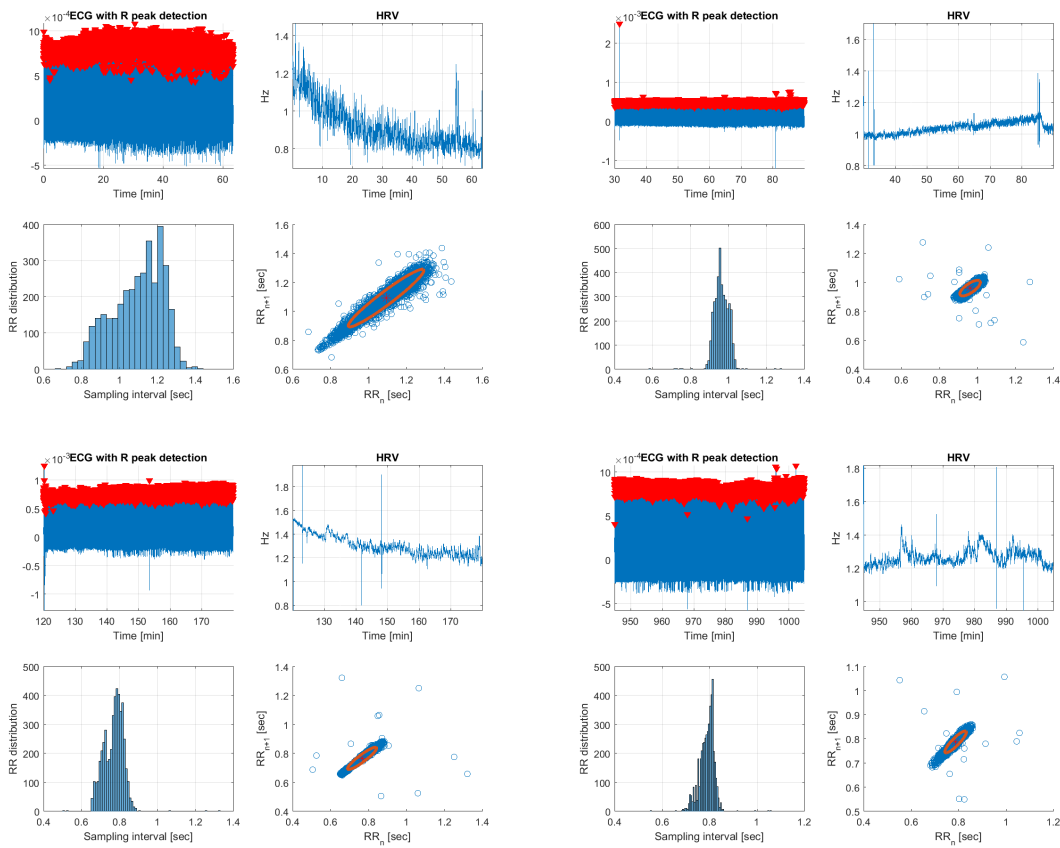


Figure 4.22: Poincare plots of 160317 from pre(top left), post1(top right), post2(bottom left) and post3(bottom right)

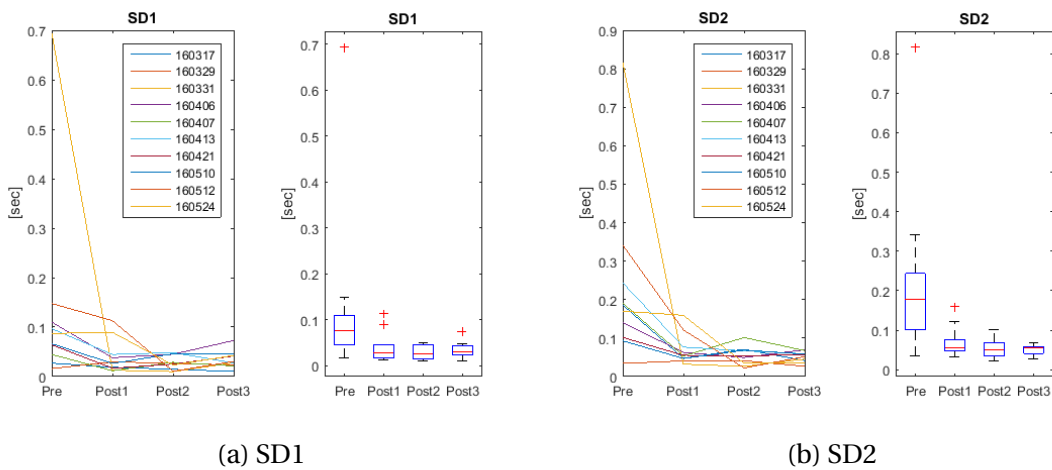


Figure 4.23: Evolution for SD1 and SD2

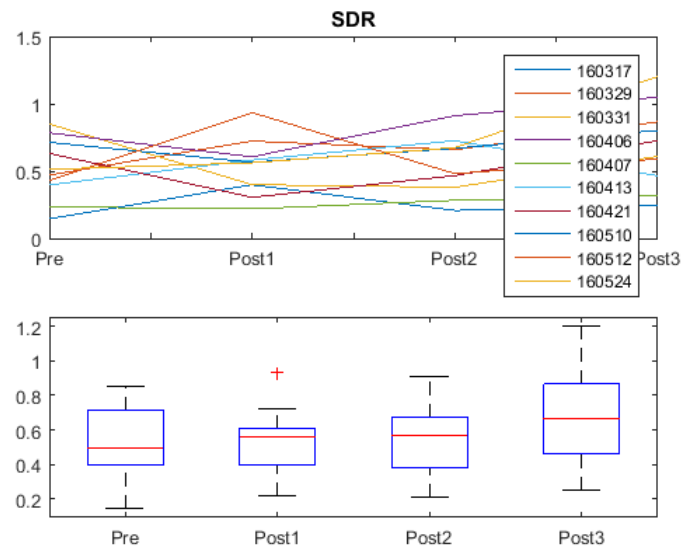


Figure 4.24: Evolution for the ratio $SD1/SD2$

Chapter 5

Discussion

The discussion will mostly cover the results from the analysis of the patients data. The application for the frequency analysis is a working application, it has some improvements which could be done such as implement the two applications in one, other analysis methods and smarter loading of the signals. Some discussion about the analysis set up follows in the first section, thereafter follows the discussion around the analysis.

5.1 Application and analysis set up

As the ECG signal not was meant for the actual study, but just the source for the HRV signal, it could have been wise to do some processing of the ECG signal. This could give a better HRV signal as there would not be that much variations in the R peaks. This can sometimes be seen in the HRV signals as a spike up or down depending on if the program detected a R peak to much or to little. This was not done because of a misunderstanding, where it was believed that the ECG signals was one of the signals of interest and not the HRV.

As seen in figure 3.12 the removal of the motion artifacts removes a lot of the low frequency interesting content but, it also removes some of the noise. The removal of the motion artifacts makes it possible to detect the HR frequency, this means it might have been wise to use this method as this could revealed some more peaks and given better data.

5.2 Peak detections

The patients data is gathered from only 10 patients, this is a fairly small data set, which decreases the confidence of the analysis. The few number of patients gets even more critical when it is not possible to detect peaks in all the hypothesized sub-bands. This leaves two variables(peak frequency and peak value) varying from 0 to 10 detections. The last variable(power) is independent from the peak detection and gives a value for all the 10 patients.

The peak detections shows that there is detected peaks in most of the sub-band with on average 70-80% detections for HR,Resp, Neuro, eMeta and VLE. This shows that there is some activity in these frequency ranges. The Myo sub-band has only 20-47% detection which is very low. This is strange as this is one of the most studied low frequency sub-bands[37],[38]. The peak detection algorithm could be more sophisticated with a prominence criteria, this would exclude

some peaks which might be noise. At the same time with this criteria it would not detect peaks which is barely higher than the noise, which could be seen for the heart rate in the LDF signal some times. It is believed that it detects more "correct" peaks than peaks known to be wrong, this is of course hard to say for certain as the low frequency content is very little studied. An idea would be to add the prominence of the peak as a variable for determining the validity of the peak and variables corresponding to the peak.

5.3 Trend analysis

As the signals HRV, LDF and BP are obtained in different ways, this gives different kind of noise sources. All the signals are though measuring global variables of the same system. This gives an idea to a theory that if there is a similar trend in the different signals this must be from a underlying physiological activity. This theory is used in defining the sub-bands, but could also be used to see if there are some changes in the underlying physiology in different time segments. In our case this is used to see if the cardiac surgery is giving some changes in the chosen variables before and in the three different time segments after surgery.

5.3.1 Heart rate

The heart rate is easily detected in both LDF and BP. The peak frequency shows a clear trend that could distinguish the different time segments. Also for the power variable it is possible to see a trend through out the time segments. All the peak frequency variables also show a statistical change from before surgery to the next morning. The fact that the same variable from the different signals shows the same evolution indicates that there has been a change in the underlying physiology.

5.3.2 Respiratory rate

The respiratory peak frequency shows a clear trend of the mean in each segment, but with high variance. The high variance in the variables brings uncertainty to the trend. For the peak value variable there is no clear trend, but there is shown a statistical change from pre to the post3 segment in two of the signal, the BP and HRV. These two signals have opposite trends and are therefor considered as a random change, maybe because of to little data.

For the power variable there is a clear trend for the mean, similar to the trend of the power variable of the HR sub-band. But the high variances makes only the BP signal give a statistical change in power.

5.3.3 Myogenic activity

In the myo sub-band there was very few peak detections, this induces great uncertainty around the variables dependent on the peak detection. For the peak frequency there is no common trend in the signals, but the variables from the LDF signals has a similar trend to the respiratory sub-band peak frequency trend. The peak value shows no clear trend but for the variables from the HRV signal it is seen a significant change in peak value, quite similar to the change in the

resp sub-band for the same variable and signal. For the power it is no clear trend for all the signals, if anything there is an opposite trend in LDF and BP compared to the trend in the HR, and resp sub-bands for the same variable.

5.3.4 Neurogenic activity

For the neurogenic activity there is no clear trend in peak frequency, but the peak value has a very distinct trend for all the signals, all these also shows a statistical change from pre to post3. The power variables have the same trend from the LDF and BP signals, but the variance is much higher in this variable.

5.3.5 Metabolic activity

In the eMeta sub-band there is some different trends and similarities but, the most evident is in the peak value variable where all the signals, shows a similar trend with a high value pre operative a short oscillation and much lower value in post3 than pre operative, this is similarly to the neuro sub-band. There is shown a statistical change from all the signals in the peak value variable from before to after surgery.

The peak frequency shows some similarity between LDF and BP but the interquartile range and the variance is large. It is interesting that the power variables from LDF and HRV has the same evolution.

5.3.6 VLF

The VLF sub-band has only one evident trend, that is in the peak value which shows a clear trend similar to the evolution in the Neurogenic and eMeta sub-bands. There is also a statistical change in the peak value from before the surgery to the next morning.

5.3.7 Similarities

It is seen that the HR, resp and partly the myo sub-bands have a similar trend for the peak frequency with a high value before surgery, decrease to the post1 increase to post2 and then a decrease in post3. The HR and resp sub-band also have a similarity in the evolution of the power, where the trend is opposite the one in the peak frequency. This evolution is also partly seen in the myo sub-band, especially for the LDF and BP signal. This might be to keep a cardiac output at a steady level. Lower frequency needs higher power to push more blood from a higher stroke volume[39]. This could be seen as a way to keep the stability of the system. The relation between the heart rate, stroke volume, blood pressure and resistance of the blood vessels are seen in equation 2.8.

The peak value shows a very distinct trend for the lower sub-bands, neuro, eMeta and VLF, from a high value before surgery, decrease after surgery a small increase to the post2 segment and decrease to the last segment post3. The values changes from high before to much lower in last segment. This change is shown as statistical significant.

Table 5.1: Number of statistical significant changed variables from pre to post3

	HR	Resp	Myo	Neuro	eMeta	VLF	Tot
Statistical significant variables	4	4	2	4	5	3	22
Total variables	6	9	9	9	9	9	54
%	67	44	22	44	55	33	40

5.4 Pre vs Post3

The change from before the surgery(pre segment) to the next morning(post3 segment) shows that 22 of the variables are from populations with different means. This means a statistical change in 22 of the 54 variables.

It is specially seen a change in the lowest sub-band, neuro, eMeta and VLF and for the peak_value where there is a statistically change for all the peak_value variables of these sub-bands. This is 9 of the 22 variables that have changed statically. This means that almost 50% of the statistically significant changes happen in 9 of the 54 variables that is 17% of the variables. For the HRV signal all the peak_value variables has a statistical significant change.

By looking at the other variables with a statistical significant change it is seen that these are distributed evenly on the remaining variables, with a slight lean towards the HR and resp sub-band.

5.5 Poincarè analysis

The Poincare analysis shows a decrease in complexity for the HRV after the surgery. The quantitative variables from the ellipse fitting technique shows a statistically significant drop in SD1 and SD2 with a significant level of 0.15. This is specially seen in SD2 with significant p-values lower than 0.05. This is quite similar to the results from Laitio et al. [40] and the general decrease in complexity by Lakusic et al. [11]. For the ratio SDR it is seen an increase in the median, but not significantly. Laitio et al. has in their paper got significance level above 0.01 and 0.001 for SD1 and SD2, but they have a much larger data set.

The decrease in complexity is also seen for HRV in the low frequency sub-bands neuro, eMeta and VLF peak_value variable. By comparing the boxplots for SD1 (figure 4.23a), SD2 (figure 4.23b) and the peak_value (figures 4.14, 4.17, 4.20) from the lower frequency bands it is seen quite a similar trend. This is expected as these variables are linked. A low frequency oscillation would increase the overall variability of the signal, which is measured by the SD2 variable. A decrease in the low frequency would be seen in the spectrum by a lower value for this frequency, and therefor also decrease the SD2 variable.

Chapter 6

Summary and Conclusion

This thesis has investigated the low frequency content from the cardiovascular system by using three different signals. These signals are; heart rate variability, blood pressure and a flow signal of the blood (Laser doppler flow). All the signals are global variables of the cardiovascular system collected in completely different manner. The low frequency content from these three different signals has been compared for patients doing cardiac surgery. Four time segments of one hour each has been collected, one before the surgery (pre operative segment) and three after surgery (post operative segments, post1, post2 and post3, are seen in table 3.2). The low frequency evolution over these segments has then been analysed. The frequency analysis has been done using a continuous wavelet transform, averaging the frequencies over the time segment. This produces three frequency spectrum's for each time segment, one for each of the signals heart rate variability, blood pressure and laser doppler flow. The evolution of these spectrum's over the time segments are then studied. A Poincare analysis for the HRV signal has been done to verify some of the results.

6.1 Conclusion

There are two main findings in the analysis. First there is a similar trend in sub-bands HR, resp and partly the myo sub-band, where the peak frequency for all shows a similar evolution over the time segments. This is seen in the figures 4.3 4.7 and 4.10. Also for the power variable there is a similar trend over the time segments. It is interesting that this trend is opposite to the peak frequency trend. As discussed this might be to keep some kind of stability in the system. The evolution for the power variables are seen in the figures 4.5, 4.9 and 4.12.

Second finding is the similar trend in the lower sub-bands, neuro, eMeta and VLF. For the mentioned sub-bands the peak value variable has all the same evolution over the time segments. This is seen in the figures 4.14, 4.17 and 4.20. These variables also shows a statistical significant change from before the surgery to the last and most stable segment after the surgery, this is seen in the table 4.8. The trend from the peak value also recur in and is strengthened by the variables from the Poincare analysis. The values from the Poincare analysis show significant decrease from before to after surgery. This is similar to the findings in the study by Laitio et al. [40] and Lakusic et al. [11].

6.2 Recommendations for Further Work

For further work it is important to increase the amount of data. This would give a better statistical foundation.

Finding a better way of comparing time-frequency evolution without averaging either time segments or the frequency spectrum would give a much better understanding of the smaller and transient reactions of the cardiovascular system. It would be interesting to compare the CWT coefficients for time-frequency. Also improving the frequency spectrum comparison without using variables and compare the entire spectrum would be interesting. This gives a much higher degree of freedom, than with just a few averaged variables.

By looking at frequency spectrum's in relation to each other might also preserve the inter-personal differences and give more accurate results. This would possibly reduce the variance in the variables if the variables were dependent on the previous variable.

Introduction of a control group could validate the effects of the operation. It would be interesting to compare if the low frequency content from a patient how has gone through heart surgery is more similar a healthy subject.

Appendix A

Cwt mean plots

This appendix shows all the frequency plots for the patients for every signal and every time segment. The signals are ordered as one signal per column and the time segments are one time segment per row. this gives the set up as shown in table A.1.

Table A.1: Shows set up for the cwt mean plots

	HRV	BP	LDF
Pre	Pre HRV	Pre BP	Pre LDF
Post1	Post1 HRV	Post1 BP	Post1 LDF
Post2	Post2 HRV	Post2 BP	Post2 LDF
Post3	Post3 HRV	Post3 BP	Post3 LDF

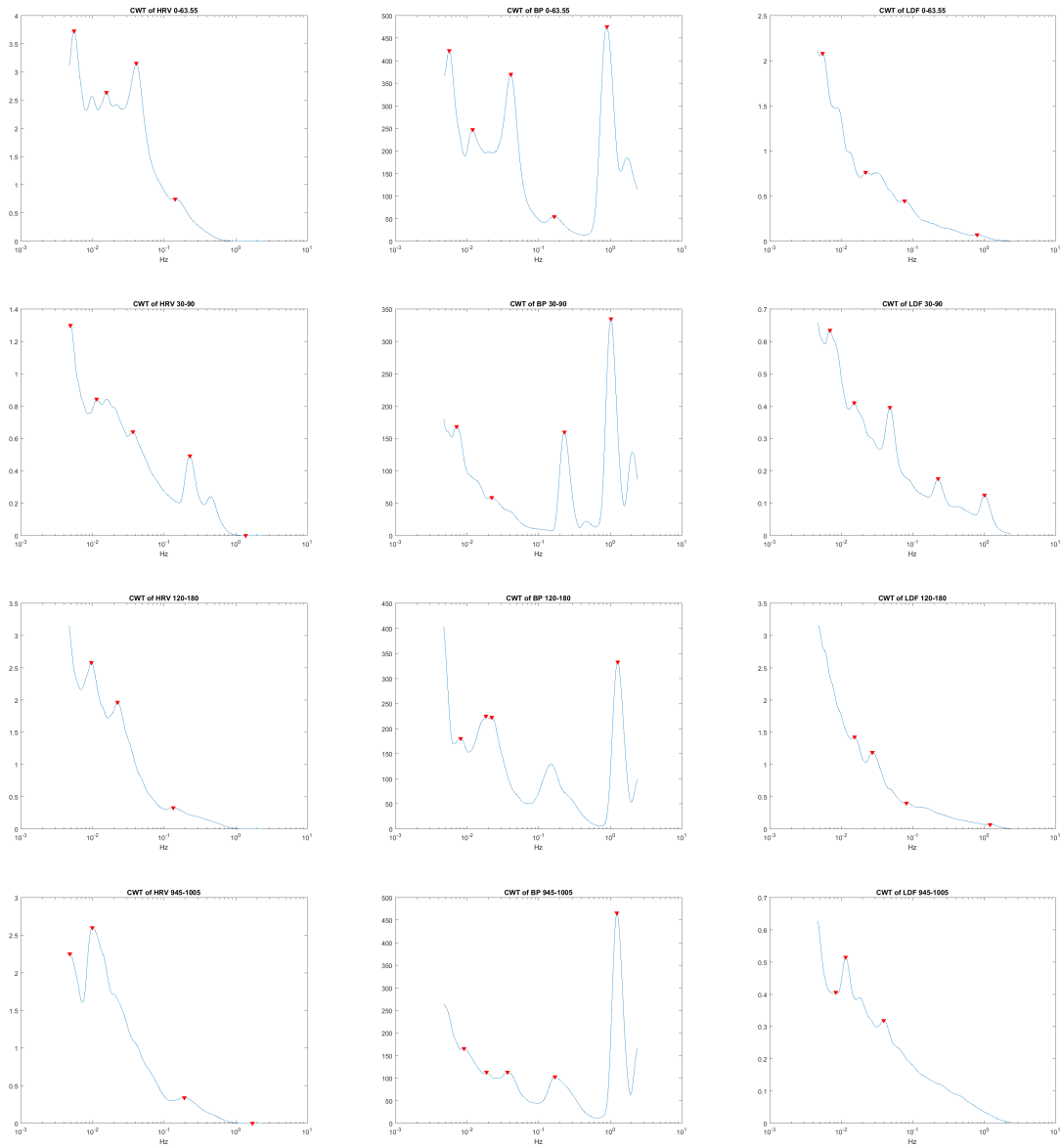


Figure A.1: CWT mean of 160317

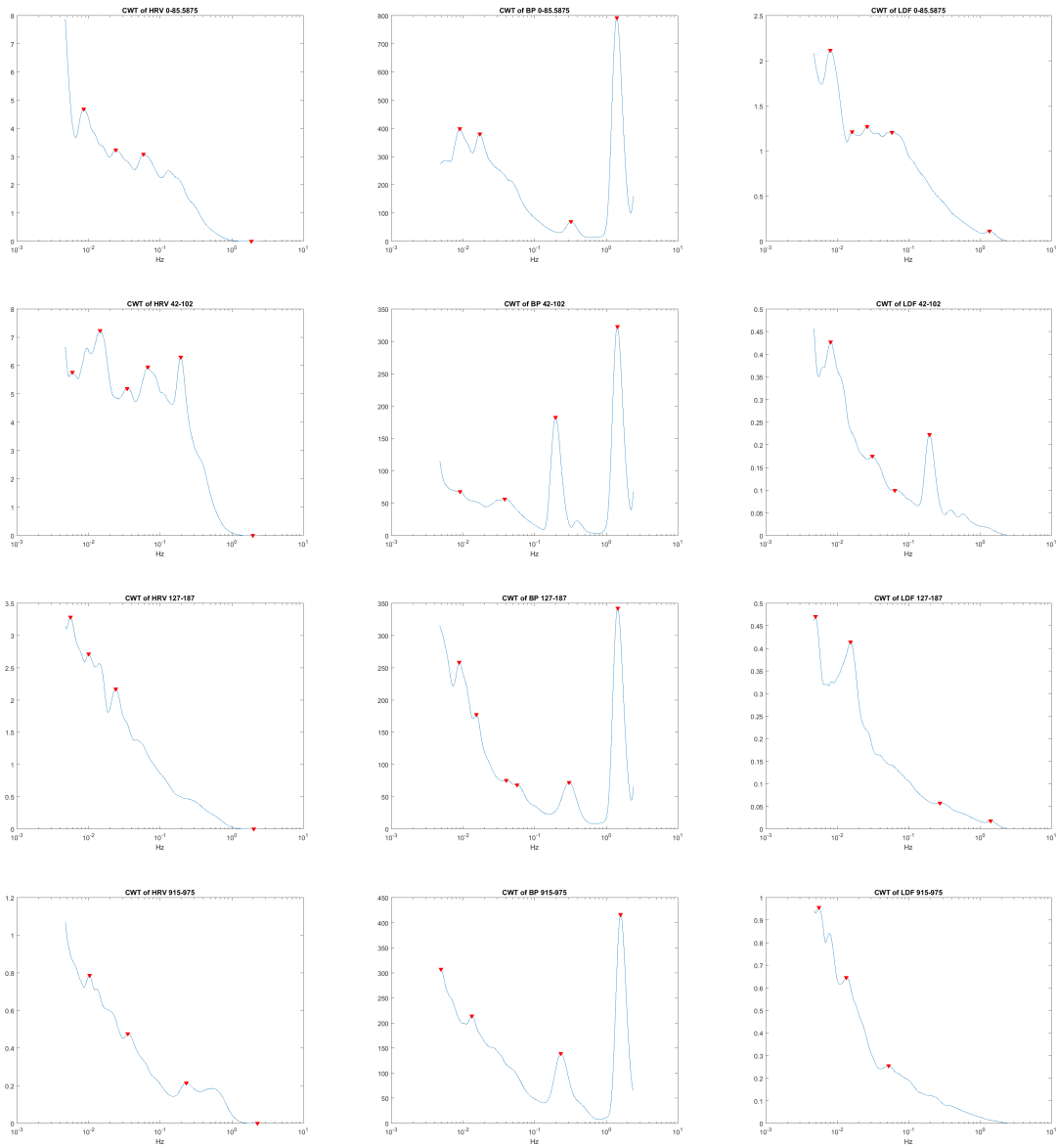


Figure A.2: CWT mean of 160329

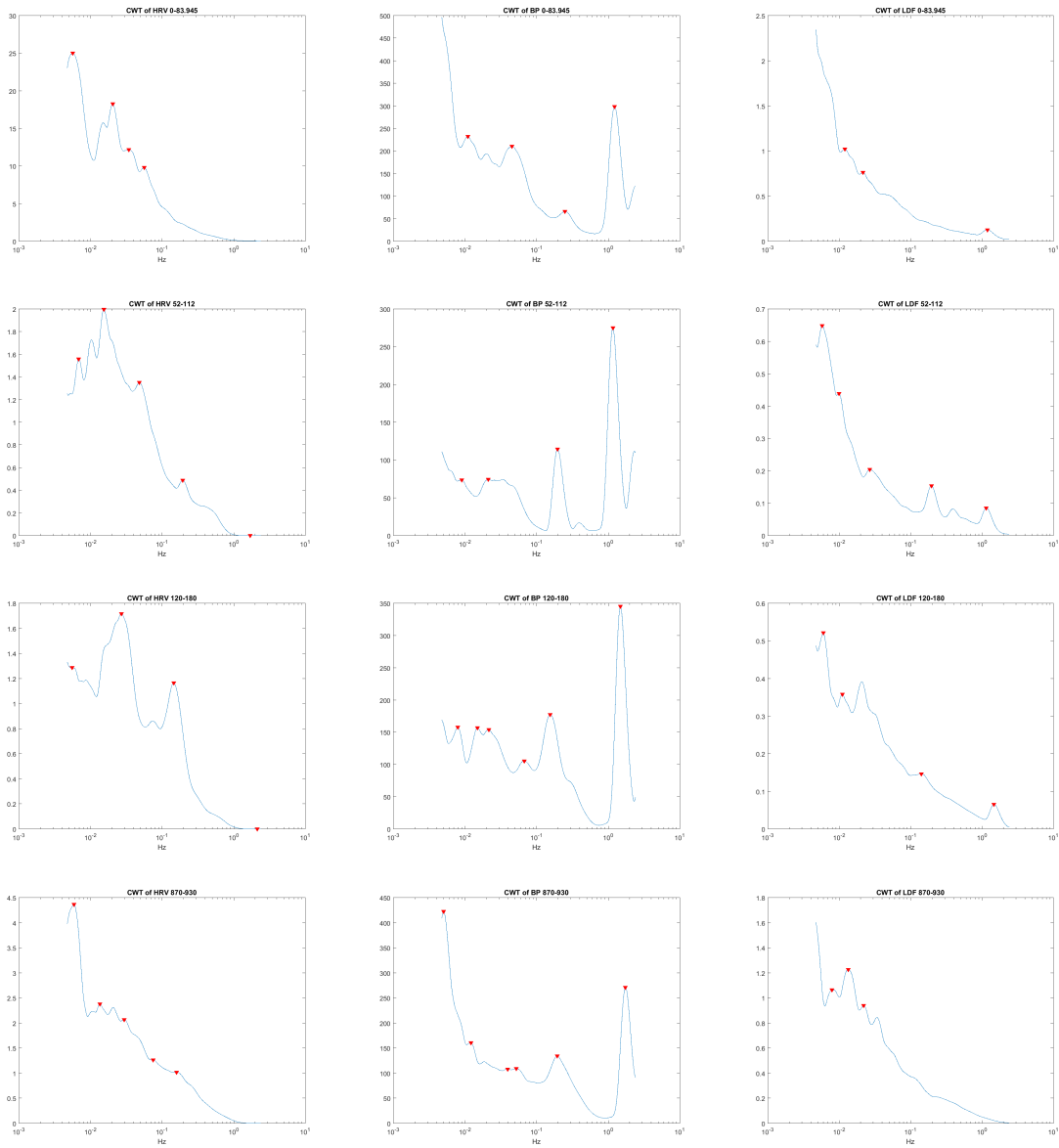


Figure A.3: CWT mean of 160331

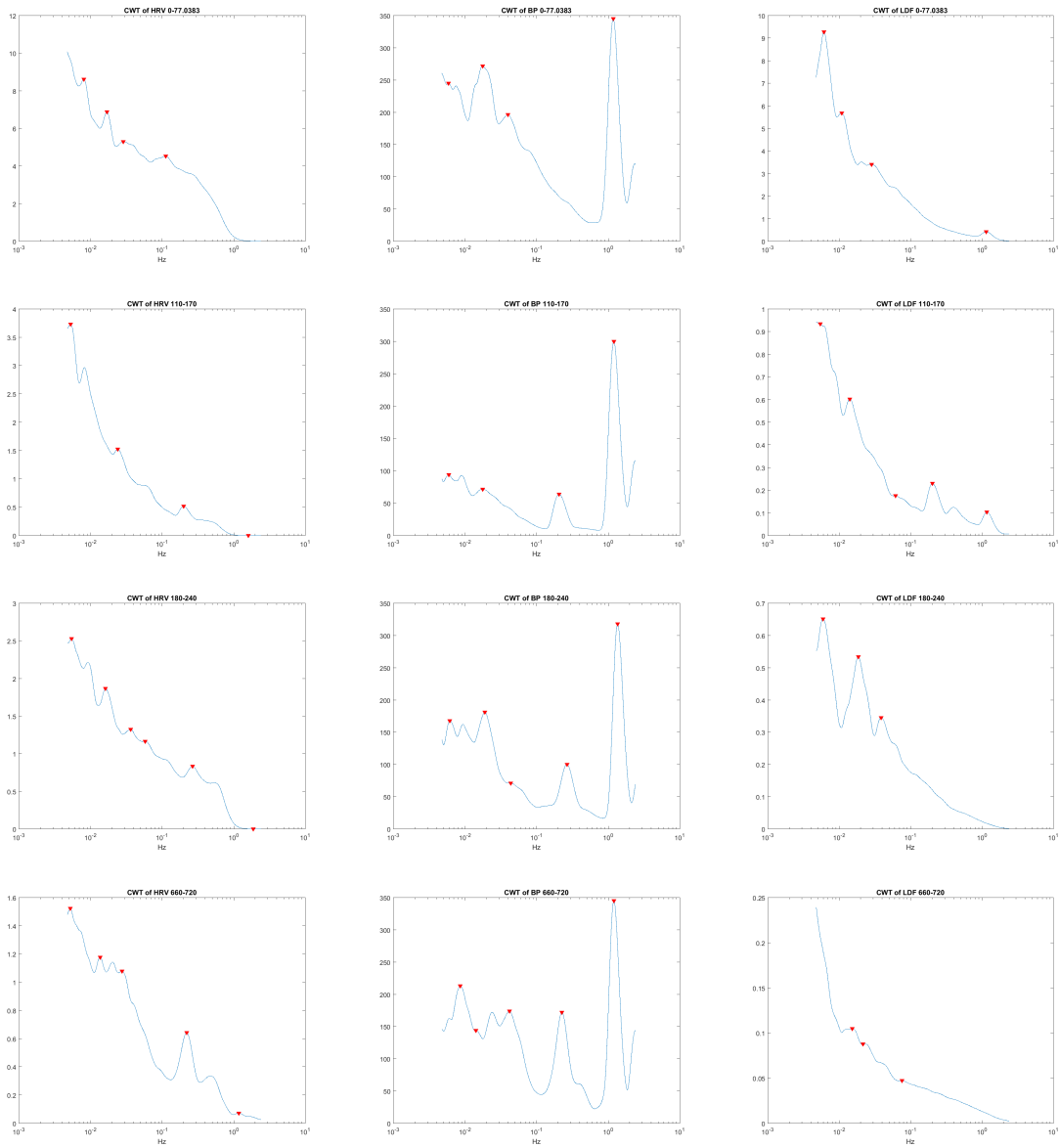


Figure A.4: CWT mean of 160406

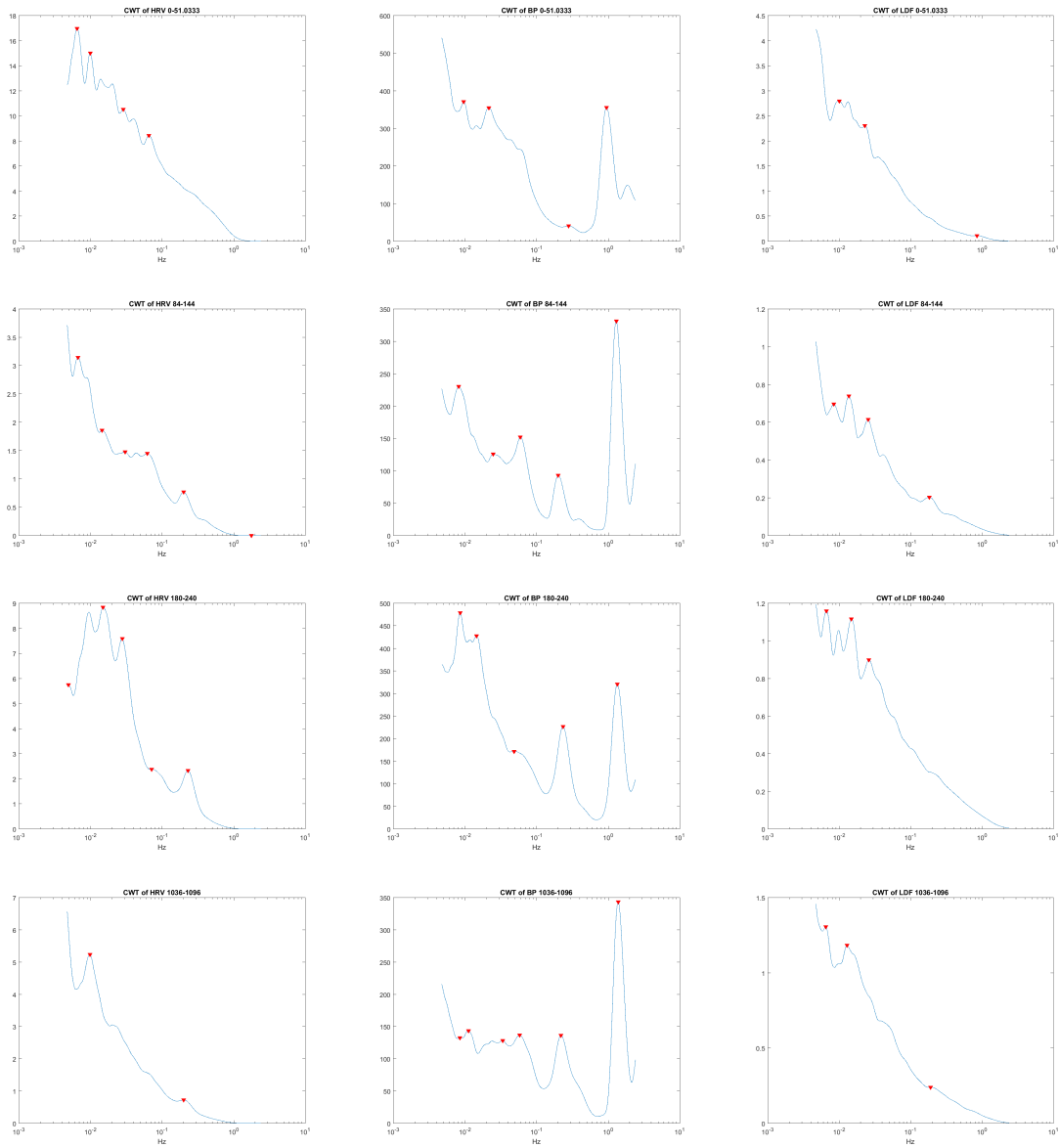


Figure A.5: CWT mean of 160407

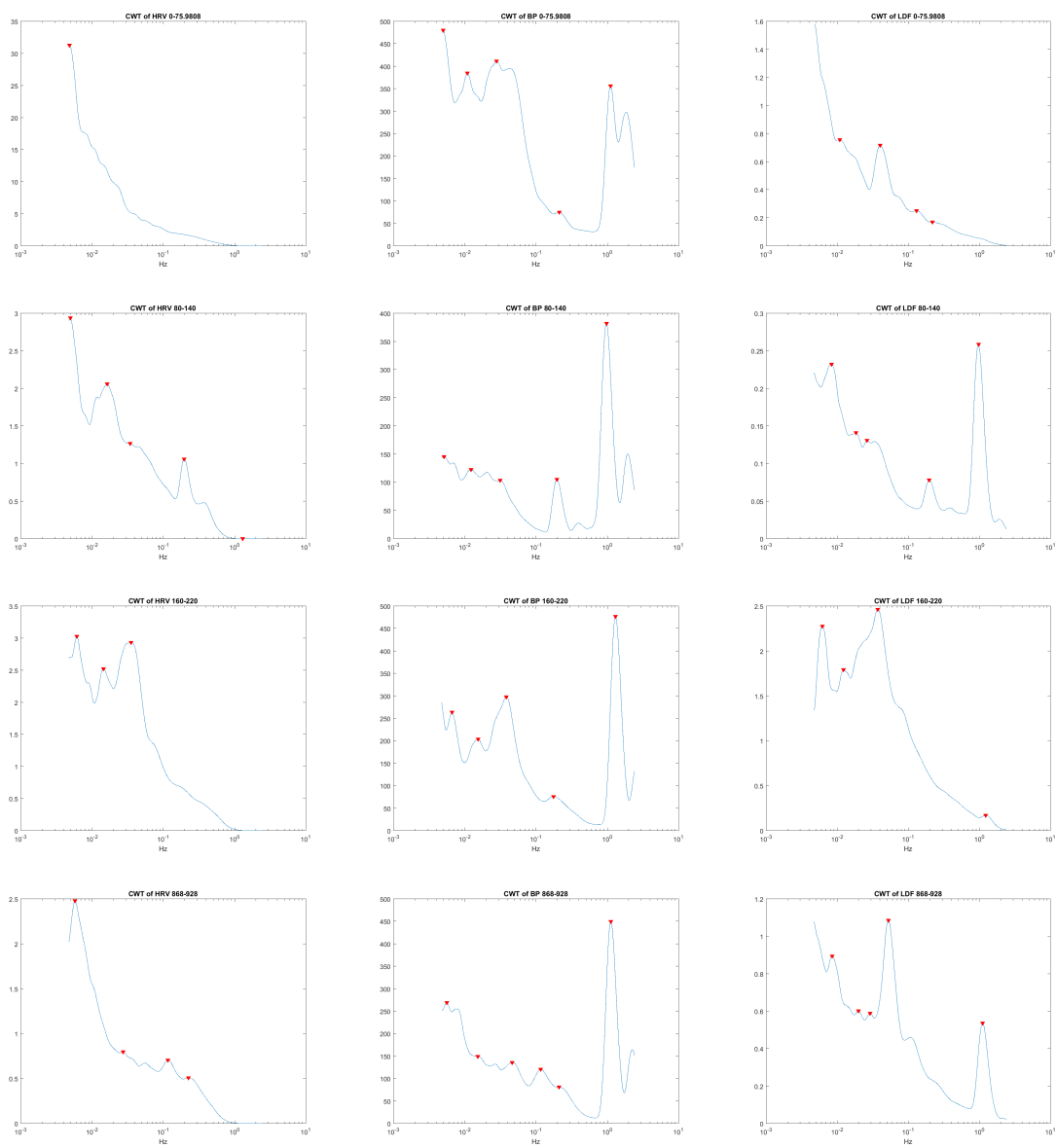


Figure A.6: CWT mean of 160413

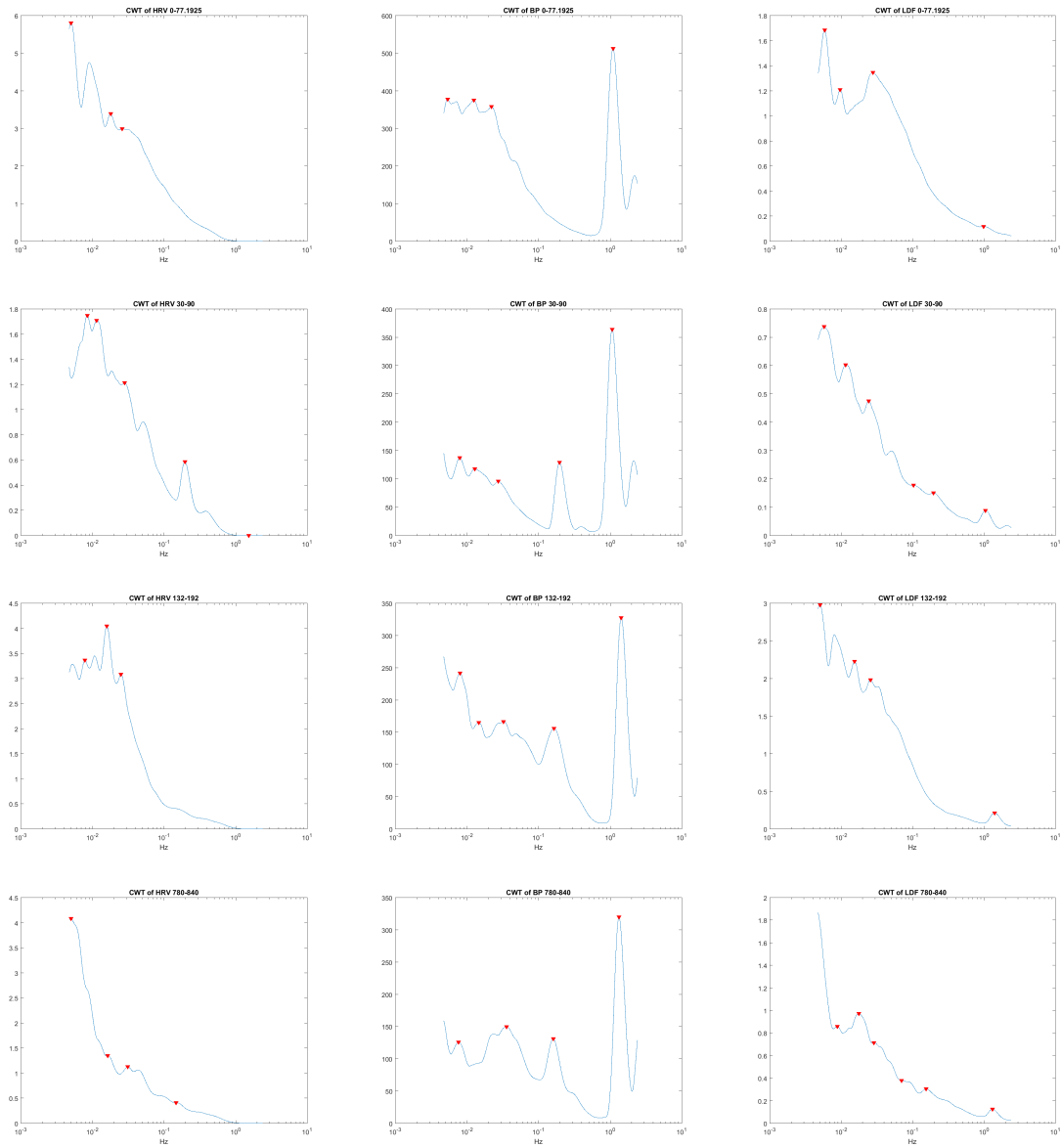


Figure A.7: CWT mean of 160421

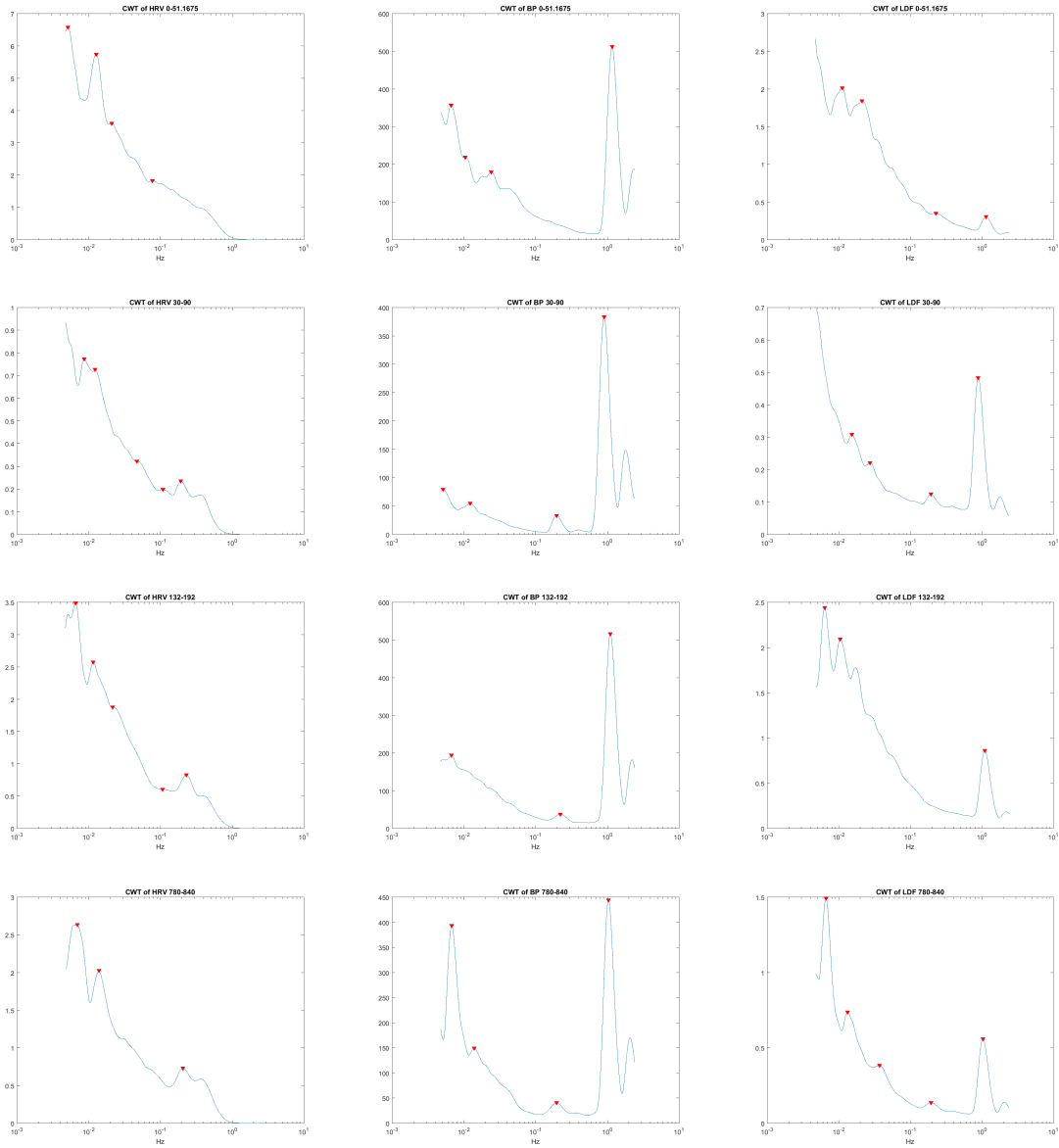


Figure A.8: CWT mean of 160510

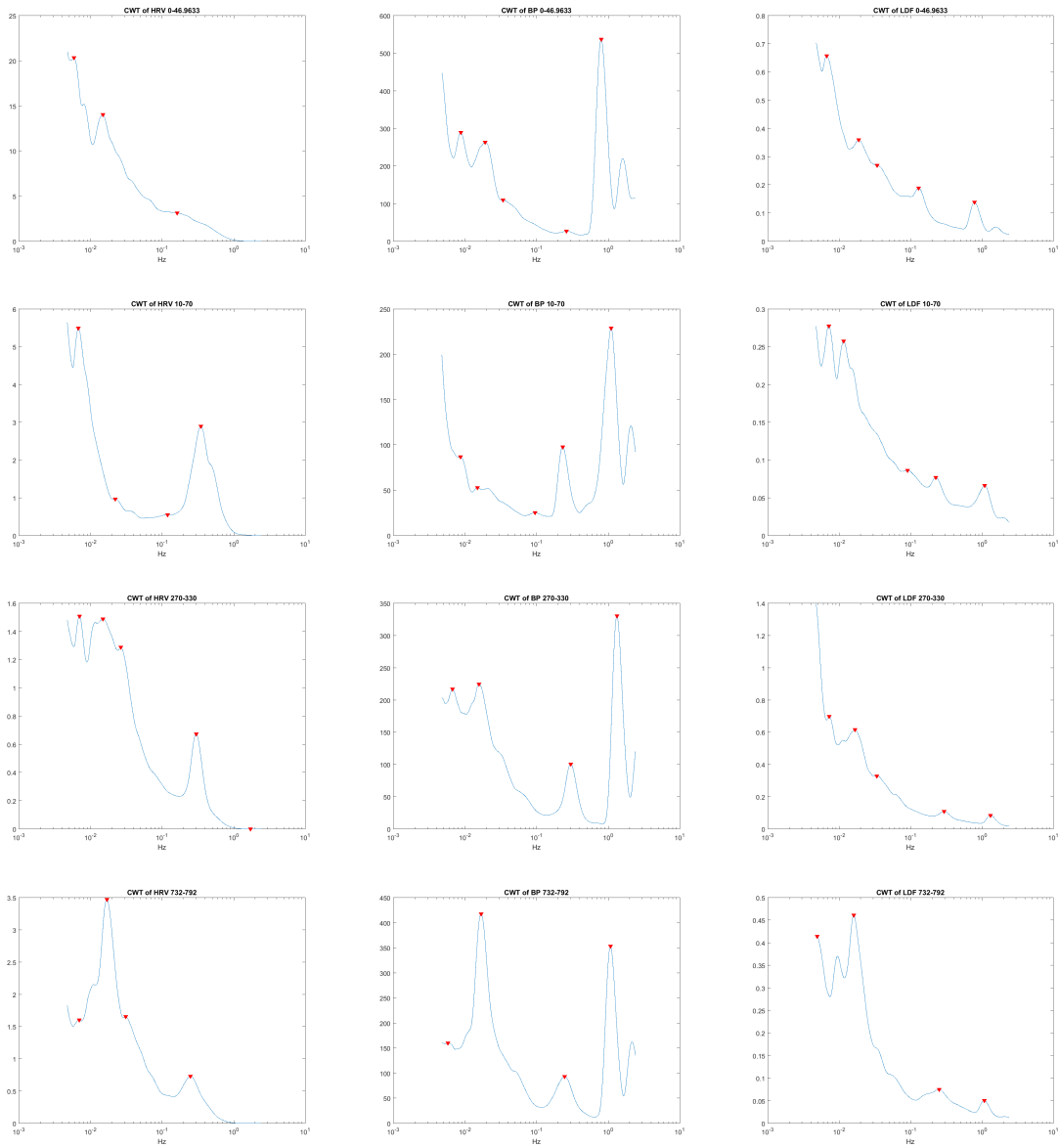


Figure A.9: CWT mean of 160512

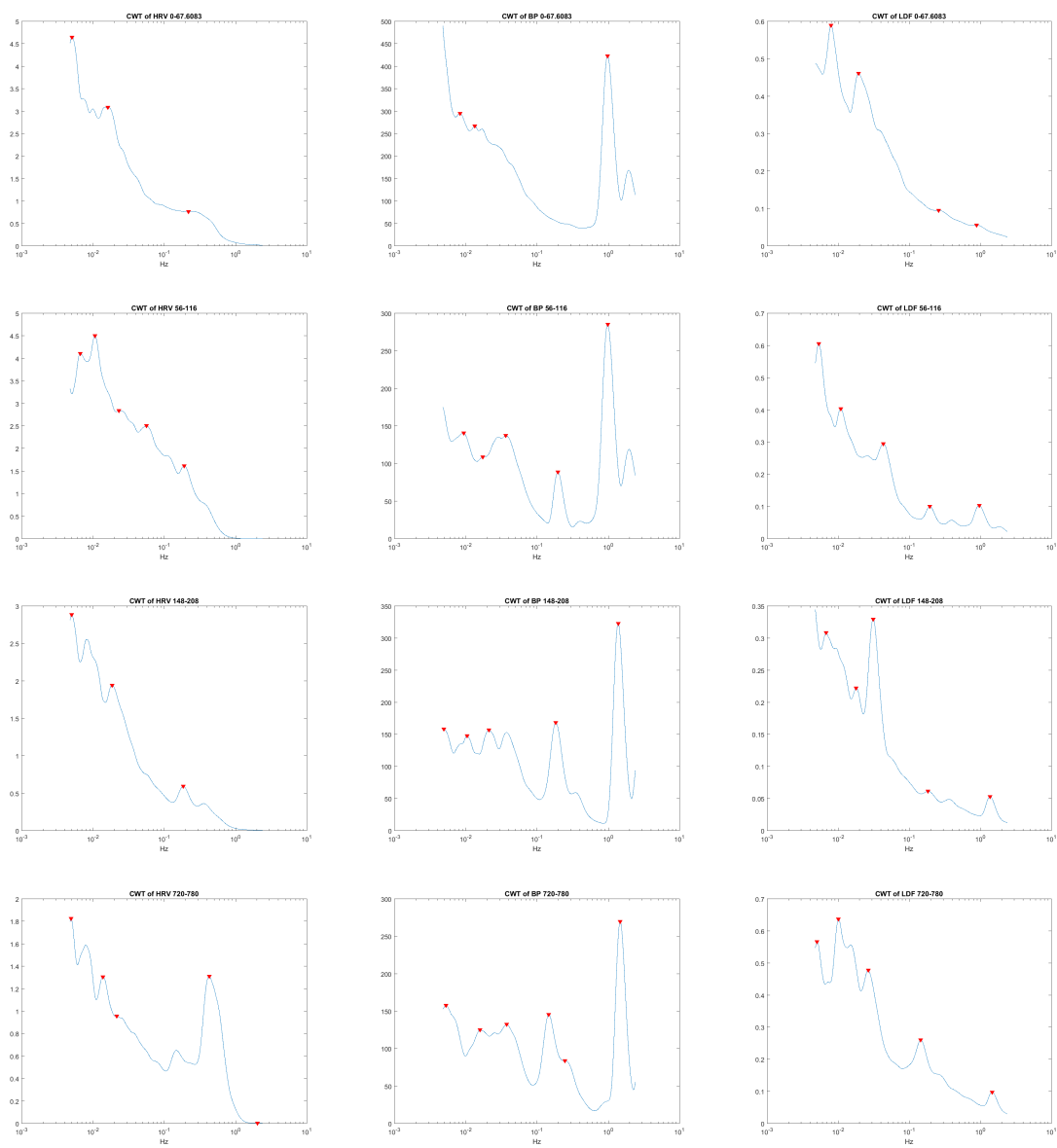


Figure A.10: CWT mean of 160524

Appendix B

Poincare plots

This appendix shows all the Poincare plots for all the patients. It is four plots for each analysed time-segment, all four time-segments are shown in the same figure. The four plots to the upper left is from the pre segment, upper right is from post1, down left is from post2 and down right is from post3.

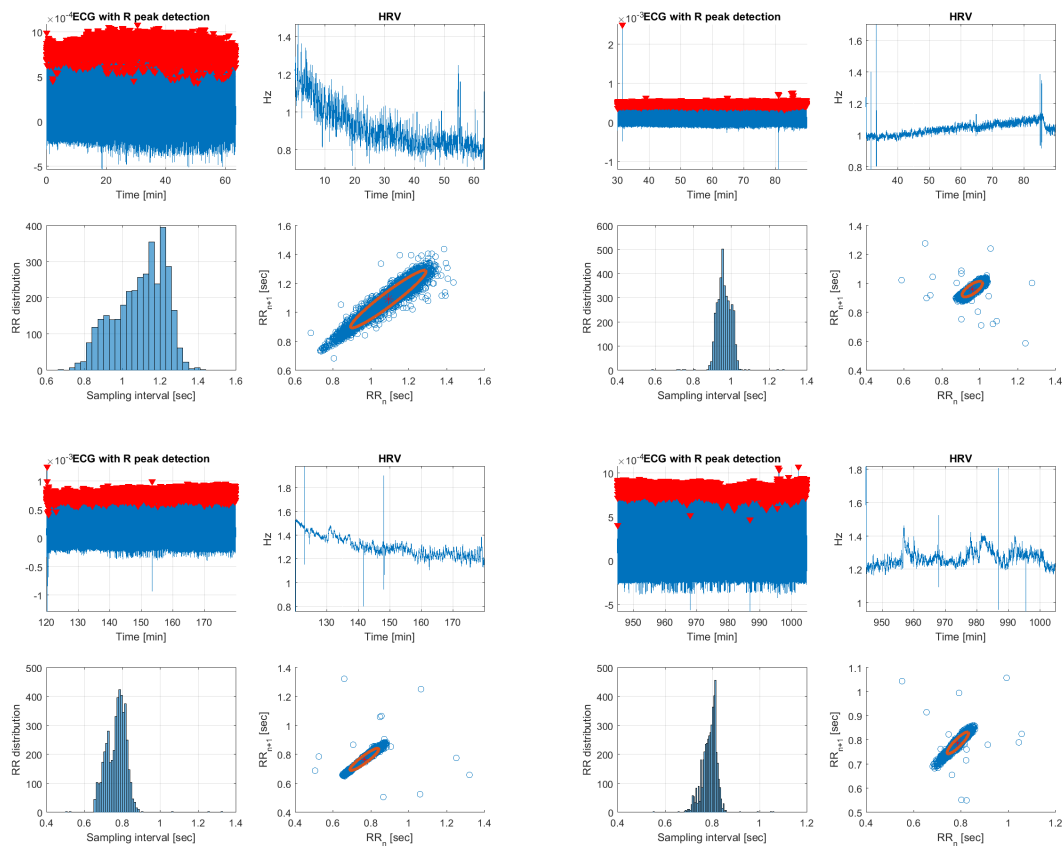


Figure B.1: Poincare plots of 160317

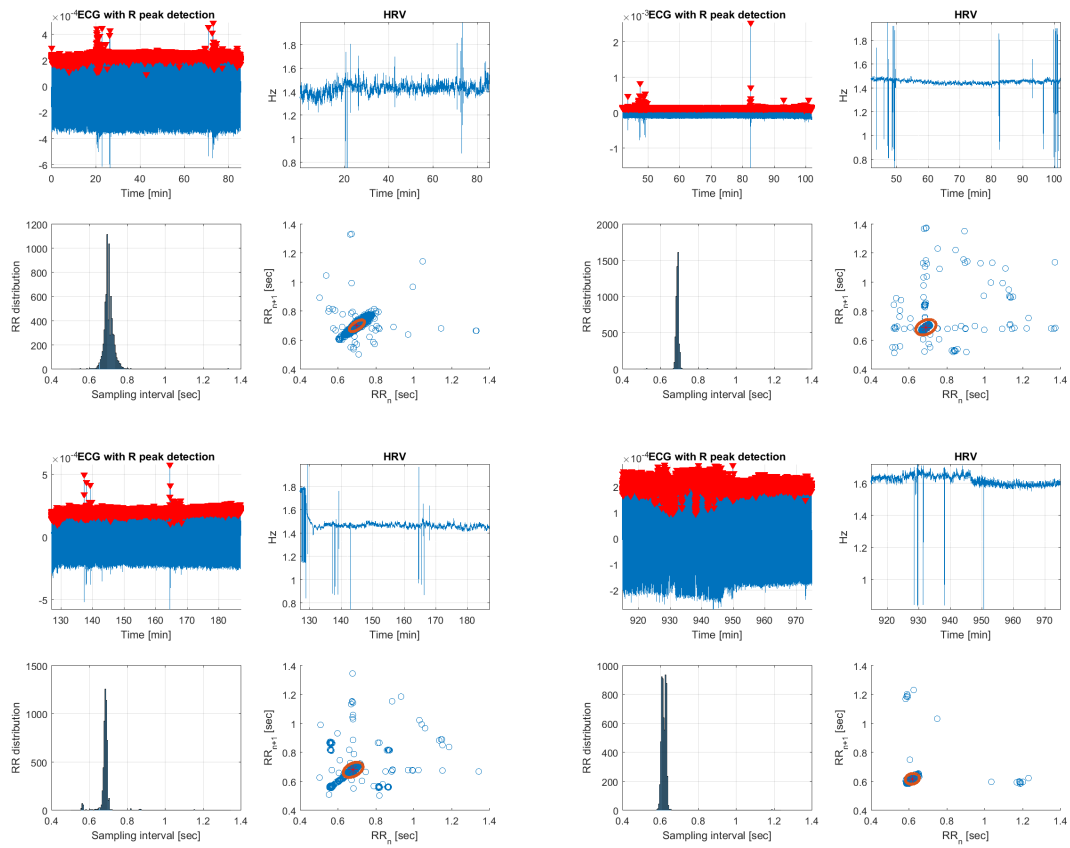


Figure B.2: Poincare plots of 160329

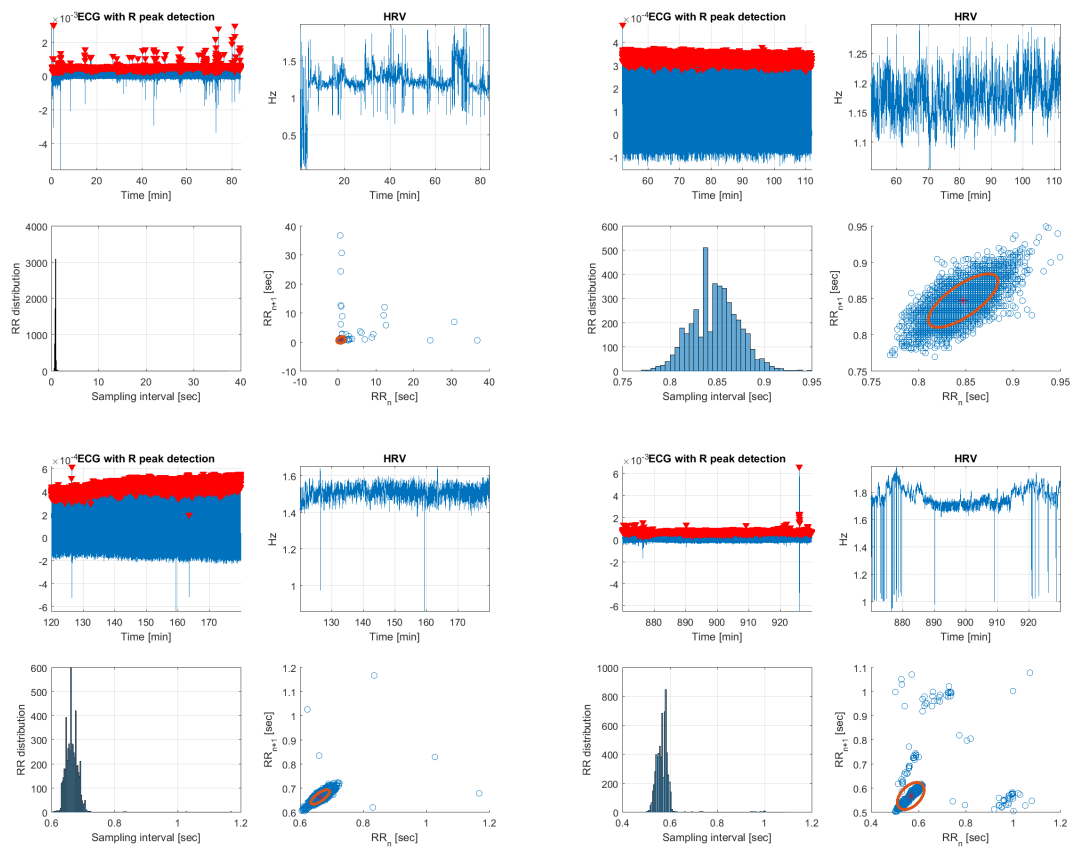


Figure B.3: Poincaré plots of 160331

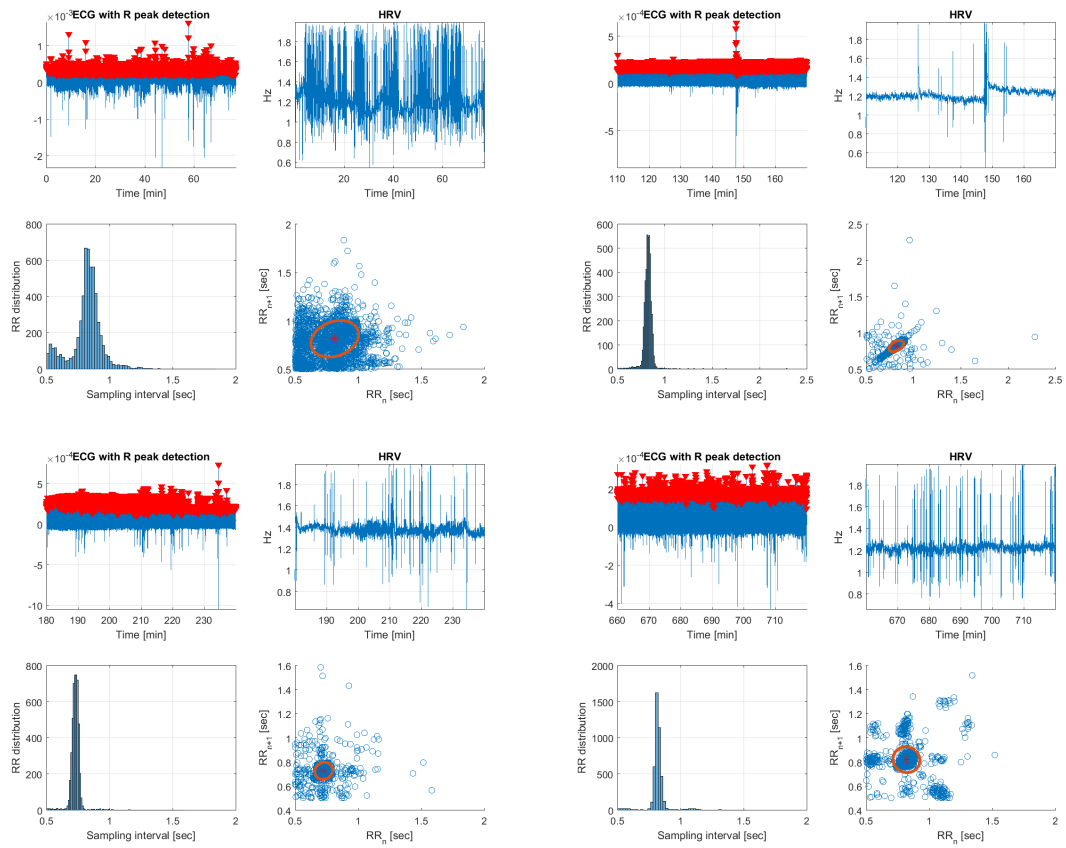


Figure B.4: Poincare plots of 160406

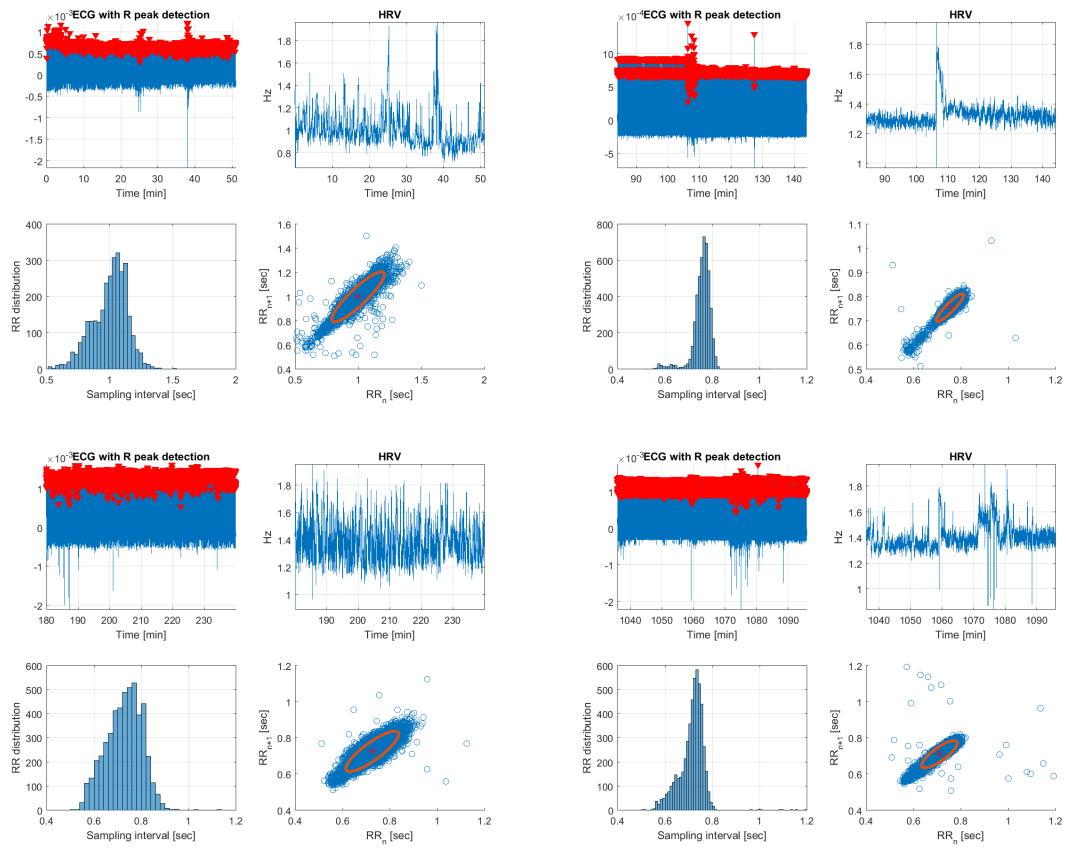


Figure B.5: Poincaré plots of 160407

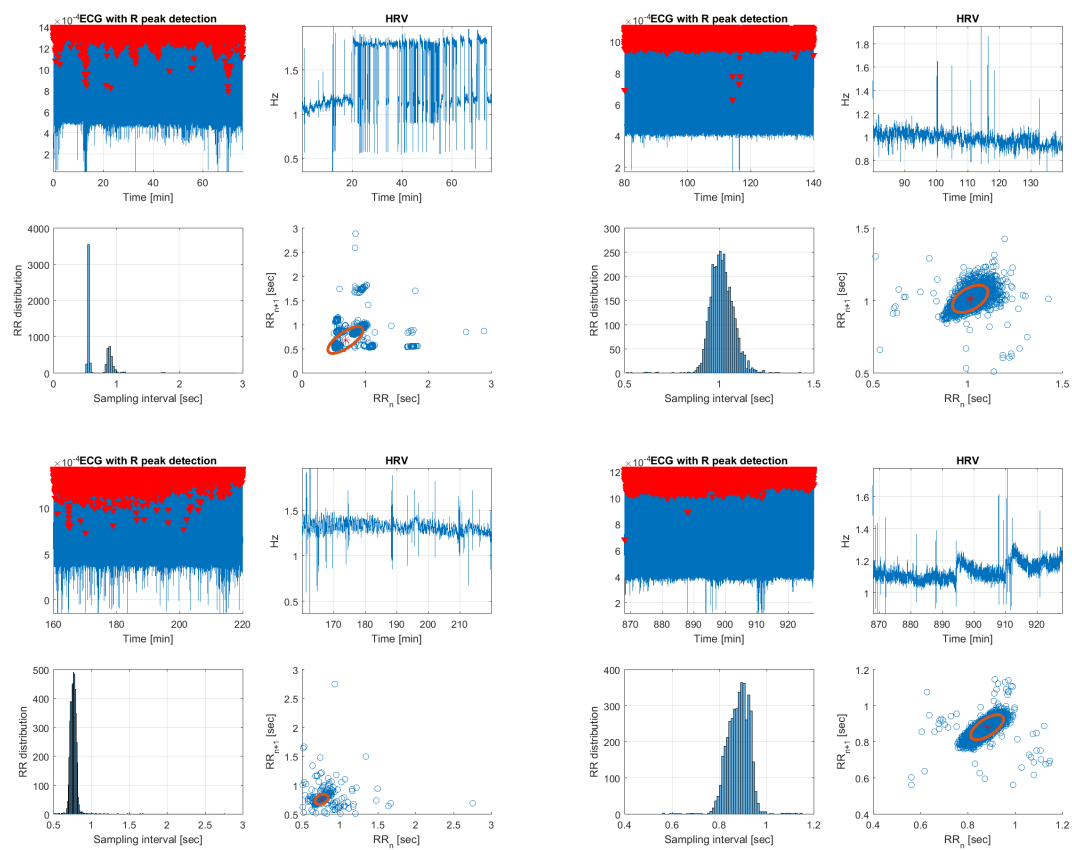


Figure B.6: Poincare plots of 160413

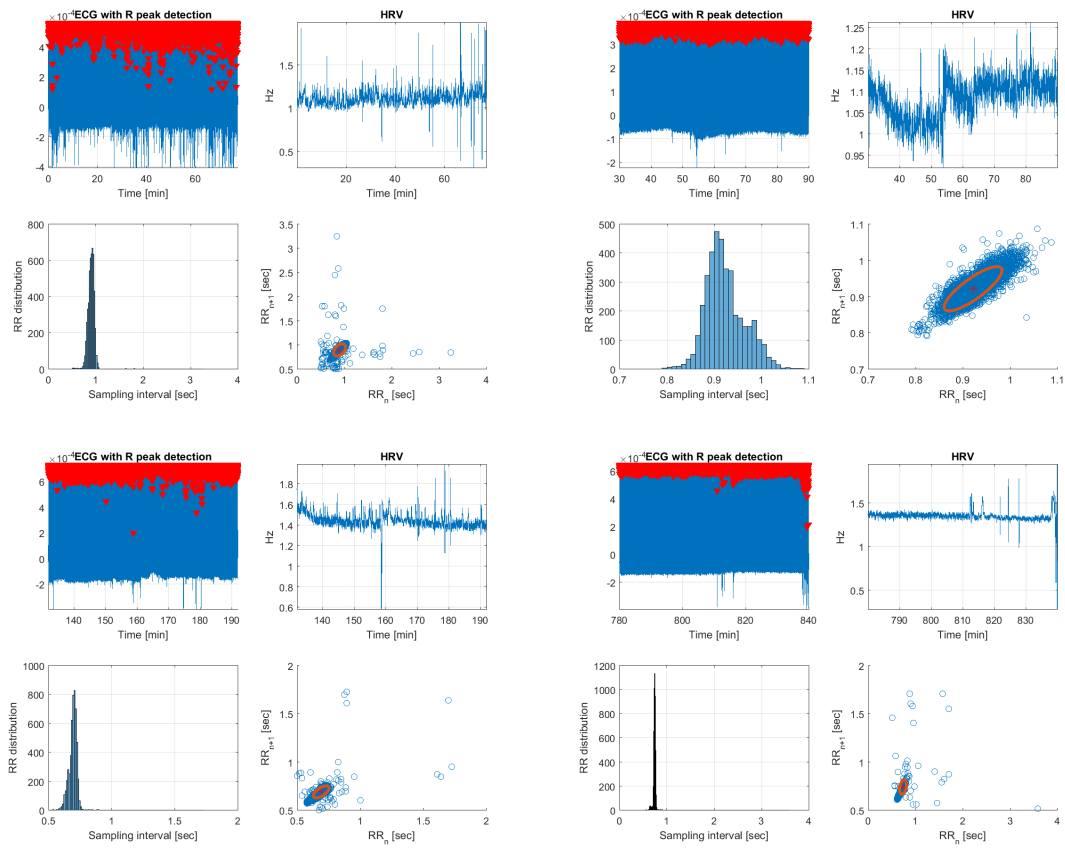


Figure B.7: Poincaré plots of 160421

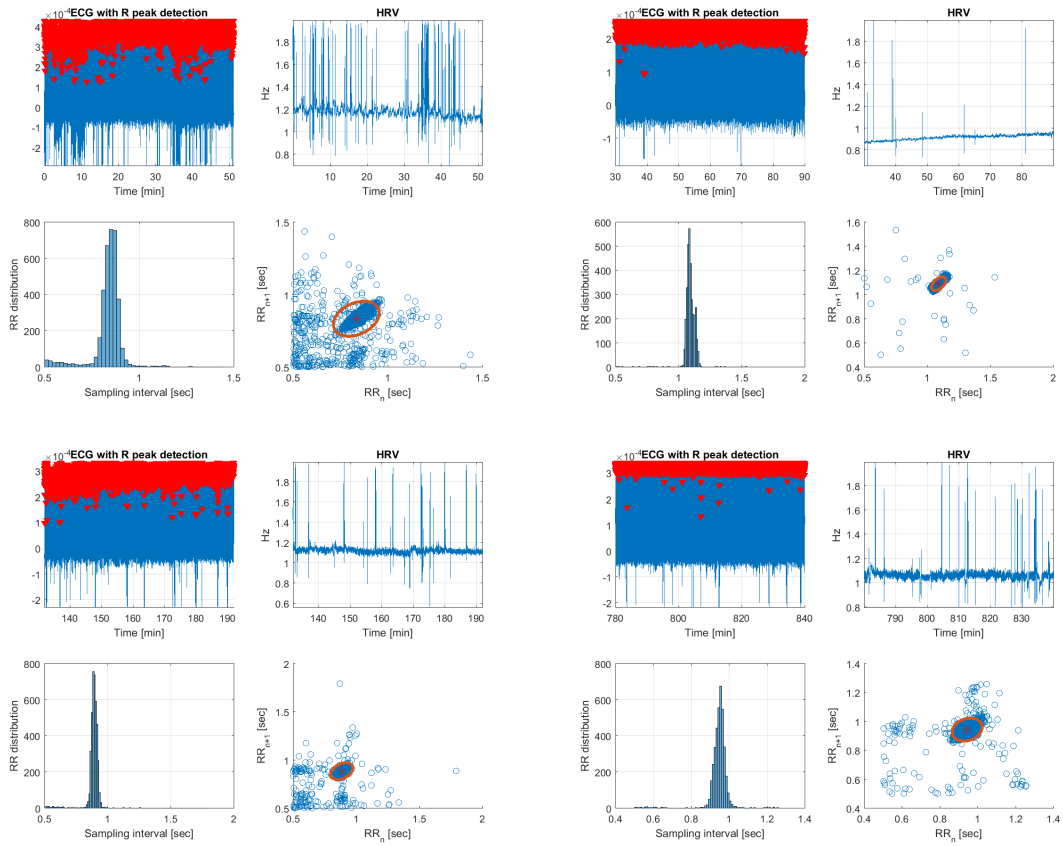


Figure B.8: Poincare plots of 160510

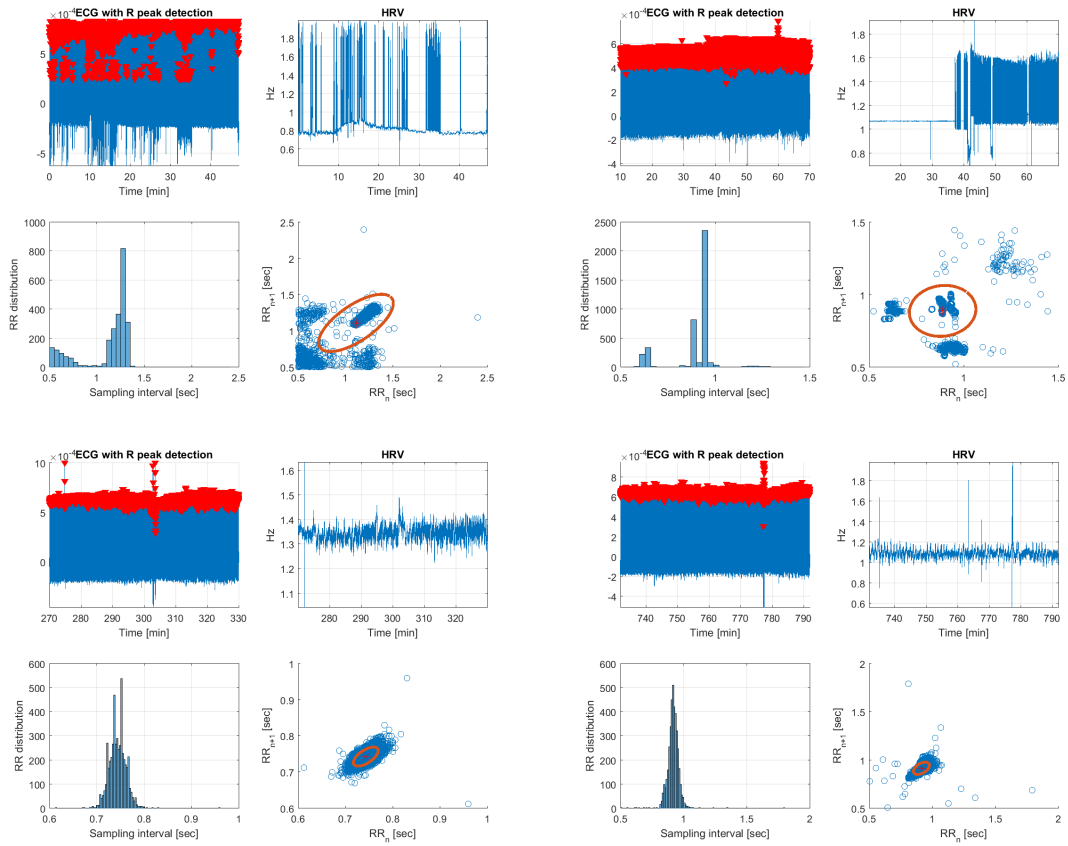


Figure B.9: Poincare plots of 160512

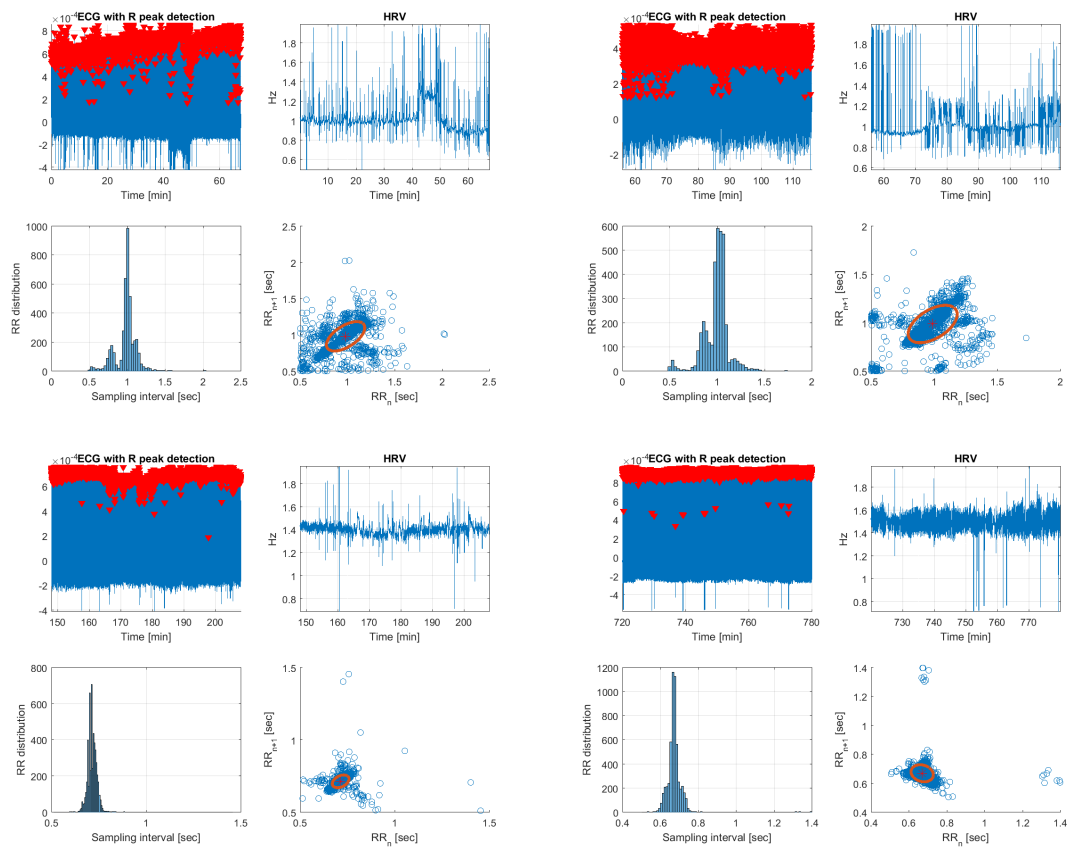


Figure B.10: Poincare plots of 160524

Appendix C

Attached files

The following is content in the attached zip-file *code*:

- **Functions**, different Matlab functions saved as .m files.
- **GUI_filer**, files to run the applications
 - **data_exc_GUI.m**, is the pre program.
 - **master_GUI.m**, is the analysis program.
- **Scripts**, different scripts used through the Master thesis work.

Raw data could be found at the OneDrive folder(this folder is owned by the medical student Bjørn Gardsjord Lio):

- https://studntnu-my.sharepoint.com/personal/bjorngar_ntnu_no/Documents/Hovedoppgave/20V16

Analysis data and figures could be found at the OneDrive folder:

- https://studntnu-my.sharepoint.com/personal/kristils_ntnu_no/Documents/Master/Figures_f_b

Bibliography

- [1] Skjærvold NK, Axelsson FET, Lio BG. Circulatory oscillations in post cardiac surgery patients. 2016 Jun;.
- [2] Wikipedia. Circulatory system; 2016. Page Version ID: 718187561. Available from: https://en.wikipedia.org/w/index.php?title=Circulatory_system&oldid=718187561.
- [3] Wikipedia. Cardiac output; 2016. Page Version ID: 720493262. Available from: https://en.wikipedia.org/w/index.php?title=Cardiac_output&oldid=720493262.
- [4] Wikipedia. Electrical conduction system of the heart; 2016. Page Version ID: 715177840. Available from: https://en.wikipedia.org/w/index.php?title=Electrical_conduction_system_of_the_heart&oldid=715177840.
- [5] Wikipedia. Electrocardiography; 2016. Page Version ID: 721281175. Available from: <https://en.wikipedia.org/w/index.php?title=Electrocardiography&oldid=721281175>.
- [6] wikipedia. Doppler effect; 2016. Page Version ID: 720407870. Available from: https://en.wikipedia.org/w/index.php?title=Doppler_effect&oldid=720407870.
- [7] Megaemg. Electrocardiogram (ECG) and Heart Rate Variability (HRV) | Mega Electronics Ltd; 2016. Available from: <http://www.megaemg.com/knowledge/heart-rate-variability-hrv/>.
- [8] Karmakar CK GJPM Khandoker AH. Standard Poincaré plot. A standard Poincaré plot (lag | Open-i; 2009. Available from: https://openi.nlm.nih.gov/detailedresult.php?img=PMC2743693_1475-925X-8-17-1&req=4.
- [9] Lio BG, Axelsson F. Circulatory oscillations in post cardiac surgery patients; 2016.
- [10] Bracic M, Stefanovska A. Wavelet-based analysis of human blood-flow dynamics. Bull Math Biol. 1998 Sep;60(5):919–935. Available from: <http://www.ncbi.nlm.nih.gov/pubmed/9739620>.
- [11] Lakusic N, Mahovic D, Kruzliak P, Cerkez Habek J, Novak M, Cerovec D. Changes in Heart Rate Variability after Coronary Artery Bypass Grafting and Clinical Importance of These Findings. Biomed Res Int. 2015;2015. Available from: <http://www.ncbi.nlm.nih.gov/pmc/articles/PMC4452832/>.

- [12] Najarian K, Splinter R. Biomedical Signal and Image Processing. Biomedical engineering. Taylor & Francis; 2005. Available from: <https://books.google.no/books?id=VCjPXACbx5EC>.
- [13] Blinowska KJ, Zygierewicz J. Practical Biomedical Signal Analysis Using MATLAB®. CRC Press; 2011.
- [14] Wikipedia. Blood pressure; 2016. Page Version ID: 716267658. Available from: https://en.wikipedia.org/w/index.php?title=Blood_pressure&oldid=716267658.
- [15] Wikipedia. Stroke volume; 2016. Page Version ID: 705248132. Available from: https://en.wikipedia.org/w/index.php?title=Stroke_volume&oldid=705248132.
- [16] wikipedia. Vascular resistance; 2016. Page Version ID: 719440240. Available from: https://en.wikipedia.org/w/index.php?title=Vascular_resistance&oldid=719440240.
- [17] Medscape. Blood Pressure Measurement; 2016. Available from: http://www.medscape.com/viewarticle/563819_5.
- [18] Eun HC. Evaluation of skin blood flow by laser Doppler flowmetry. Clin Dermatol. 1995 Aug;13(4):337–347.
- [19] Rajan V, Varghese B, Leeuwen TG, Steenbergen W. Review of methodological developments in laser Doppler flowmetry. Lasers Med Sci. 2008 Jan;24(2):269–283. Available from: <http://link.springer.com/article/10.1007/s10103-007-0524-0>.
- [20] wikipedia. Heart rate; 2016. Page Version ID: 719944450. Available from: https://en.wikipedia.org/w/index.php?title=Heart_rate&oldid=719944450.
- [21] C Guger GE. Heart-Rate Variability and Event-Related ECG in Virtual Environments. 2004;p. 240–245.
- [22] Malik M, Bigger JT, Camm AJ, Kleiger RE, Malliani A, Moss AJ, et al. Heart rate variability. European Heart Journal. 1996 Mar;17(3):354–381. Available from: <http://eurheartj.oxfordjournals.org/content/17/3/354>.
- [23] Wikipedia. Frequency domain; 2015. Page Version ID: 689132256. Available from: https://en.wikipedia.org/w/index.php?title=Frequency_domain&oldid=689132256.
- [24] wikipedia. Fourier transform; 2016. Page Version ID: 719260147. Available from: https://en.wikipedia.org/w/index.php?title=Fourier_transform&oldid=719260147.
- [25] wikipedia. Parseval's theorem; 2016. Page Version ID: 709346158. Available from: https://en.wikipedia.org/w/index.php?title=Parseval%27s_theorem&oldid=709346158.
- [26] Wikipedia. Fast Fourier transform; 2016. Page Version ID: 712035039. Available from: https://en.wikipedia.org/w/index.php?title=Fast_Fourier_transform&oldid=712035039.

- [27] Wikipedia. Wavelet; 2016. Page Version ID: 719674061. Available from: <https://en.wikipedia.org/w/index.php?title=Wavelet&oldid=719674061>.
- [28] {ECE Northwestern}. Advanced Concepts (Wavelet Toolbox); 2016. Available from: http://www.ece.northwestern.edu/local-apps/matlabhelp/toolbox/wavelet/ch06_a26.html.
- [29] Huikuri HV, Seppänen T, Koistinen MJ, Airaksinen J, Ikäheimo MJ, Castellanos A, et al. Abnormalities in beat-to-beat dynamics of heart rate before the spontaneous onset of life-threatening ventricular tachyarrhythmias in patients with prior myocardial infarction. *Circulation*. 1996 May;93(10):1836–1844.
- [30] Torrence C, Compo GP. A practical guide to wavelet analysis. *Bulletin of the American Meteorological society*. 1998;79(1):61–78. Available from: [http://journals.ametsoc.org/doi/abs/10.1175/1520-0477\(1998\)079%3C0061:APGTWA%3E2.0.CO;2](http://journals.ametsoc.org/doi/abs/10.1175/1520-0477(1998)079%3C0061:APGTWA%3E2.0.CO;2).
- [31] Alfaouri M, Daqrouq K. ECG signal denoising by wavelet transform thresholding. *American Journal of applied sciences*. 2008;5(3):276–281. Available from: https://www.researchgate.net/profile/Khaled_Daqrouq/publication/26516250_ECG_Signal_Denoising_By_Wavelet_Transform_Thresholding/links/00b7d523c1c6ac1e9b000000.pdf.
- [32] Erçelebi E. Electrocardiogram signals de-noising using lifting-based discrete wavelet transform. *Computers in Biology and Medicine*. 2004 Sep;34(6):479–493. Available from: <http://www.sciencedirect.com/science/article/pii/S0010482503000908>.
- [33] Akay M. Introduction: Wavelet transforms in biomedical engineering. *Ann Biomed Eng*. 1995 Sep;23(5):529–530. Available from: <http://link.springer.com/article/10.1007/BF02584452>.
- [34] Parati G, Saul JP, Rienzo MD, Mancia G. Spectral Analysis of Blood Pressure and Heart Rate Variability in Evaluating Cardiovascular Regulation A Critical Appraisal. *Hypertension*. 1995 Jun;25(6):1276–1286. Available from: <http://hyper.ahajournals.org/content/25/6/1276>.
- [35] Kastrup J, Bülow J, Lassen NA. Vasomotion in human skin before and after local heating recorded with laser Doppler flowmetry. A method for induction of vasomotion. *Int J Microcirc Clin Exp*. 1989 Apr;8(2):205–215.
- [36] Braun SR. Respiratory Rate and Pattern. In: Walker HK, Hall WD, Hurst JW, editors. *Clinical Methods: The History, Physical, and Laboratory Examinations*. 3rd ed. Boston: Butterworths; 1990. Available from: <http://www.ncbi.nlm.nih.gov/books/NBK365/>.
- [37] Karemaker JM. Autonomic integration: the physiological basis of cardiovascular variability. *J Physiol*. 1999 Jun;517(Pt 2):316. Available from: <http://www.ncbi.nlm.nih.gov/pmc/articles/PMC2269362/>.

- [38] Julien C. The enigma of Mayer waves: Facts and models. *Cardiovascular Research*. 2006 Apr;70(1):12–21. Available from: <http://cardiovascres.oxfordjournals.org/content/70/1/12>.
- [39] Rhoades R, Bell DR. *Medical Physiology: Principles for Clinical Medicine*. Lippincott Williams & Wilkins; 2009.
- [40] Laitio TT, Huikuri HV, Kentala ES, Mäkikallio TH, Jalonen JR, Helenius H, et al. Correlation properties and complexity of perioperative RR-interval dynamics in coronary artery bypass surgery patients. *Anesthesiology*. 2000 Jul;93(1):69–80.